ROLE OF JMJD5 IN LIVER CANCER

A THESIS SUBMITTED TO
THE DEPARTMENT OF MOLECULAR BIOLOGY AND GENETICS
AND THE GRADUATE SCHOOL OF ENGINEERING AND SCIENCE OF
BILKENT UNIVERSITY
IN PARTIAL FULFILLMENT OF THE REQUIREMENTS
FOR THE DEGREE OF
MASTER OF SCIENCE

By

Engin Demirdizen

August, 2013

I certify that I have read this thesis and that in my opinion it is fully adequate, in scope and in quality, as a thesis for the degree of Master of Science.

Prof. Dr. Mehmet Öztürk (Advisor)

I certify that I have read this thesis and that in my opinion it is fully adequate, in scope and in quality, as a thesis for the degree of Master of Science.

Assoc. Prof. Dr. Rengül Çetin-Atalay

I certify that I have read this thesis and that in my opinion it is fully adequate, in scope and in quality, as a thesis for the degree of Master of Science.

Assist. Prof. Dr. Bala Gür-Dedeoğlu

Approved for the Graduate School of Engineering and Science:

Director of Graduate School of
Engineering and Science
Prof. Dr. Levent Onural

ABSTRACT

ROLE OF JMJD5 IN LIVER CANCER

Engin Demirdizen
M.S. in Molecular Biology and Genetics
Supervisor: Prof. Dr. Mehmet Öztürk
August 2013, 94 Pages

Being one of the most common cancer types in human population, hepatocellular carcinoma (HCC) has high rate of deaths due to the challenges in its diagnosis and treatment. In recent years, epigenetic regulators have come into play in HCC research to overcome with those challenges. As potential drug targets, histone demethylases has drawn a lot of interest. In this respect, several studies have focused on a specific member of this family, JMJD5, suggesting its possible function in tumor suppression, while the opposite argument has also been proposed by several reports. Preceding studies on JMJD5 in our lab also pointed to a possible tumor suppressor function. Hence, this study aimed to elucidate the role of JMJD5 in liver cancer development using SNU449 HCC cell line stably expressing JMJD5. For this purpose, stable clones overexpressing wild-type and mutant JMJD5 as well as controls were generated. A comparative analysis of these clones was performed. No definite results could be obtained for the effect of JMJD5 on cell proliferation, but the number of cells in G1 declined, whereas that in G2/M inclined in clones expressing wild-type and mutant JMJD5, suggesting that JMJD5 affects cell cycle progression. In addition, cell motility was decreased, while anchorage-independent colony formation ability was enhanced in both mutant and wild type JMJD5-expressing clones. Decrease in cell motility is considered to be anti-tumoral, whereas anchorage-independent growth is a malignant change. Our findings suggest that JMJD5 may have a quite complex role in liver tumorigenesis. Further in vivo studies may help to clarify some of these apparently conflicting in vitro effects.

Keywords: JMJD5, liver cancer, hepatocellular carcinoma, tumor suppressor.

ÖZET

JMJD5'İN KARACİĞER KANSERİNDEKİ ROLÜ

Engin Demirdizen
Moleküler Biyoloji ve Genetik, Yüksek Lisans
Tez Yöneticisi: Prof. Dr. Mehmet Öztürk
Ağustos 2013, 94 Sayfa

İnsan popülasyonunda en sık görülen kanser tiplerinden biri olarak, teşhis ve tedavisindeki zorluklardan dolayı karaciğer kanseri (Hepatoselüler Karsinom, HSK) yüksek ölüm oranına sahiptir. Bu zorlukların üstesinden gelebilmek için son yıllarda HSK araştırmalarında epigenetik düzenleyiciler kullanılmaya başlandı. Potensiyel ilaç hedefleri olarak histon demetilazlar çok ilgi çekmektedir. Bu bakımdan, pek çok çalışma karşıt delilleri de diğer çalışmalarda iddia edilmesine rağmen tümör baskılanmasında olası bir görevi olduğunu ileri sürerek bu ailenin bir üyesi olan JMJD5'e odaklanmıştır. Labımızda JMJD5 üzerindeki daha önce yapılan çalışmalar da olası bir tümor baskılama görevine işaret etmiştir. Bu yüzden bu çalışma JMJD5'i stabil olarak ifade eden SNU449 HSK hücre hattını kullanarak JMJD5'in karaciğer kanseri gelişimindeki rolünü ortaya çıkarmayı amaçlamıştır. Bu amaç için normal ve mutant JMJD5'i olduğundan fazla ifade eden stabil klonlarla birlikte kontroller oluşturuldu. Bu klonların kıyaslamalı analizi yapıldı. JMJD5'in hücre çoğalmasına etkisi hakkında kesin sonuçlar elde edilemedi, ancak G2/M'deki hücre sayısı normal ve mutant JMJD5 ifade eden klonlarda artarken, G1'deki hücre sayısı azaldı. Bu sonuç JMJD5'in hücre döngüsü ilerleyişini etkilediğini ileri sürüyor. Buna ek olarak, mutant ve normal tip JMJD5 ifade eden klonlarda dayanaktan bağımsız koloni oluşum kapasitesi artarken hücre hareketliliğinin azaldığı gözlendi.. Hücre hareketliliğinde azalma tümör önleyici olarak düşünülürken dayanaktan bağımsız büyüme kötü huylu bir değişimdir. Bulgularımız JMJD5'in karaciğer kanseri oluşumunda oldukça karmaşık bir rolü olabileceğine işaret ediyor. Daha fazla in vivo çalışma, görünüşe göre çelişkili in vitro etkilerin bazılarına açıklık getirmeye yardım edebilir.

Anahtar sözcükler: JMJD5, karaciğer kanseri, hepatoselüler karsinom, tümör baskılayıcı.

TO MY FAMILY

.

ACKNOWLEDGEMENTS

I am greatly thankful to many people who make this thesis possible.

First of all, I would like to thank my thesis supervisor Prof. Dr. Mehmet Öztürk for his supervision throughout this project, great ideas, encouragement and understanding. I always admired his extensive knowledge in molecular biology, enthusiasm and excitement about science. It was a privilege for me to work in his laboratory as a M.Sc. student.

Secondly, I am grateful to Gökhan Yıldız for his guidance and valuable support in almost every part of this project. I would also like to thank Emre Yurdusev and Tamer Kahraman for their crucial contributions to this work.

All the past and present members of our group, especially Umur Keleş, Derya Soner Dilek Çevik, Ayşegül Örs, Dr. Çiğdem Özen, Hande Topel, Merve Deniz Abdüsselamoğlu, Yusuf İsmail Ertuna, Dr. Hani Alotaibi, Umar Raza and Andaç Kipalev have been wonderful colleagues and friends during my M.Sc. study.

Other members in our lab, particularly Ender Avcı, Pelin Telkoparan, Mehmet Şahin, İhsan Dereli, Damla Gözen, Sıla Özdemir, Gurbet Karahan, Nilüfer Sayar, Verda Ceylan Bitirim, Defne Bayık, Gözde Güçlüler, Ece Akhan, Merve Aydın have always been good friends for me.

I would also like to thank Füsun Elvan, Bilge Kılıç, Sevim Baran, Yıldız Karabacak and Abdullah Ünnü in the Department of Molecular Biology and Genetics for their invaluable help.

I would like to thank Dr. Uygar Tazebay and Dr. Yoshihiro Izumiya for donating SNU449-TRex cells and pLTRE-KDM8 plasmids, respectively.

Finally, I would like to thank The Scientific and Technological Research Council of Turkey (TÜBİTAK) for supporting me during the master study through BİDEB 2210 scholarship.

TABLE OF CONTENTS

LIST OF TABLES

LIST OF FIGURES

CHAPTER 1

INTRODUCTION

1.1 Hepatocellular carcinoma

Among all types of liver cancer, hepatocellular carcinoma (HCC) is the most widely encountered, comprising 83 % of all cases [1]. As a common disease, HCC is the fifth and seventh most widespread cancer in populations of men and women, respectively [2]. Being the sixth most prevalent neoplasm, HCC is also ranked third among the cancers most frequently causing death, with only 14 % 5-year survival rate [3, 4].

1.1.1 Aetiologies of hepatocellular carcinoma

The major aetiological factors regarding HCC include infection with hepatitis B (HBV) and C virus (HCV), contributing to about 70 % of all cases, excessive alcohol intake and aflatoxin contamination in the food resources [1, 2, 5]. Other risk factors, including female oral contraceptive use for a long time, certain metabolic diseases, diabetes, obesity, non-alcoholic fatty liver disorders (NAFLD) and non-alcoholic steatohepatitis, are also minorly responsible for the causation of HCC [1, 5]. The frequency of HCC occurrence changes in the world based on geographical distribution of causative agents. HBV infection plays a major role in most Asian and African countries, whereas HCV infection is the primary reason for HCC in United States and most European countries. Heavy alcohol drinking in western societies and dietary aflatoxin contamination in South China and Sub-Saharan Africa are primary causes of HCC development in these regions [2].

1.1.2 Pathogenesis of hepatocellular carcinoma

The cause of hepatocellular carcinoma can be literally attributed to cirrhosis-stimulating circumstances in the host microenvironment [1]. HBV-HCV infections and alcohol overconsumption lead to inflammation, many rounds of hepatocyte loss and regeneration, oxidative stress and permanent fibrotic activity, ultimately resulting in cirrhosis [1, 6]. After liver is injured, genomic stability is lost through blockage of DNA repair, carcinogenic agents and epigenetic alterations, which starts conversion of normal hepatocytes into malignancy [6, 7]. As the genetic damage accumulates, self-expanding dysplastic nodules arise, and they progressively give rise to well-differentiated, moderately differentiated and poorly differentiated metastatic HCC [7].

Genomic changes, including chromosome abnormalities and genetic mutations are commonly observed in HCC [1]. Loss of 4q and gain of 1q, 8q, 17q are the most widespread changes in the chromosome [5]. Mutations detected in HCC cases mainly occur in p53, β-catenin, Axin1, p16, hTERT, ErbB receptor family and MET receptor [1, 5, 8]. Epigenetic mechanisms, such as DNA methylation, mutations in epigenetic factors and differential expression of miRNAs, have been found to be associated with HCC pathogenesis [5]. As a key component in HCC development, inhibition of p53 and p16, coupling with hTERT activation, drives liver cells into bypassing senescence and immortalization [9].

1.2 Epigenetics, cancer and HCC

The field of hereditary alterations which do not occur in base sequence of DNA but affect gene expression is defined as epigenetics [10]. This inherited knowledge is encoded by chemically modified nucleotides and proteins binding to the chromatin in eukaryotic genomes. Gene expression patterns are deeply differentiated upon epigenetic changes because accessibility of genes and chromatin architecture are modulated [11]. There are four major mechanisms of epigenetic modification: DNA methylation, covalent modifications of histones, microRNAs and non-covalent actions of nucleosome remodeling machineries and histone variants [10].

Abnormal functioning in epigenetic mechanisms is equally important as genetic events in the onset and development of carcinogenesis [12]. As evidence suggests, the function of key epigenetic players changes earlier than cell transformation into malignancy, thereby playing a critical role in cancer development [13, 14]. In terms of discovery of early diagnostic biomarkers, risk consideration and tracing of the disease, more elaborated knowledge on epigenetic mechanisms could provide promising improvements [13].

Methylation patterns of genome, histone modification status and expression levels of chromatin-regulating factors are globally altered in cancer epigenome [10]. Hypomethylation in the global scale and hypermethylation in the CpG islands of tumor suppressor promoters are commonly detected in the cancer cells [10, 12]. According to mapping studies covering whole chromatin, most widely observed histone modifications in cancer are diminished histone-4 lysine 16 acetyl (H4K16ac), H4K20 methyl (H4K20me3) levels and varying H3K9, H3K27 methylations, all of which leads to gene silencing. Upregulated histone deacetylases (HDACs) levels, changing histone acetyl transferases (HATs) levels and aberrant histone methyltransferases (HMTs) activity underlie those modifications, being other characteristics of cancer. Histone lysine demethylases (HDMs), many of which possess Jumonji C domain, have also been associated with cancer, several of them being upregulated in prostate cancer. Nucleosome remodeling complexes were shown to act together with DNA methylations and histone modifications on silencing of tumor suppressors *via* compacting nucleosome settlement in promoter regions. Compared to normal tissues, miRNA expression levels also exhibit wide range of changes in tumor [10].

In the context of HCC, DNA methylation abnormalities, influencing mutations in epigenetic factors and changes in miRNA expression profiles have newly been identified with a raising concern [5]. Promoter hypermethylation in tumor suppressor genes and genome-wide hypomethylation have been characterized in HCC [15]. EZH2, which constitutes the catalytic part of polycomb repressive complex 2 (PRC2) and generates H2K27me3 repressive mark, is upregulated in HCC and correlates with the aggresiveness of HCC [5, 16]. HDACs-1, -2 and -3; enzymes involved in

DNA methylation, including DNMT1, DNMT3A and DNMT3B; and CENPA histone variant levels have also been shown to exhibit elevation in HCC samples compared to non-tumor liver samples [5].

1.3 Histone demethylases

Similar to the histone methylation through histone methyltransferases, which regulate chromatin architecture and transcription, HDMs play key functions in the cellular mechanisms, including development and involvement in disease. Histone demethylases so far identified have been shown to be important in normal processing of the cells, playing a diverse range of biological roles and also targeting non-histone proteins as substrates [17].

1.3.1 Histone lysine demethylase (HDM) family

Recently discovered histone lysine demethylases including amine oxidase family and Jumonji C (JmjC) domain-containing enzyme family has proved that histone lysine methylation is reversible. The first member of histone lysine demethylases discovered was lysine-specific demethylase 1(LSD1), also known as KDM1 [18]. The first member to be elucidated in JmjC family was F-box and Leu-rich repeat protein 11 (FBXL11), also known as JHDM1A and KDM2A, which was reported to demethylate H3K36me1 and H3K36me2 [17]. With the discovery of JMJD2, which is capable of demethylating H3K9me3/me2 and H3K36me3/2, and many others, trimethylation on histone lysine residues were also indicated to be reversible [19]. Up to now, demethylation events targeting H3K4, H3K9, H3K27, H3K36 and H4K20 have been detected in 18 members of 30-member JmjC family, as summarized in Table 1.1 [17].

Table 1.1: List of histone lysine demethylases, their specific substrates and related diseases.

(Adapted from Kooistra and Helin, 2012 [17])

Name	Synonyms	Histone substrates	Non-histone substrates	Association with human disease
LSD demethylases				
LSD1	AOF2, BHC110, KDM1A	H3K4me1, H3K4me2, H3K9me1, H3K9me2	p53, E2F1, DNMT1	Overexpression in prostate cancer, undifferentiated malignant neuroblastoma, oestrogen-receptor-negative breast cancer, bladder cancer, lung and colorectal carcinoma and silencing/downregulation in breast cancer
LSD2	AOF1, KDM1B	H3K4me1, H3K4me2		Amplification and overexpression in urothelial carcinoma
JMJC demethylases				
JMJD7				
HIF1AN				
HSPBAP1				
JMJD5	KDM8	H3K36me2		
JMJD4				
JMJD6	PSR, PTDSR	H3R2, H4R3		Overexpression in chronic pancreatitis
JMJD8				
FBXL10	JHDM1B, KDM2B	H3K36me1, H3K36me2, H3K4me3		Overexpression in various leukaemias and bladder carcinoma
FBXL11	JHDM1A, KDM2A	H3K36me1, H3K36me2	p65, NF-κB	
KIAA1718	JHDM1D	H3K9me1, H3K9me2, H3K27me1, H3K27me2		
PHF8	JHDM1F	H3K9me1, H3K9me2, H4K20me1		Mutation and deletion associated with X-linked mental retardation and cleft lip/palate
PHF2	JHDM1E	H3K9me2	ARID5B	Mutation or silencing/downregulation in breast carcinoma and head and neck squamous cell carcinoma
HR				
KDM3B				
JMJD1A	JHDM2A, TSGA, KDM3A	H3K9me1, H3K9me2		Overexpression in malignant colorectal cancer, metastasized prostate adenocarcinoma, renal cell carcinoma and hepatocellular carcinoma
JMJD1C				

JMJD3	KDM6B	H3K27me2, H3K27me3		Overexpression in various cancers including lung and liver carcinomas and several haematological malignancies, in neutrophils of patients with ANCA vasculitis and in primary Hodgkin's lymphoma
UTX	KDM6A	H3K27me2, H3k27me3		Mutation in multiple tumour types including multiple myeloma, oesophageal squamus cell carcinoma, renal clear cell carcinoma, transitional cell carcinoma, chronic myelomonocytic leukaemia, overexpression in breast cancer and deletion in Kabuki syndrome
UTY				
JMJD2A	JHDM3A, KDM4A	H3K9me2, H3K9me3, H3K36me2, H3K36me3, H1.4K26me2, H1.4K26me3		Silencing/downregulation in bladder cancer and overexpression in breast cancer
JMJD2C	JHDM3C, GASC1, KDM4C	H3K9me2, H3K9me3, H3K36me2, H3K36me3, H1.4K26me2, H1.4K26me3		Amplification in oesophageal cancer, breast cancer, medulloblastoma and translocation in lymphoma
JMJD2B	JHDM3B, KDM4B	H3K9me2, H3K9me3, H3K36me2, H3K36me3, H1.4K26me2, H1.4K26me3		Overexpression in malignant peripheral nerve sheath tumour
JMJD2D	JHDM3D, KDM4D	H3K9me2, H3K9me3, H3K36me2, H3K36me3, H1.4K26me2, H1.4K26me3		
JARID1B	PLU1, KDM5B	H3K4me2, H3K4me3		Overexpression in bladder cancer, prostate cancer and breast cancer
JARID1C	SMCX, KDM5C	H3K4me2, H3K4me3		Mutation in mental retardation, in autism and in renal carcinoma
JARID1D	SMCY, KDM5D	H3K4me2, H3K4me3		Deletion in prostate cancer
JARID1A	RBP2, KDM5A	H3K4me2, H3K4me3		Silencing/downregulation or deletion in melanoma, translocation in acute leukaemia and mutation in ankylosing spondylitis
JARID2				Mutation associated with non-syndromic cleft lip, spina bifida and congenital heart defects

MINA				
NO66		H3K4me2, H3K4me3, H3K36me2, H3K36me3		Overexpression in non-small cell lung cancer

1.3.2 Regulation of histone demethylase activity

Several mechanisms that control histone demethylase activity include modulation of gene expression, settlement into the target *via* certain domains or as a component of protein complexes and modifications at the post-translational level [17, 20]. For the recruitment of the enzyme to the histones, high numbers of weak associations in the chromatin surroundings are utilized [18]. It turned out that in their recruitment sites, in place of switching on/off activity, they are involved in fine-tuning of the transcriptional regulation [17].

1.3.3 Biochemical mechanism of histone lysine demethylation

LSD1 carries out demethylation through flavin adenine dinucleotide (FAD)-dependent amine oxidation. In this mechanism, imine intermediate is formed due to oxidation of target methyl group on lysine by FAD, which is followed by hydrolysis of the intermediate product and release of demethylated lysine and formaldehyde. Because of chemical restrictions, LSD1 could only conduct its function on lysines with mono or dimethylation, whereas JmjC domain-containing histone lysine demethylases (JHDMs) catalyze the reaction at all three levels of histone methylation. In JHDM mechanism, target methyl group is converted into a hydroxymethyl group, with the involvement of α-ketoglutarate (α-KG) and Fe^{2+} as cofactors; then release of the hydroxymethyl group in formaldehyde form occurs, generating unmethylated lysine residue [18].

1.3.4 HDMs in relation to cancer

Several lines of study point to the fact that genetic changes and protein deregulations in histone demethylases are commonly encountered in cancer and these proteins are

considered as targetable candidates for drug research [19]. Suppressive effect of LSD1 on p53 and E-cadherin proposes that it might stimulate tumorigenesis [17, 21]. JMJD2 proteins, namely JMJD2A, JMJD2B and JMJD2C, have potentially oncogenic property, as evidenced by high expression of all in prostate cancer and contribution of JMJD2C to the cancer cell proliferation [19]. In breast cancer cells, JARID1B was shown to be upregulated [21]. In a hematopoetic mouse model, mutation in FBXL10 was detected, suggesting its possible tumor suppression activity. Upon triggering of senescence depending on RAS oncogene induction in primary human epithelial cells, JMJD3, JMJD6 and KIAA1718 were shown to be overexpressed, addressing a possible involvement of these factors in inducing senescence [19].

1.4 Role of JMJD5 in H3K36 demethylation and protein hydroxylation

1.4.1 Role of JMJD5 in histone demethylation

1.4.1.1 Biological importance of H3K36 methylation

Histone methyltransferases known as SET2/KMT3 family carry out H3K36 methylation, which is generally found in body region of transcriptionally active genes. Consistently, this mark has been proposed to function in elongation of transcripts and inhibition of transcriptional start in this region [22]. Being related to actively transcribed chromatin in majority of the cases, methylation at H3K36 is also known to play roles in silencing of extra X chromosome, replication of DNA, DNA damage response, alternative splicing and methylations of DNA [23].

1.4.1.2 JMJD5 in the literature

JMJD5 was first demonstrated to play a role in connection between histone modulation and circadian clock regulation, having an evolutionary conservation from plants to humans [24]. In *Arabidopsis,* JMJD5 accumulation in both cytoplasm and

nucleus was detected, suggesting differential roles in both regions [25]. JMJD5, depending on its localization, might be carrying out protein hydroxylation in soluble part of nucleus and histone demethylation in chromatin [26]. According to the preliminary analyses, presence of an LXXL motif on N-terminus of JMJD5, required for interaction with nuclear receptors; and association with SUV39H1 and SETDB1 histone methyltransferases were predicted, implying complicated regulatory mechanisms [27]. Biochemical and functional analyses on JMJD5 revealed that it could most probably act as a protein hydroxylase rather than histone demethylase [28]. Hydroxylating NFATc1 and leading to its degradation, JMJD5 suppresses differentiation of precursor osteoclasts [26].

Through removing methyl marks on H3K36me2, JMJD5 induced cyclin A1 expression, functioning as a key factor in cell cycle progression of breast cancer cells [27]. JMJD5 deletion in mouse embryos resulted in an embryonic lethal phenotype due to the overexpression of *Cdkn1a* gene, which encodes $p21^{cip1}$ cyclin-dependent kinase inhibitor, through demethylation of H3K36 [29]. As a potential oncogene, JMJD5 was also proposed to inhibit p53-$p21^{cip1}$ pathway and p53-mediated cell cycle arrests in mouse embryos [30]. In contrast, histone demethylase-free action and decreased JMJD5 expression in lung cancer was detected, suggesting a possible function in tumor inhibition [31]. Furthermore, in an insertional mutagenesis study using mice lacking Blm, JMJD5 was identified as a candidate tumor suppressor [32].

1.4.2 Role of JMJD5 in protein hydroxylation

Metazoans, ranging between worms and humans, have a set of adaptive mechanisms against low oxygen conditions primarily controlled by hypoxia-inducible factor-α (HIF-α in short) [33]. The putative oncogenic roles of many HIF-target genes and elevated expression of HIF-α on several solid tumors suggest its potential tumor-inducing role [34]. Its accumulation, interaction with other partners and degradation are regulated by HIF-prolyl hydroxylases (HPHs), which constitute a subfamily among dioxygenases. These enzymes were also described in HIF-independent hydroxylation activities on several other substrates [33]. Exemplifying the first discovered protein hydroxylation event in the cell, HIF-α hydroxylation is performed

by EGLN hydroxylases on proline residue at high levels of oxygen and by factor-inhibiting HIF-α (FIH) on asparagine residue at intermediate levels of oxygen [35].

1.4.2.1 Hydroxylation activities of JMJD5 and its related proteins

Biochemical analysis on JMJD5 structure suggests a possible protein hydroxylase function rather than histone demethylation [28]. Recently, it was also documented that JMJD5 hydroxylates NFATc1 (nuclear factor of activated T-cells calcineurin-dependent 1), a critical transcription factor in osteoclastogenesis, and helps its proteasomal degradation [26]. Consistently, JmjC domain-containing enzymes involved in protein and nucleic acid hydroxylation, such as FIH-1, JMJD6, TWY5 and HSPBAP1 seem to be more homologous to JMJD5 depending on structural and sequential comparisons [28]. FIH-1 is responsible for the hydroxylation of HIF-α at Asparagine 803 under medium level of oxygen, resulting in HIF-α inhibition [19]. JMJD6 was detected to act as a lysyl hydroxylase on an RNA splicing protein U2AF65 (U2 small nuclear ribonucleoprotein auxiliary factor 65-kDa subunit), and its previously documented histone arginine demethylation role was disproved [36]. TYW5 (tRNA yW-synthesizing enzyme 5) was reported to catalyze hydroxylation of wybutosine (yW), a nucleoside located in $tRNA^{Phe}$ whose modification is required for proper translation of phenyl alanine, to its derivative [37]. HSPBAP1 (heat-shock protein 27 (Hsp27) -associated protein 1) was put forward as a potential protein hydroxylase of Hsp27 to block its activity [19].

CHAPTER 2

OBJECTIVES AND RATIONALE

Due to the absence of early biomarkers, liver injury-related restrictions on drug use and resistance against cytotoxic agents used for cancer therapy; HCC is lethal. As the genetic, molecular and aetiological mechanisms are better understood, the severe problems that liver cancer therapy is confronted could be dealt with [1]. Epigenetics, in this perspective, could provide progression in discovery of early diagnostic biomarkers, risk consideration and tracing of the disease [13]. In particular, several lines of study point to histone demethylases as targetable candidates for drug research [19]. JMJD5, a member of JmjC domain-containing histone lysine demethylase family, has recently been suggested to have a putative tumor suppressor role [31, 32]. Our past and current group members have also demonstrated its downregulation from the early onset of liver disease to hepatocellular carcinoma (see Figures 4.2 and 4.3 in "Results" section), suggesting a key role for this gene in normal functioning of liver and hepatocarcinogenesis. These results led to come up with the hypothesis that JMJD5 might have a tumor suppressor function in liver, its deficiency possibly contributing to the development of liver disease and carcinoma. In this study, we aimed at analysis of biological roles of JMJD5, with a particular focus on its tumor suppressor activity, applying genetic, molecular biological, phenotypic and morphological assays using hepatocellular carcinoma-derived SNU449 cell line. The outcomes of this study are expected to make important contributions to the liver cancer research in regards of candidate drug targets and biomarker identification.

CHAPTER 3

MATERIALS AND METHODS

3.1 MATERIALS

3.1.1 General Laboratory Reagents

The chemicals majorly used in this research were purchased from Sigma-Aldrich (St. Louis, MO, USA) and Merck (Darmstadt, Germany). The commonly used reagents, including ethanol, methanol, haematoxylene and Bradford reagents, were from Sigma-Aldrich (St. Louis, MO, USA). Ponceau S and DMSO were purchased from Applied Biochemia (Darmstadt, Germany). Nucleospin RNA II total RNA isolation kit and plasmid mini-prep kit was from Macherey-Nagel (Duren, Germany). Plasmid midi-prep kit was bought from Promega (Madison, WI, USA). Fluorescent mounting medium was from Dako. ECL Prime detection kit used for western blot was from Amersham Pharmacia Biotech Company (Buckinghamshire, UK). Agarose used in gel electrophoresis was purchased from Conda (Madrid, Spain). Agar, yeast extract and tryptone were puchased from Gibco (Carlsbad, CA, USA).

3.1.2 Cell culture materials and reagents

All the plastic equipments, including petri dishes, plates, flasks and cryovials, were bought from Corning Life Sciences Incorporated, (Corning, NY, USA). Dulbecco's modified Eagle's medium (DMEM) and Roswell Park Memorial Institute (RPMI) 1640 media were purchased from GIBCO (Life Technologies, Carlsbad, CA, USA). Powder DMEM High Glucose was from USBiological (Swampscott, Massachusetts, USA). Non-essential amino acids, trypsin-EDTA, penicillin/streptomycin, L-glutamine, fetal bovine serum (FBS), Optimem reduced serum medium, puromycin

and blasticidin were all from GIBCO. Serological pipettes and sealed-cap polycarbonate centrifuge tubes were from Costar Corporation (Cambridge, UK). Lipofectamine 2000 was purchased from Invitrogen.

3.1.3 Bacterial Strains

E. coli DH5α strain was used in this study.

3.1.4 Nucleic acids

DNA molecular weight markers and 6X loading dye were purchased from MBI Fermentas GmbH (Germany). pLTRE-FLAG-KDM8, pLTRE-FLAG-KDM8H321A and pLTRE-FLAG-empty plasmids were constructed and donated by Yoshihiro Izumiya from Sacramento, CA, USA.

3.1.5 Electrophoresis, photography and spectrophotometry

Agarose gel electrophoresis apparatus was from Thermo Electron Corporation. Gel imaging software, power supplies Power – PAC200 and Power – PAC300 were from Bio Rad Laboratories (CA, USA). Beckman Du640 UV-visible spectrophotometer from Beckman Instruments Incorporation (CA, USA) was used for Bradford assay to quantify proteins. Nucleic acid concentrations were determined by using NanoDrop from Thermo Scientific (Wilmington, USA).

3.1.6 Antibodies

Antibodies used in different assays are indicated in the following table together with their catalog numbers, and working dilutions.

Table 3.1: The list of the antibodies with their catalog numbers and working dilutions

(WB: western blotting, IP: immunoperoxidase staining, FC: flow cytometry, IF: immunofluorescence)

Antibody	Company and catalog number	Dilution
Calnexin (rabbit, polyclonal)	Sigma, C4731	1:5000 (WB)
Anti-mouse-HRP	Sigma, A0168	1:5000 (WB)
Anti-rabbit-HRP	Sigma, 6154	1:5000 (WB)
Anti-rabbit/Mouse HRP link	Dako, K8000	Working solution was used without dilution.
Flag M2 (mouse, monoclonal)	Sigma, F1804	1:1000 (WB), 1:200 (IP), 1:200 (FC), 1:200 (IF)
IgG1-FITC isotype control (mouse, monoclonal)	Immunotools, 21275513	1:25 (FC)
Anti-mouse-FITC	Dako, F0479	1:250 (FC)
JMJD5 (rabbit polyclonal)	Abcam, ab83011	1:1000 (WB)
BrdU (mouse, monoclonal)	Dako, M0744	1:500 (IF)
Flag (rabbit, polyclonal)	Sigma, F7425	1:500 (IF)
Anti-mouse Alexa Fluor 488	Invitrogen, A11029	1:500 (IF)

Anti-rabbit Alexa Fluor 568	Invitrogen, A11011	1:500 (IF)

3.2 SOLUTIONS AND MEDIA

3.2.1 General solutions

50X Tris Acetate EDTA (TAE)	242 g Tris base, 57.1 ml glacial acetic acid and 18.6 g EDTA were dissolved in 1 liter ddH_2O. 1X working dilution is used.
10X Phosphate Buffered Saline (PBS)	80 g NaCl, 2 g KCl, 14.4 g Na_2HPO_4, 2.4 g KH_2PO_4 in 1 liter ddH_2O 1X working dilution is used. Before use in cell culture, it is autoclaved.
Ethidium bromide	10 mg/ml stock is prepared by dissolving in ddH_2O. Working concentration is 30 µg/ml.

3.2.2 Bacteria solutions

Luria-Broth (LB) medium	10 g bacto-tryptone, 5 g bacto-yeast extract and 10 g NaCl were dissolved in 1 liter of water. For LB agar plates, 15 g/L bacto agar was added and autoclave-sterilized.
Ampicillin	100 mg/ml stock solution was dissolved in ddH_2O.

	100 µg/ml working concentration was used.

3.2.3 Immunofluorescence staining solutions

Acetone: methanol fixation reagent	Acetone and methanol were mixed in 1 to 1 ratio.
Blocking solution	10% FBS, 0.3% Triton X-100 in 1X PBS
Antibody dilution solution	1 % BSA, 0.3% Triton X-100 in 1X PBS
DAPI (4',6-diamino-2-phenylindole)	0.1-1 µg/ml working concentration in ddH_2O.

3.2.4 Immunoperoxidase staining solutions

Acetone: methanol fixation reagent	Acetone and methanol were mixed in 1 to 1 ratio.
3% H_2O_2 solution	It was prepared mixing 30% H_2O_2 with methanol and ddH_2O. (For example, 3 ml H_2O_2, 10 ml methanol and 17 ml ddH_2O)
Blocking solution	10% FBS, 0.3% Triton X-100 in 1X PBS
DAB solution	DAB chromogen and its substrate from Dako were used according to the manufacturer's protocol.
DAPI (4',6-diamino-2-phenylindole)	0.1-1 µg/ml working concentration in

	ddH_2O.

3.2.5 BrdU incorporation assay solutions

BrdU	Stock solution concentration is 10 mg/ml in ddH2O. 30 μM working concentration is used.
2N HCl	8.62 ml of 37% HCl is added to 16.36 ml ddH_2O.

3.2.6 Sodium Deodecyl Sulphate (SDS) – Polyacrylamide Gel Electrophoresis (PAGE) and immunoblotting solutions

In this study, tris-glycine gels and buffers were prepared manually according to a conventional protocol in our lab. To prepare 5% stacking gel, ddH_2O, 30% acrylamide mix, 1.0 M Tris-HCl pH 6.8, 10% SDS, 10% ammonium persulphate and TEMED were mixed successively, in certain volumes. For the resolving gel, depending on concentration of the gel, same solutions were mixed in certain volumes, this time using 1.5 M Tris-HCl pH 8.8 instead of 1.0 M Tris-HCl pH 6.8. Wet transfer was applied on PVDF membrane. 5X sample loading buffer, and denaturing agent (β-mercaptoethanol) were purchased from Invitrogen.

NP-40 lysis buffer	50 mM Tris HCl, 150 mM NaCl, 1% NP-40, 0.1% SDS, 1X protease inhibitor cocktail
10X SDS Running buffer	144 g glycine and 30 g Tris were dissolved in dH_2O, 50 ml 10% SDS was added, and the volume was completed to 1 L. Working solution is 1X.
10X Transfer buffer	72 g glycine and 58 g Tris were dissolved in dH_2O, 2 ml 10% SDS was

	added, and the volume was completed to 1 L. Working solution is 1X containing 20% EtOH.
10X Tris buffered saline (TBS)	12.19 g trisma base and 87.76 g NaCl were dissolved in 1 L of ddH2O, and pH is adjusted to 8. Working concentration is 1X.
TBS-tween 20 (TBS-T)	0.2% Tween 20 was dissolved in 1X TBS.
Blocking solution	5% (w/v) non-fat dry milk was dissolved in 0.2% TBS-T.
Ponceau S	0.1% (w/v) Ponceau S and 5% (v/v) acetic acid were dissolved in 0.2 % TBS-T.

3.2.7 SRB assay solutions

10 % TCA fixation solution	10 % TCA is dissolved in water.
0.4 % SRB staining buffer	0.4 % SRB dye powder is dissolved in 1 % acetic acid.
Tris base, unbuffered	10 mM, pH 10.5

3.2.8 Wound healing assay solutions

Crystal Violet solution	1 % crystal violet solution is prepared in 2 % ethanol.

3.2.9 Flow cytometry analysis solution

Propidium iodide buffer	50 µg/ml propidium iodide, 0.1 mg/ml RNase A and 0.5% TritonX-100 in PBS

3.3 METHODS

3.3.1 Commonly used methods

3.3.1.1 Agarose gel electrophoresis

Restriction enzyme digestion products and plasmid DNAs generally were run, separated and checked with this technique. Agarose gels were prepared in desired weight/volume concentrations by dissolving agarose in 1X TAE buffer using microwave heat. When the solution was cool enough, ethidium bromide, reaching to 30 µg/ml concentration, was added. 1X TAE buffer was also used for the gel run. Mixed with 6X loading dye, samples were loaded into the wells and run at 120 V, for the various time durations with respect to the size of the products. Visualization of DNA fragments was carried out by gel imaging device under UV light, and product sizes were compared with those of DNA ladder.

3.3.1.2 Computer and Software Tools

NCBI website at http://www.ncbi.nlm.nih.gov/ and Ensembl Genome Browser website at http://www.ensembl.org/index.html/ were utilized to learn all sequences, transcripts variants exon-intron information about the genes. PROSITE internet tool at http://prosite.expasy.org/ developed by Swiss Institute of Bioinformatics (Lausanne) was used for conserved domain search. A plasmid Editor (ApE) programme created by M. Wayne Davis was used for plasmid map construction, restriction digestion design and cloning.

3.3.2 Constructing the plasmids

The plasmids donated by Yoshihiro Izumiya were constructed by this group in a set of cloning processes. 3X Flag tag and RsrII site was inserted into the multiple cloning site of pcDNA5/FRT/TO vector (Invitrogen) under CMV promoter containing Tet operator sequences. JMJD5 variant 2 open reading frame (ORF) was inserted into RsrII site. The construct between XhoI sites which contains Tet-CMV promoter, 3X Flag tag, JMJD5 ORF and BGH polyadenylation signal was cut out from pcDNA5/FRT/TO vector and inserted into pLKO.1 no-stuffer vector (Addgene) between XhoI sites. Newly generated plasmids were named as pLTRE-FLAG-KDM8, pLTRE-FLAG-KDM8H321A and pLTRE-FLAG-empty.

3.3.3 Cell culture methods

3.3.3.1 Cell lines and growth conditions of cells

HepG2-Trex, SNU449-Trex stable cell lines and SNU449-Trex-derived stable clones, namely EGEM-W1, EGEM-W2, EGEM-W3, EGEM-W4, EGEM-M1, EGEM-M2, EGEM-M3, EGEM-E1, EGEM-M2-C2, EGEM-M2-C4, EGEM-W4-C2, EGEM-W4-C3, were cultured in complete DMEM or RPMI medium.

Complete DMEM and RPMI media contained 10 % FBS, 1 % penicillin/streptomycin and 1 % non-essential amino acids. The incubation of cells was conducted in humidified incubators with 37 C° temperature and 5 % CO_2 level. Cells were passaged in 2-3 day frequency when the confluency was reached.

3.3.3.2 Thawing the cells

Taken from either nitrogen tank or -80 C° freezer, the desired cell lines were incubated on ice for a few minutes and thawed at 37 C° in water bath in a few minutes. The thawed cell suspension was transferred to a 15 ml falcon tubes and mixed with several milliliters of fresh medium, immediately. Cells were spinned down at 1500 rpm for 3 min. DMSO was removed together with the supernatant

using aspirator. The pellet was resuspended in several milliliters of complete medium and transferred to either a 25 cm^2 flask or 100 mm dish according to the size of the pellet. Rocked gently back and forth to evenly distribute the cells, flask or dish was incubated in the incubator at 37 C° in 5% CO_2 overnight. Next day, dead cells were removed and washed with 1X PBS, and the medium was replenished.

3.3.3.3 Passaging the cells

Before passaging the cells, the old growth medium was removed by aspiration, and the cells were washed with 1X PBS. After the removal of PBS, trypsin-EDTA was added onto the cells in dishes or plates. The added volume of the trypsin-EDTA was dependent on the surface area of the dish or plate. For example, 500 µl volume was added to the 100 mm dishes. The cells were left to incubate in incubators for a few minutes until all the cells were detached from the surface. The detached cells were mixed thoroughly by adding fresh medium and pipetting up and down with serological pipettes. Then, the cells were divided into suitable dishes or flasks with desired dilutions. The growth media, trypsin-EDTA and 1X PBS were stored at 4 C°. FBS was heat-inactivated at 55 C° for 30 min, filter-sterilized, aliquoted and stored at -20 C°. Before use, all media and solutions were warmed up in water bath at 37 C°.

3.3.3.4 Cryopreservation of the cells

After reaching 60-70% confluency, cells were washed with PBS, detached by trypsin-EDTA and collected with medium into 15-ml falcon. Cell suspension was centrifuged at 1500 rpm for 3 min, and the supernatant was aspired. The cell pellet was then resuspended in freezing medium containing 10 % DMSO in complete medium. Cells were transferred to the cryotubes, and first stored at -20 C° for 1 hour and later at -80 C° overnight. Nitrogen tanks were used for long term storage.

3.3.3.5 Transient transfection of cells using Lipofectamine 2000

After washing with 1X PBS and trypsinizing, cells were counted on hemocytometer, and 6 x 10^5 cells/well were cultured on 6-well plates in antibiotic-free medium. Cell confluency on the plates should be 90-95% after 24h. Preceding transfection, the media were aspirated, cells were washed with 1X PBS and 1.5 ml OptiMem I Reduced Serum Medium was given into each well. 250 µl/well diluted DNA mix was prepared by mixing 4 µg of plasmid of interest per well with OptiMem I Reduced Serum Medium. 250 µl/well diluted lipofectamine 2000 mix was prepared by mixing 10 µl of lipofectamine 2000 transfection reagent per well with OptiMem I Reduced Serum Medium. After gently mixed, the mixtures were incubated for 5 minutes at room temperature. Diluted DNA and diluted lipofectamine mixtures were combined and incubated for 20 minutes at room temperature. 500 µl of complexes was divided into each well, completing the volume to 2 ml. The cells were incubated in transfection media at 37 C° in 5% CO_2 for 4-6 hours. Then, transfection media were removed, 2 µg/ml doxycycline (Sigma)-containing complete RPMI 1640 medium was given to the Dox (+) cells, whereas only complete RPMI was given to Dox (-) cells. The cells were incubated at 37 C° in 5% CO_2 for 24, 48 and 72 hours.

3.3.3.6 Stable transfection of cells with lentiviral vectors

3.3.3.6.1 Production of viral particles

HEK293T cells were seeded in such a way as to reach 30-40 % confluency in the following day, and incubated at 37 C° overnight.

Transfection mixes (The required amounts per well for 6-well plate transfection are shown.)

Express-In™ (Open Biosystem)		Calcium phosphate (CaP)	
Mix A		Mix A	
TransLenti Viral ORF Packaging mix (OpenBiosystem)	2 µl	TransLenti Viral ORF Packaging mix (Open Biosystem)	2 µl
Lentiviral vector	0,5-1µg	Lentiviral vector	0,5-1µg
Optimem	500 µl	$CaCl^2$ (1M)	120 µl

		ddH^2O	360 µl
Mix B		Mix B	
Express-In™ (Open Biosystem)	20 µl	2xHBS	500 µl
Optimem	480 µl		

(In addition to the lentiviral transfection vectors, pLEX JRed TurboGFP vector mix was prepared (Evrogen) to check working of transfection in every step of the process.)

A and B mixes were prepared separately and left to wait for 5 minutes. Then two mixes were combined and left to wait for 20 minutes at room temperature. Completing the volume to 2 ml with complete growth medium, the whole mixtures were added to HEK293T cells, and plates were incubated at 37 C° overnight. Next day, transfection medium was changed with fresh complete medium.

3.3.3.6.2 Infection

The day after the transfection of HEK293T cells, SNU449-TRex cells targeted for transfection were seeded on 6-well plates to reach 30-40 % confluency and incubated overnight at 37 C°. 48 hours after than HEK293T cell transfection, 2 ml media of these cultures which contain viral particles were taken, 8 µg/ml polybrene was added, and the media were passed through 42 µm filter. Media of HEK293T cells were replenished. The media of target SNU449-TRex cells were removed, and the filtered media containing viral particles and polybrene were added to them. Target cells were incubated at 37 C° overnight. By collecting the media from HEK293T cells every other day, target cells were infected three times in total for efficient transfection.

3.3.3.6.3 Selection

24 hours after third infection, target SNU449-TRex cells were selected under 9 µg/ml puromycin concentration, dose being dependent on kill curve of this cell line. After 1-week selection, all the control cells were dead, while colonies appeared on infected cells.

3.3.4 Total protein extraction from cultured cells

Cells were trypsinized and collected in the pellet. For lysis, cells were mixed up with the adequate amount of RIPA buffer by pipetting and vortexing every 5 minutes up to 15 minutes. To fragment DNA and increase lysing efficiency, sonication and 3-minute boiling processes were applied. Cell lysates were centrifuged at 4 C° at 13,000 rpm for 40 minutes. Supernatants were saved in clean eppendorf tubes, and stored at -80 C°.

3.3.5 Western blotting

For quantification of protein lysates, Bradford assay was applied. A standard curve was drawn with respect to absorbance values of serially diluted BSA proteins of known concentrations. The concentrations of sample proteins were calculated by putting the absorbance values of them as y values in the standard curve equation. Upon mixing with Bradford reagent, a blue- colored complex is formed, giving an absorbance maximum at 595 nm on the spectrophotometer. For sample preparation, 5X SDS loading dye and 5% b-mercaptoethanol in loading dye were added in appropriate amounts to 15-30 ug protein lysates, and the volume was completed by ddH_2O. Denaturation of samples was done at 100 C° for 10-12 minutes.

All the SDS-PAGE gels and buffers were manually prepared. 12% Tris-glycine gel was used for the better resolution of about 50 kD Flag-JMJD5 conjugate protein. 1X SDS running and 1X SDS transfer buffers were prepared according to the commonly used recipes in the lab. Transfer buffer contained 20 % ethanol, and PVDF membrane was used for the transfer.

Blocking of the obtained membranes was conducted overnight at 4 C° with 5 % BSA or milk in 0.3 % TBS-T, according to the suggested protocols for each specific antibody. Primary antibody incubation was done for 1 hour at room temperature with gentle shaking at certain antibody dilution ratios. Membranes were washed for 5, 15 and 5 minutes with 0.3 % TBS-T. Membrane was incubated with HRP-conjugated secondary antibodies for 1 hour at room temperature with gentle shaking at certain antibody dilution ratios. The membrane was additionally washed with TBS-T as in

the previous case. Then, for chemiluminescent detection, ECL prime western blot detection kit from Thermoscientific was applied according to the manufacturer's protocol. Development of the X-ray films with chemiluminescent emission was performed for certain time periods according to the specific antibody.

3.3.6 Immunofluorescence staining

SNU449-TRex cells were seeded on sterile coverslips in 12-well plates in 15,000 cells/well number in order to reach subconfluency on the day of immunoperoxidase staining after 3-day culturing. Doxycycline induction, as being 2 μg/ml, was done in the first day of experiment after cells were attached to the surface for 48 hours. Being washed with 1X PBS, the cells were both fixed and permeabilized with acetone-methanol (1:1) mixture at -20 C° for 10 minutes. Then cells were washed with 1X PBS three times for 5 minutes each. Blocking was applied with 10 % FBS, 0.3 % Triton X-100 in 1X PBS for 1 hour at 37 C°. Primary antibody was diluted in a buffer containing 1 % BSA, 0.3 % Triton X-100 in 1X PBS depending on the specific antibody and applied directly onto the coverslips drop by drop. The coverslips were incubated at 37 C° for 2 hours. Then cells were washed three times with 0.3 % 1X PBS-T for 5 minutes each and incubated with fluorescent dye-conjugated secondary antibody for 1 hour at room temperature in dark. Washing of the secondary antibody was performed similar to the primary antibody. DAPI counterstaining was performed by diluting 1/10,000 in ddH_2O and applying for 3 minutes at room temperature. The excessive counterstain was removed by ddH_2O washing, and mounting of coverslips onto the slides was done with DAKO mounting medium. Fluorescent microscope (ZEISS) was used to examine the samples.

3.3.7 Immunoperoxidase staining

SNU449-TRex cells were seeded on sterile coverslips in 6-well plates in 15,000 cells/well number in order to reach subconfluency on the day of immunoperoxidase staining after 3-day culturing. Doxycycline induction, as being 2 μg/ml, was done in the first day of experiment after cells were attached to the surface for 48 hours. Being

washed with 1X PBS, the cells were both fixed and permeabilized with acetone-methanol (1:1) mixture at -20 C° for 10 minutes. Then cells were washed with 1X PBS three times for 5 minutes each. To stop endogenous peroxidase activity, hydrogen peroxide was added to each well and incubated for 10 minutes at room temperature in dark. The cells were again washed with 1X PBS three times for 5 minutes each. Blocking was applied with 10 % FBS, 0.3 % Triton X-100 in 1X PBS for 1 hour at room temperature. Primary antibody was diluted in blocking solution depending on the specific antibody and applied directly onto the coverslips. The coverslips were incubated at 37 C° for 2 hours. Then cells were washed twice with 0.3 % 1X PBS-T for 2 minutes each and incubated with secondary antibody (DAKO, anti-mouse and anti-rabbit together) for 1 hour at room temperature in dark. Washing of the secondary antibody was performed similar to the primary antibody. DAKO-DAB Chromogen solution was prepared according to the manufacturer's protocol, added onto only one coverslip as drops, left to wait until reaction occurs and gives brown-colored product, and time was recorded. Then each well was treated with this substrate for determined amount of time. After reaction was stopped with ddH_2O, Haemotoxylin (Mayer's, Sigma) counterstaining was performed for 3-5 minutes. The excessive counterstain was removed by ddH_2O washing, and mounting of coverslips onto the slides was done with DAKO mounting medium. Light microscope (ZEISS) was used to examine the samples.

3.3.8 Bromodeoxyuridine (BrdU) and Flag double immunofluorescence staining

SNU449-TRex clones were seeded on 12-well plates in 30,000 cells/well density, and fresh medium containing both doxycycline and BrdU was given to all cells. After 4-hour incubation, all medium was removed. The medium with doxycycline but without BrdU was added, and cells were incubated in this medium for 48 hours. Following fixation in 70 % ice-cold ethanol at -20 C° for 10 minutes, cells were washed with 1X PBS three times for 5 minutes each. Blocking was applied with 10 % FBS, 0.3 % Triton X-100 in 1X PBS for 1 hour at 37 C°. Primary Flag polyclonal antibody (Rb) was diluted in a buffer containing 1 % BSA, 0.3 % Triton X-100 in 1X

PBS depending on its working dilution ratio and applied directly onto the coverslips drop by drop. The coverslips were incubated at 37 C° for 2 hours. Then cells were washed three times with 0.3 % 1X PBS-T for 5 minutes each. Alexa 568-conjugated anti-Rabbit secondary antibody was applied in its specific dilution ratio at room temperature for 1 hour, and three times washing with 0.3 % 1X PBS-T was done. Then fixation was repeated with 70 % ice-cold ethanol at -20 C° for 10 minutes in order to keep Flag primary and secondary antibodies attached to their targets. 2 N HCl treatment for 30 minutes at 37 C° was applied to denature double stranded DNA structure. Neutralization was carried out with borate buffer, and cells were washed with 1X PBS three times. BrdU primary antibody treatment was applied at 37 C° for 1 hour and followed by PBS-T washes three times. Alexa 488-conjugated anti-mouse secondary antibody incubation was performed at room temperature for 1 hour, and it was washed with PBS-T three times. DAPI counterstaining was performed by diluting 1/10,000 in ddH_2O and applying for 3 minutes at room temperature. The excessive counterstain was removed by ddH_2O washing, and mounting of coverslips onto the slides was done with DAKO mounting medium. Fluorescent microscope (ZEISS) was used to examine the samples.

3.3.9 Flow cytometry analysis of JMJD5 - expressing clones

Being treated with doxycycline as previously mentioned, cells were rinsed with 1X PBS, trypsinized and divided into 15 ml falcons. Then cells were centrifuged at 1500 rpm for 5 minutes. Pellets were resuspended in 70 % PBS-ice cold ethanol, and tubes were incubated at -20 C° for 15 minutes for fixation and permeabilization. Cells were centrifuged at 1800 rpm for 8 minutes, PBS-ethanol solution was removed, and pellets were washed with 1X PBS. Primary antibody solution was prepared in 0.1 % PBS-T, being 1:200 dilution for Sigma mouse M2 monoclonal anti-flag antibody. The pellets were resuspended in 100 µl of primary antibody solution and incubated at room temperature for 1 hour with a few-time vortexing. Mouse IgG1-FITC isotype control was applied as being 4 µl in 100 µl of 0.1 % PBS-T and incubated in the same manner. After 1X PBS-T wash, Sigma FITC-conjugated anti-mouse secondary antibody, being properly diluted in 0.1 % PBS-T, was applied to the cells for 30

minutes in the dark with gentle agitation. After 1X PBS-T wash, for DNA staining, cells were incubated at 37 C° for 30 minutes in 500 µl propidium iodide buffer containing 50 µg/ml Sigma propidium iodide, 0.1 mg/ml Thermoscientific RNase A and 0.5 % Triton X-100. After cells were washed twice with 1X PBS and resuspended in appropriate amount of PBS, cell cycle analysis was performed using BD Accuri C6 Flow Cytometer (BD Biosciences, San Jose, CA) and BD Accuri C6 CFlow Sampler software.

3.3.10 RNA sample preparation and hybridization to chip

Total RNA isolation from triplicate samples of empty and wild type JMJD5 clones was performed with Nucleospin RNA kit (MN, Düren, Germany) according to the manufacturer's protocol. RNA quality was checked using Agilent Bioanalyzer 2100 kit and software (Agilent Technologies, Santa Clara, CA, USA) according to the manufacturer's protocol. RNA isolates were hybridized to Affymetrix HG_U133_Plus2 chips, applying Affymetrix 3' IVT hybridization protocol in Bilkent University Bilgen Affymetrix Center for microarray analysis.

3.3.11 Bioinformatics data analyses of JMJD5 microarray samples

Heatmap of JMJD5 probe set (Figure 4.2) was generated using the publically available microarray dataset (GSE6765) [38] downloaded from the gene expression omnibus website. The dataset was normalized using the RMA normalization method. Heatmap was generated using Cluster 3.0 software [39] and Java TreeView software [40].

Microarray raw files of three replicates of empty vector over-expression samples (EGEM_e1a, EGEM_e1b, and EGEM_e1c) and three replicates of wild type (wt) JMJD5 over-expression samples (EGEM_w4a, EGEM_w4b, and EGEM_w4c) were normalized with the RMA method using the BRB_Array_Tools Version 4.2.0 developed by Dr. Richard Simon and BRB-ArrayTools Development Team. Class comparison tool of the BRB_Array_Tools program was used to determine the list of

significantly (>1.5 fold and $p<0.05$) differentially expressed genes between empty vector and wt JMJD5 samples.

In order to determine differing biological mechanisms as a result of over-expression of JMJD5 in SNU449 cells, gene set enrichment analysis (GSEA) experiments were performed using normalized microarray data together with C5_ALL gene ontology gene sets or C6_ALL oncogenic signatures curated gene lists of molecular signature databases (MSigDB).

3.3.12 Sulphordamine B (SRB) assay for cell proliferation

EGEM-w2, EGEM-w4, EGEM-m2, EGEM-m3 and EGEM-e1 clones were seeded on 96-well plates in 2000 cells/well density in triplicates for both Dox (+) and Dox (-) conditions. All the outer wells were filled with 200 µl PBS. Next day, fresh medium containing doxycycline was added to Dox (+) wells, completing the volume in each well to 300 µl and letting the final doxycycline concentration be 2 µg/ml. Cells were cultured for 6 days, replenishing doxycycline from top of the wells every 2 days. Upon reaching the over-confluency, cells were taken out for SRB fixation and staining protocol. The media were discarded very gently, and wells were washed slowly with 200 µl 1X PBS. Fixation was done with 10 % TCA for 1 hour at +4 C° for 1 hour in dark. Cells were washed 4-5 times with dH_2O, and plates were allowed to dry overnight on the bench. 0.4 % SRB solution was prepared by dissolving SRB powder in 1 % acetic acid and applied to the wells as 50 µl/well at room temperature for 20 minutes in dark. After discarding the dye, the plates were washed five times with 1 % acetic acid on plate washer device (BioTek). The plates were left to dry in fume hood for 1 hour, and then they were scanned. 10 mM pH 10.5 cold Tris base from + 4 C° was added into each well, and dye was dissolved by shaking 10 seconds on plate shaker. OD values were then read on Elisa reader (BioTek) at 515 nm primary wavelength, using KC Calbiochem program.

3.3.13 SRB assay for Adriamycin resistance

SNU449 TRex, EGEM w4-C2, EGEM w4-C3, EGEM m2-C2, EGEM m2-C4 and EGEM-e1 clones were seeded on 96-well plates in 5000 cells/well density in triplicates. All the outer wells were filled with 200 µl PBS. Next day, medium containing 2X adriamycin and doxycycline was added to all wells, completing the volume in each well to 200 µl and letting the final doxycycline concentration be 2 µg/ml. Adriamycin concentration range was arranged between 10 µg/ml and 0. The cells were incubated for 72 hours, and SRB staining protocol was performed as explained above.

3.3.14 Wound healing assay

Cells were seeded on 6-well plates as 4 x 10^5 cells/well in complete RPMI medium. Next day, wounding was done with FT200 pipette. Cells were washed with 1X PBS twice. Complete RPMI medium containing 2 µg/ml doxycycline was given to the cells. Cells were incubated at 37 °C, 5 % CO2 for 48 hours. Photos were taken at 0, 24 and 48 hours using the inverted light microscope. 48 hour- cultured cells were then fixed with acetone-methanol (1:1) at -20 °C for 10 minutes and washed with 1X PBS three times. Staining with 1 % cystal violet in 2 % ethanol was performed for 30 minutes at room temperature in dark. Following washing with ddH_2O several times, the photos of the stained cells were taken again.

3.3.15 Soft agar colony formation assay

3.3.15.1 Preparation of base agar

All the glassware, materials and water were sterile. 1 % agar solution was prepared by dissolving in water heating with microwave and cooled to 40 °C in a water bath. 2X DMEM medium, prepared from its powder form adding the missing components according to its datasheet, with 20 % FBS, 2 % penicillin-streptomycin and 2 % non-essential amino acids was left to wait with 1 % agar solution in the water bath for about 30 minutes to equilibrate them. Two solutions were mixed in equal volumes in

order to obtain 0.5 % agar in 1X DMEM, 10 % FBS, 1 % penicillin-streptomycin and 1 % non-essential amino acids. 1 ml of the mixture was put into each well of 6-well plates and allowed to wait for 5 minutes for solidification of agar.

3.3.15.2 Preparation of top agar

0.7 % agar solution was prepared in water and left to equilibrate with 2X DMEM containing 20 % FBS, 2 % penicillin-streptomycin and 2 % non-essential amino acids in water bath, as described above. Adherent cells were trypsinized and counted. They were divided into 15-ml falcon tubes in such a way as to obtain 10,000 cells in 100 µl volume of medium per each falcon tube. 6-well plates were labeled properly. 2 ml of 2X DMEM containing 20 % FBS, 2 % penicillin-streptomycin and 2 % non-essential amino acids; and 2 ml of 0.7 % agar were added to a tube of cells, mixed and divided as 1 ml/well into 6-well plates. Only one tube at a time was performed not to allow agar to solidify early. Plates were incubated at 37 C° in a humidified incubator for 3-4 weeks. Agar media were feeded with 1 ml complete culture medium containing 2 µg/ml doxycycline. The colonies were counted, and their photos were taken under inverted light microscope.

CHAPTER 4

RESULTS

4.1 JMJD5

4.1.1 Knowledge about JMJD5 on NCBI

Jumonji domain containing 5 (JMJD5), also known as KDM8, is a protein coding gene located in chromosome 16 at 16p12.1 locus in the neighborhood of *NSMCE1*, *FLJ21408* and *EEF1A1P38*, genes. Existing bioinformatics information about JMJD5 obtained from NCBI and PROSITE web tools are illustrated in Figure 4.1.

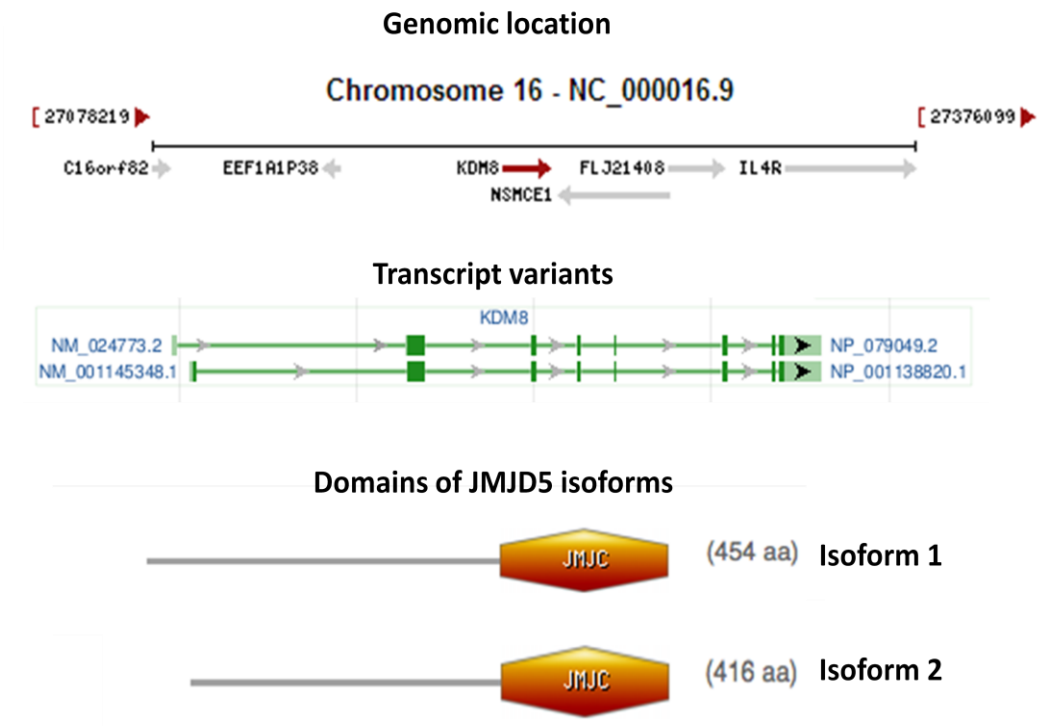

Figure 4.1: Genomic location, transcript variants and conserved domains of JMJD5 isoforms

Two transcript variants are present in humans for this gene. The lengths of variant 1 and 2 are 2531 bp and 2481 bp, encoding 454-amino acid and 416-amino acid long isoform 1 and 2, respectively. The molecular weights of isoform 1 and 2 are 51 kD and 47 kD, respectively. Splice variant 1 has 8 exons, all of which encode the isoform 1. Splice variant 2 has also 8 exons, 7 of which encode isoform 2, translation being started from an alternative exon at downstream. Conserved domain search indicates that both isoforms have catalytic JmjC domain at C-terminus.

4.2 Expression Levels of JMJD5 in Healthy-Diseased Liver and HCC Cell Lines

4.2.1 In Vivo JMJD5 Expression

Alteration of JMJD5 mRNA and protein levels between different stages of liver disease was determined by our lab members in previous studies. Microarray analysis of liver samples corresponding to 8 different states of liver disease for JMJD5 expression is demonstrated in Figure 4.2.

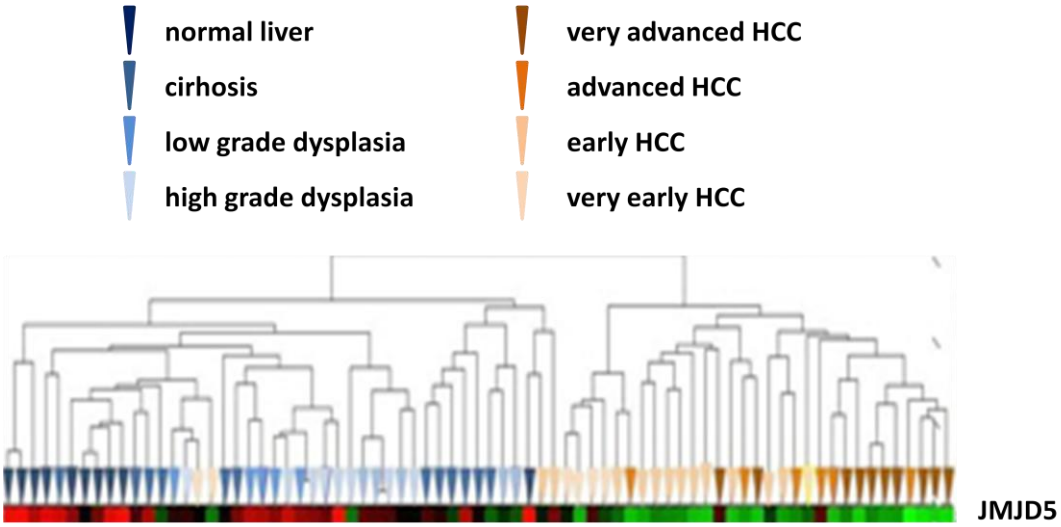

Figure 4.2: Microarray data of different liver conditions for JMJD5 levels

(Red indicates upregulation, and green indicates downregulation of the gene.)

According to the figure, there is a drastic decrease in JMJD5 expression from normal liver toward very advanced HCC, the intermediate stages also exhibiting the gradual

change with the color designation. From normal liver to dysplasia, the color turns from red to black in most cases; and from dysplasia to very advanced HCC, black color turns into light green, showing how sharply this change occurs between the stages as HCC progresses.

This tendency was also checked in protein levels with western blotting using samples from Dokuz Eylül University, İzmir (collaboration with Dr. Esra Erdal). Cirrhotic and HCC liver tissue samples from same individual patient were taken, making up 15 patients and 30 tissue samples in total. All samples were analyzed with JMJD5 polyclonal antibody in Figure 4.3 (Eylül Harputlugil and Mehmet Öztürk, personal communication).

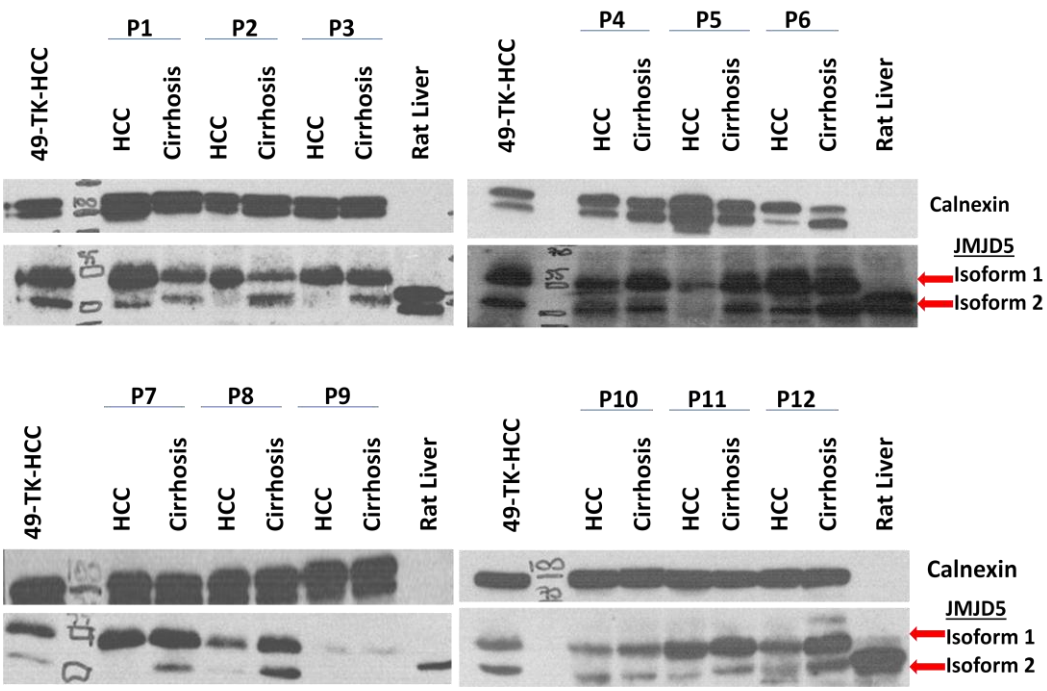

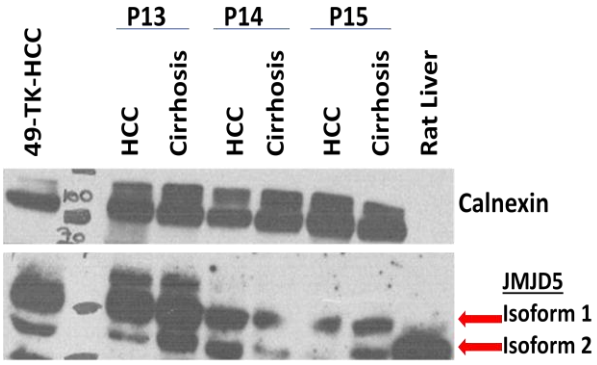

Figure 4.3: Screening for JMJD5 expression in HCC and cirrhosis sample pairs of 15 patients using western blotting technique

(P: patient; Calnexin for equal loading; rat liver and 49-TK-HCC are for positive control. Rat liver indicates 47 kD rat JMJD5 isoform 2; whereas 49-TK-HCC indicates both 51 and 47 kD human JMJD5 isoforms.)

In all of the samples 51-kD isoform 1 is visible. 47-kD isoform 2 is also seen in most of the samples with a few exceptions. Levels of both isoforms exhibited oscillations between HCC and cirrhotic samples of the same patient. JMJD5 isoform 1 levels decreased in HCC samples of 7 patients compared to their cirrhotic samples, remaining at comparable levels in 5 patients and showing an increase in 3 of them. JMJD5 isoform 2 levels, on the other hand, decreased in HCC samples of 10 patients compared to their cirrhotic samples, remaining at comparable levels in 3 patients and showing an increase in 2 of them. In majority of the cases, both isoforms were downregulated from cirrhosis to HCC. This result seems to be consistent with the previous microarray data in that the fall in JMJD5 expression might be critical in progression of cirrhosis to carcinoma. These results collectively suggest the possible tumor suppressor role of JMJD5 in normal liver and early phases of liver injury, its gradual decrease contributing to the development of cancer.

4.2.2 In Vitro JMJD5 Expression

In addition to these in vivo data, JMJD5 expression in HCC cell lines was also tested using qRT-PCR (Gökhan Yıldız and Mehmet Öztürk, personal communication).

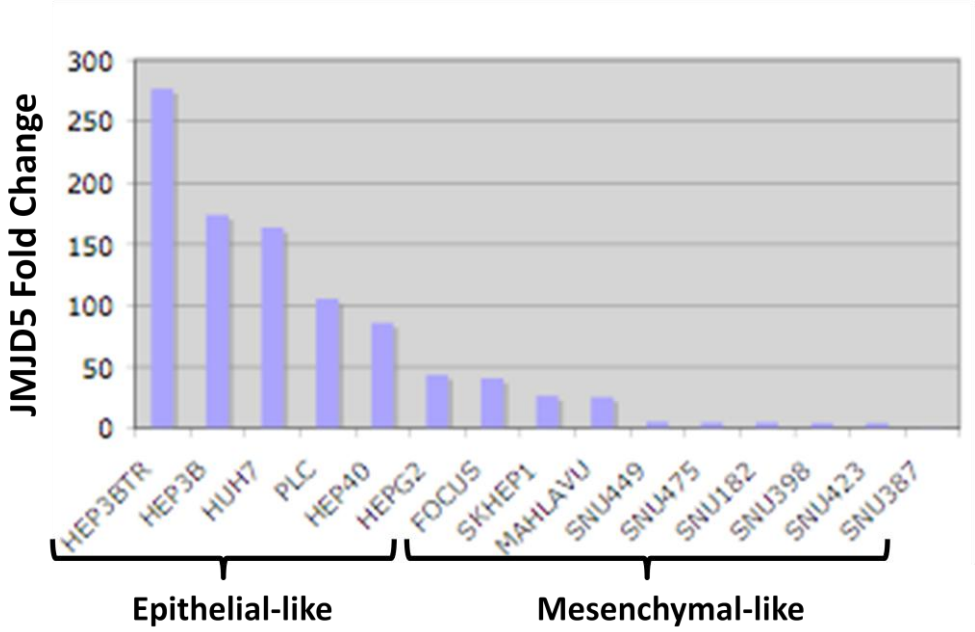

Figure 4.4: Fold change of JMJD5 expression in HCC cell lines

In Figure 4.4, fold change values indicate that JMJD5 expression in RNA levels decreases from epithelial-like HCC cell lines to mesenchymal-like HCC cell lines dramatically. This result shows that JMJD5 levels are drastically reduced as HCC becomes more advanced, suggesting the tumor suppression role for JMJD5 similar to the in vivo data.

In order to study overexpression of a gene of interest, basal levels of that gene should be relatively low in a cell type. If the expression is considerably high, the overexpression does not make very much sense in terms of the phenotype. Consistent with this phenomenon, mesenchymal-like cells seem to be suitable for overexpression analysis. Hence, SNU449 cells with highly low JMJD5 expression were used in this study as a model HCC cell line.

4.3 Maps of JMJD5 Plasmids and Restriction Enzyme Digestion Control

Tumor suppressor role of JMJD5 in liver cancer was investigated using a mesenchymal-like cell line model SNU449, which was derived from a patient with advanced-(grade II-III/IV) HCC [41]. Overexpression of JMJD5 in SNU449 cells

through its stable transfection by lentiviral vectors was planned to test JMJD5's effects on phenotype or tumor growth of this HCC cell line. SNU449-TRex clone derived from this cell line by Hani Alotaibi and Pelin Telkoparan (personal communication), which expresses Tet repressor protein, was used for the regulated expression of JMJD5. Tet-ON expression system derived from pcDNA5/FRT/TO plasmid was cloned into pLKO.1 puro vector as explained in the methods section to provide inducible JMJD5 expression by working in compatibility with SNU449-TRex cells. Figure 4.5 shows the created map of pLTRE plasmids which contain JMJD5 constructs.

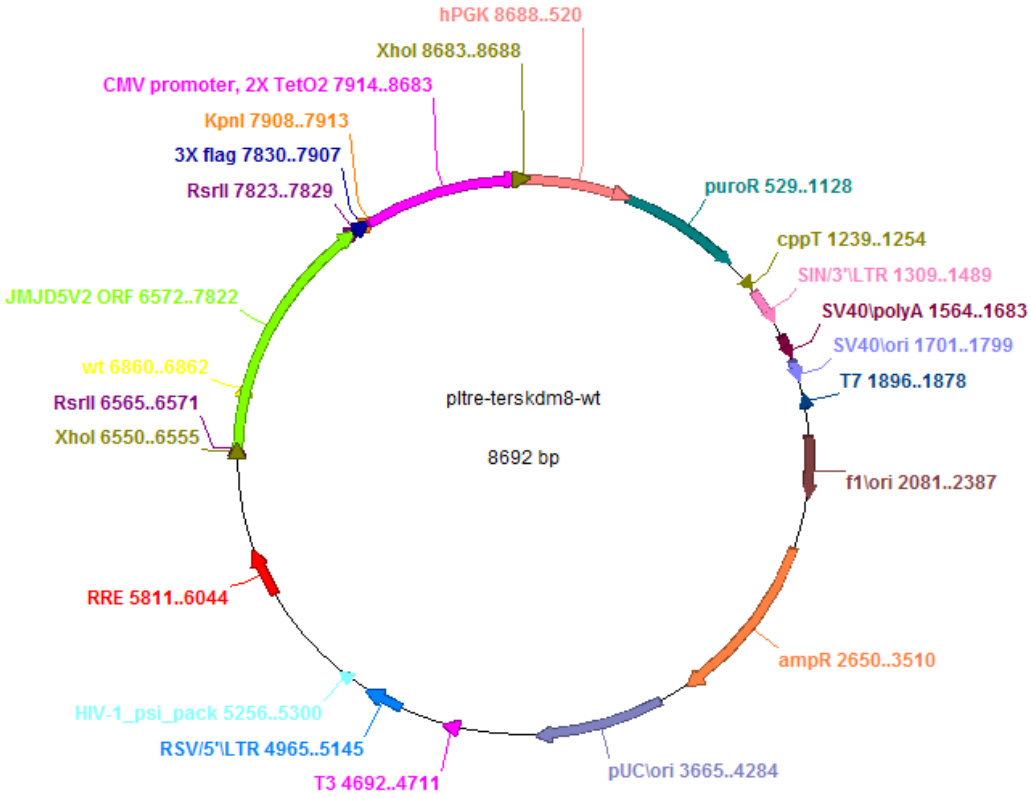

Figure 4.5: Map of pLTRE-FLAG-KDM8 plasmid

("A Plasmid Editor" (ApE) programme was used to create this map.)

Puromycin and ampicillin resistance markers are required for selection in mammalian and bacterial cells, respectively. 5' and 3' long terminal repeats (LTRs) enable the lentiviral DNA to be integrated into host genome.

The cloning of the construct occurred in the reverse direction; hence, JMJD5 is expressed in counterclockwise direction according to this map. This map illustrates the wild type JMJD5 ORF. The 3-bp mutation site in JmjC domain of JMJD5 is also demonstrated in yellow color. Those 3 basepairs only were changed to create the map of pLTRE-FLAG-KDM8H321A plasmid. The map of pLTRE-FLAG-empty plasmid was also created by deleting JMJD5 ORF between RsrII sites.

The correctness of these plasmid maps was tested by restriction enzyme digestion with *NcoI* as depicted in Figure 4.6.

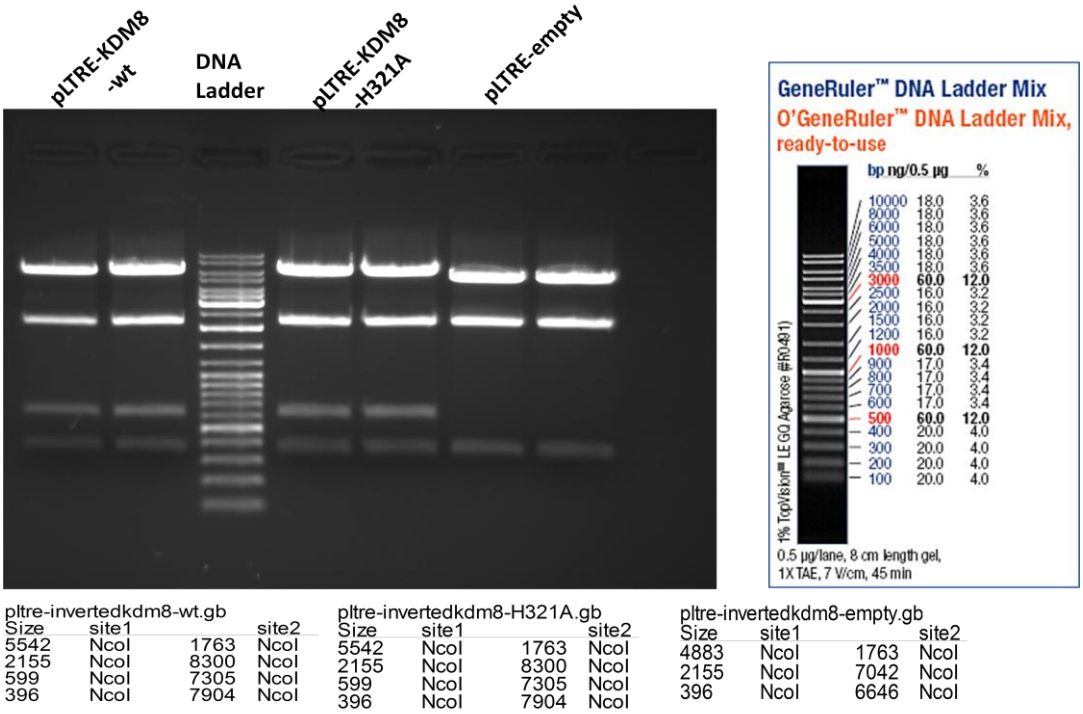

Figure 4.6: *NcoI* restriction enzyme digestion results for JMJD5 plasmids on 1 % agarose gel

(GeneRuler^{TM} DNA ladder mix is shown on the right. The expected band sizes after digestion of each plasmid are shown at the bottom of the figure and were obtained using ApE. Each plasmid was analyzed in duplicates.)

The expected band sizes after digestion of wild type and mutant plasmids were 5542 bp, 2155 bp, 599 bp and 396 bp; whereas those of empty plasmid were 4883 bp, 2155 bp and 396 bp. As compared to the migration of DNA ladder bands on the gel, all restriction digestion products seemed to give the correct bands of expected sizes. This result confirmed the maps and contents of the pLTRE plasmids.

4.4 Transient Exogenous JMJD5 Expression in SNU449-TRex Cells

4.4.1 Tet-ON Inducible Transient Expression of Exogenous JMJD5 at 24 and 48 Hours

To check whether Tet-ON system of pLTRE plasmids works or not in SNU449-TRex cells, transient transfection with the constructs and western blot detection were applied.

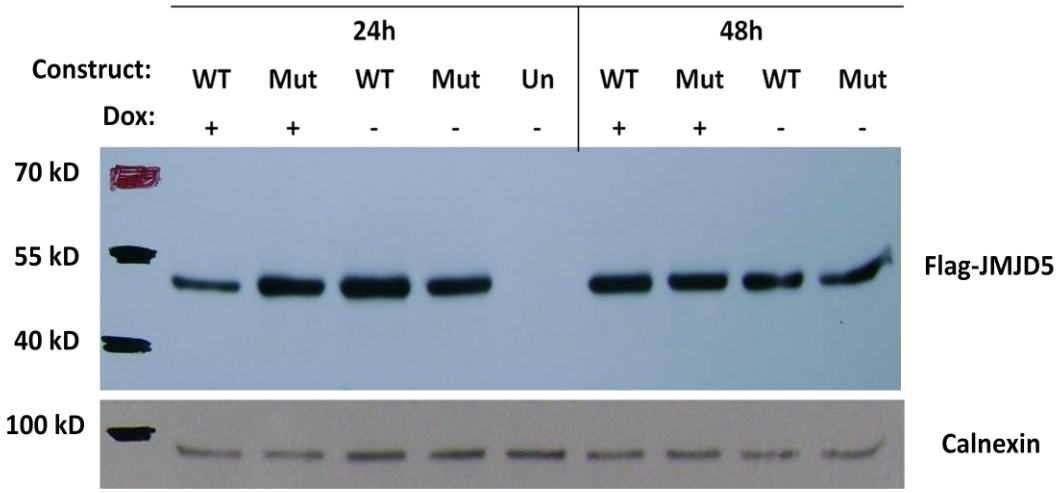

Figure 4.7: Flag-JMJD5 recombinant protein expression upon 24 h and 48 h doxycycline induction in SNU449-TRex cells transiently transfected with wild type and mutant constructs of JMJD5 gene

(WT: wild type, Mut: mutant, Un: untransfected, Dox: doxycycline)

Total protein lysates of the cells were run on SDS-PAGE gel, and N terminally-tagged JMJD5 protein was detected with Flag monoclonal antibody. Molecular weight of Flag-JMJD5 protein is about 50 kD. As seen in Figure 4.7, this band is obtained slightly below the 55 kD band of the ladder. The fact that untransfected cells do not contain this band also confirms the specificity of the antibody to the protein of interest. Contrary to the expectation, there are remarkable bands in Dox (-) cells, indicating that the expression cannot be repressed under Dox (-) condition, and there is a substantial amount of leaky expression. At 24 hour doxycycline induction, the expression does not seem to be inducible, while at 48 hour induction, there is a slightly noticeable induction as indicated by the relatively more intense bands in Dox

(+) cells than Dox (-) cells. This result suggests that JMJD5 is exogenously expressed in SNU449-TRex cells, and Tet-ON inducible system seems to work better under 48 hour doxycycline induction despite the presence of great leaky expression.

4.4.2 Tet-ON Inducible Transient Expression of Exogenous JMJD5 at 48 Hours

Since Figure 4.7 suggests that the inducible expression occurs at 48 hours, transient transfection followed by western blot detection was tested again only for 48 hour doxycycline induction in a separate experiment using the same antibody.

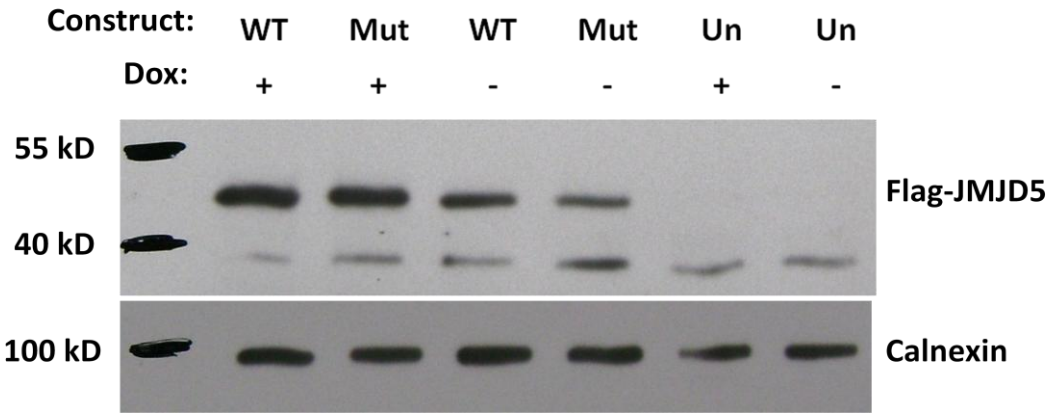

Figure 4.8: Flag-JMJD5 recombinant protein expression upon 48 h doxycycline induction in SNU449-TRex cells transiently transfected with wild type and mutant constructs of JMJD5 gene

(WT: wild type, Mut: mutant, Un: untransfected, Dox: doxycycline)

As indicated in Figure 4.8, the desired Flag-JMJD5 band is obtained around 50 kD size. Although leaky expression is still observed under no induction, the band intensities in Dox (+) wild type and mutant transfectants are much higher than those in Dox (-) cells. This result confirms that both wild type and mutant constructs of JMJD5 are expressed in an inducible manner at 48 hours when introduced into SNU449-TRex cells in a Tet-ON expression plasmid.

4.5 Determining the Optimum Drug Concentrations for Selection of Stable Colonies Using Kill Curve Method

Since pLTRE plasmid contains puromycin selective marker, cells stably transfected with these constructs are resistant to puromycin antibiotic to a certain extent. In very high doses of puromycin, even the stable cells cannot survive, or in low doses, even untransfected cells can survive. Therefore, an optimum drug concentration is required in culture medium in order to eliminate the untransfected cells but to keep transfected ones in a healthy and proliferating state. This concentration was determined using the method so-called “kill curve”.

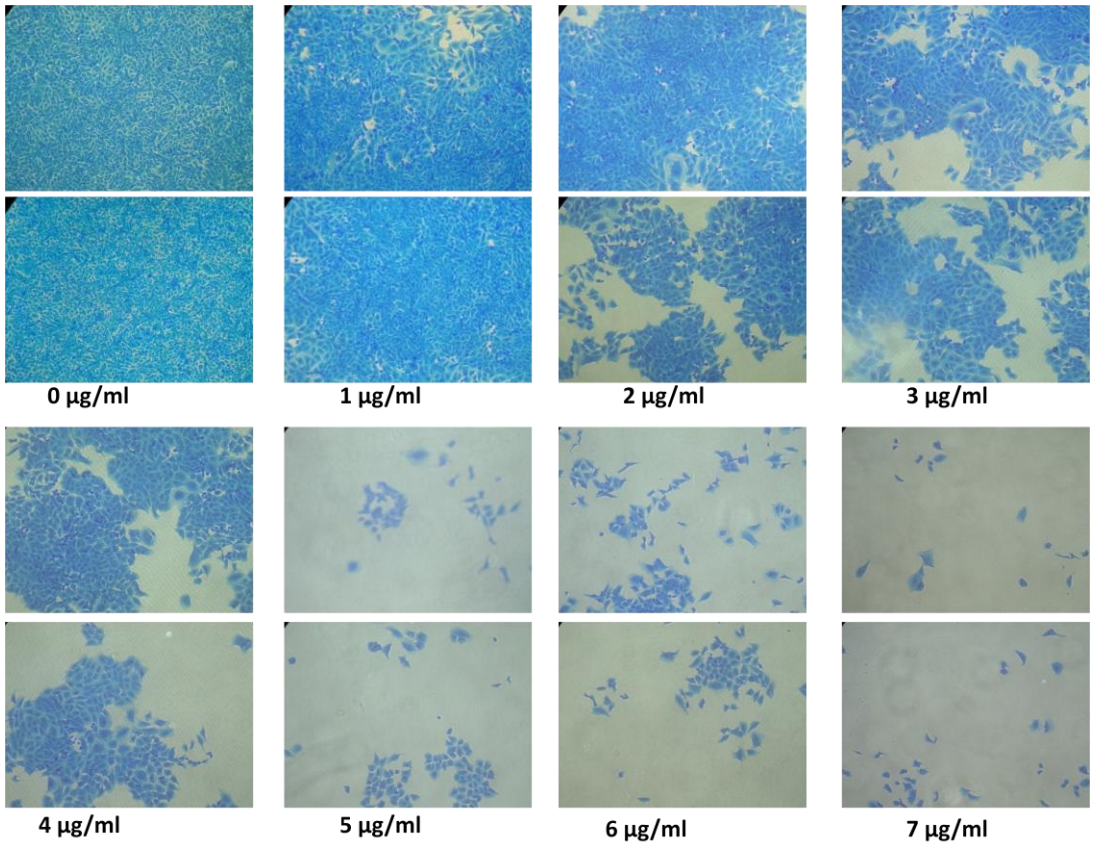

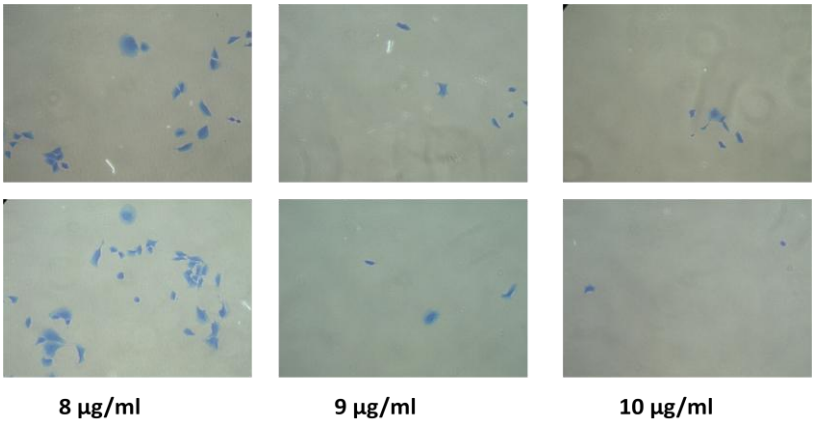

Figure 4.9: Commassie Brilliant Blue staining of untransfected SNU449-TRex cells incubated in different concentrations of puromycin for 6 days

(The duplicate images represent an average view of the plates and were taken at 10X.)

As shown in Figure 4.9, the puromycin dose sufficient to kill about all the untransfected SNU449-TRex cells at day 6, which was 9 µg/ml, was assigned to be the optimum dose. Stable lentiviral transfectants were selected under this puromycin concentration. For culture and growth of the stable clones, a lower dose of puromycin, 6 µg/ml, was used. As previously determined by Hani Alotaibi and Pelin Telkoparan for SNU449-TRex cells, 2 µg/ml blasticidin was also added to the selective growth media of the stable clones.

4.6 Tet-ON Inducible Exogenous JMJD5 Expression in Stable Clones

4.6.1 Western Blot Analysis

Stable JMJD5-expressing polyclonal cell populations were created by lentiviral transduction and antibiotic selection (Emre Yurdusev and Mehmet Öztürk, personal communication). We then tested these cells for inducible JMJD5 expression using Flag monoclonal antibody. In Figure 4.10, western blot analysis for the tested clones is illustrated. Similar to the transient expression experiments, the cells were induced with 2 µg/ml doxycycline for 48 hours.

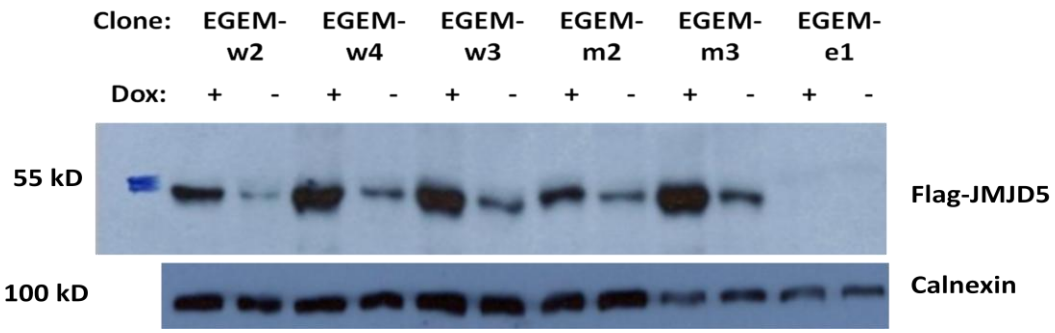

Figure 4.10: Inducible JMJD5 expression in stable clones

(EGEM: Engin-Gokhan-Emre-Mehmet, w: wild type, m: mutant, e: empty, Dox: doxycycline)

As shown in Figure 4.10, the desired Flag-JMJD5 band is observed around 50 kD in all wild type and mutant clones. Since there is no specific protein for Flag antibody binding, no band could be seen in empty clone as expected. The leakage in the Tet-ON system is still present at a considerable level in Dox (-) cells, being quite lower than in transient transfection case. Upon doxycycline induction, the increase in the expression is much clearer in all wild type and mutant clones. This result indicates that the analyzed stable clones are positive for exogenous JMJD5, and the expression is inducible.

4.6.2 Immunofluorescence Analysis

Immunoflorescence staining of stable clones were also performed using flag monoclonal antibody after 48-hour doxycycline induction.

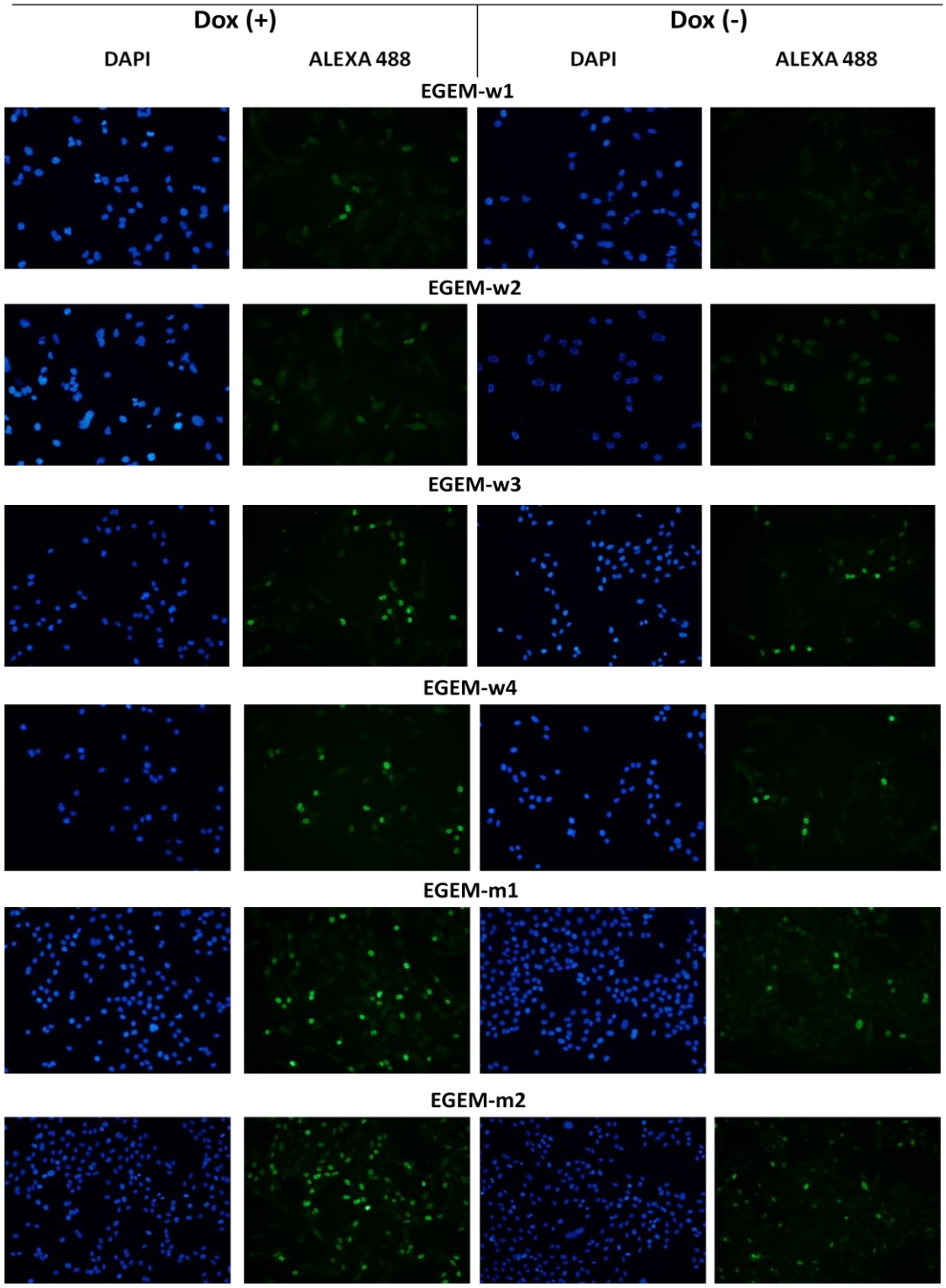
Dox (+)
Dox (-)
DAPI
ALEXA 488
DAPI
ALEXA 488
EGEM-w1
EGEM-w2
EGEM-w3
EGEM-w4
EGEM-m1
EGEM-m2

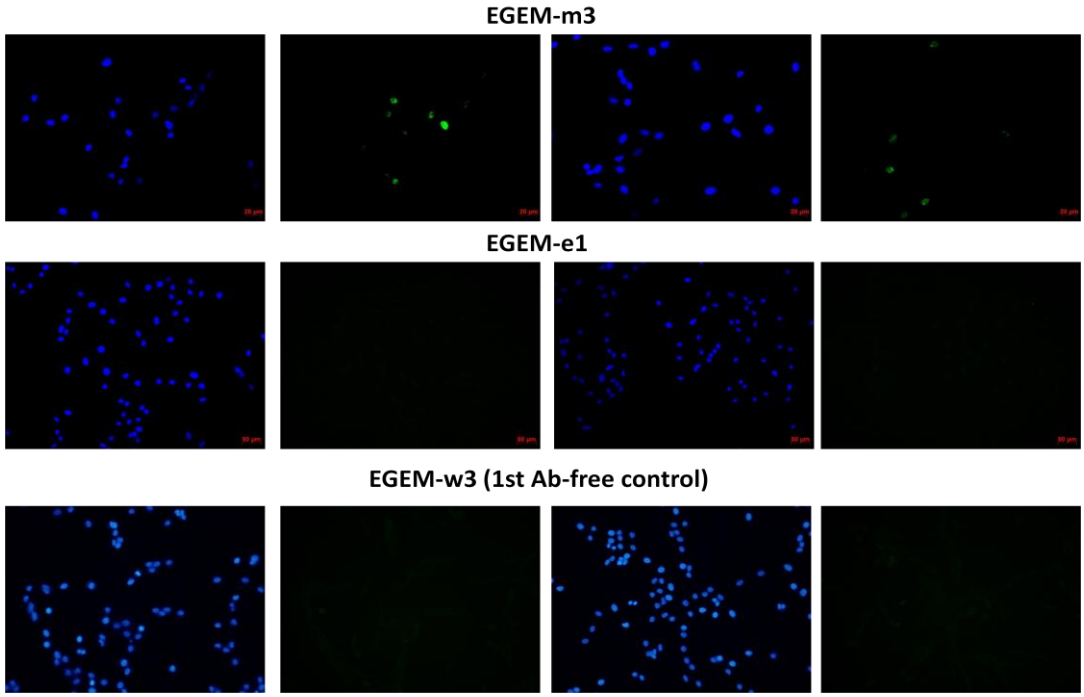

Figure 4.11: Immunoflorescence staining of stable clones for exogenous JMJD5

(The images were taken at 20X. DAPI stains nucleus (blue), and Alexa 488 stains Flag-JMJD5 (green).)

According to Figure 4.11, exogenous Flag-JMJD5 expression is detectable in all wild type and mutant clones, but the percentage positivity changes between clones. The leaky expression is present, and doxycycline induction is not so dramatic. JMJD5 positivity percentage for each clone was calculated by counting green Alexa signals and blue DAPI signals in triplicate random areas as indicated in Table 4.1.

Table 4.1: JMJD5 positivity for each clone

(Triplicate random areas were counted. The marked clones with relatively higher positivity and induction were selected for further phenotypic analyses.)

Clone	Region 1	Region 2	Region 3	Average
EGEM-w1 Dox +	12/73	7/60	12/88	14%
EGEM-w1 Dox -	0	0	0	0%
EGEM-w2 Dox +	25/64	26/70	17/56	36% *
EGEM-w2 Dox -	4/41	5/36	5/33	13%
EGEM-w3 Dox +	45/110	28/80	17/51	36%
EGEM-w3 Dox -	16/49	23/96	29/92	29%
EGEM-w4 Dox +	21/51	27/49	45/109	46% *
EGEM-w4 Dox -	16/71	10/70	17/42	26%
EGEM-m1 Dox +	46/174	77/310	63/288	24%
EGEM-m1 Dox -	29/283	37/332	11/78	12%
EGEM-m2 Dox+	117/288	119/247	101/195	47% *
EGEM-m2 Dox-	60/284	61/296	58/295	21%
EGEM-m3 Dox+	6/30	10/28	9/23	32% *
EGEM-m3 Dox-	6/35	4/27	5/18	20%

According to Table 4.1, the positivity of stable clones is not 100 %, maximally reaching up to 47 % in EGEM-m2. The leakiness is also remarkably high, even reaching up to 29 % in EGEM-w3. The mild doxycycline induction in the clones is also quantitatively detected. What is concluded from immunoflorescence staining and counting result is that JMJD5 positivity of the clones is not homogenous, quite low, even not reaching to 50 %, and the induction is weak.

4.7 Comparison of Genome-wide Expression Profiles between EGEM-w4 and EGEM-e1

Microarray expression profiles of EGEM-w4 and EGEM-e1 were compared to shed light on target genes and target pathways of JMJD5 and to reveal its association with liver carcinoma. For this purpose, two types of analyses were made. In the first one, the genes that change significantly between empty and wild type clones were

determined and listed. In the second one, gene sets were analyzed in terms of cellular pathways or oncogenic properties to find out a relationship between JMJD5 and a set of genes with a similar property.

4.7.1 Altered Genes

The genes with at least 1.5 fold significant expression change in EGEM-w4 relative to EGEM-e1were listed in Table 4.2 and 4.3.

Table 4.2: 26 genes at least 1.5 fold upregulated with significance level of 0.05 in EGEM-w4 clone compared to EGEM-e1 clone

(Fold change is the ratio of the expression level in EGEM-e1 to that in EGEM-w4. Two microarray probesets that did not match with a known gene were not shown.)

Gene	Fold ratio (control/ Wt-JMJD5	Name	Defined Genelist
ASZ1	0.39	ankyrin repeat, SAM and basic leucine zipper domain containing 1	
ENPP2	0.41	ectonucleotide pyrophosphatase/phosphodiesterase 2	Nicotinate and nicotinamide metabolism, Pantothenate and CoA biosynthesis, Purine metabolism, Riboflavin metabolism, Starch and sucrose metabolism
FAM198B	0.48	family with sequence similarity 198, member B	
EMP3	0.49	epithelial membrane protein 3	
LOC283104	0.53	hypothetical LOC283104	
FAM84B	0.53	family with sequence similarity 84, member B	
ALDH1A1	0.58	aldehyde dehydrogenase 1	Retinol metabolism

		family, member A1	
DEPTOR	0.6	DEP domain containing MTOR-interacting protein	
TPD52L1	0.6	tumor protein D52-like 1	
RDH10	0.6	retinol dehydrogenase 10 (all-trans)	
FABP5	0.61	fatty acid binding protein 5 (psoriasis-associated)	PPAR signaling pathway
FAP	0.62	fibroblast activation protein, alpha	angiogenesis, cell_cycle, cell_signaling, metastasis
TPD52L1	0.62	tumor protein D52-like 1	
IL7	0.62	interleukin 7	Cytokines and Inflammatory Response, IL-7 Signal Transduction, Regulation of hematopoiesis by cytokines, Cytokine-cytokine receptor interaction, Hematopoietic cell lineage, Jak-STAT signaling pathway, immunology
OLFML2A	0.62	olfactomedin-like 2A	
TNFAIP6	0.63	tumor necrosis factor, alpha-induced protein 6	immunology
TSPAN7	0.63	tetraspanin 7	
WNT5A	0.64	wingless-type MMTV integration site family, member 5A	Perou's- Intrinsic- Breast-Cancer-Genes, Hedgehog signaling pathway, Wnt signaling pathway, development, tsonc
RDH10	0.65	retinol dehydrogenase 10 (all-trans)	
MALL	0.65	mal, T-cell differentiation protein-like	immunology
TNFAIP6	0.65	tumor necrosis factor, alpha-induced protein 6	immunology

ERBB3	0.65	v-erb-b2 erythroblastic leukemia viral oncogene homolog 3 (avian)	Neuroregulin receptor degredation protein-1 Controls ErbB3 receptor recycling, Role of ERBB2 in Signal Transduction and Oncology, Calcium signaling pathway, cell_cycle, cell_signaling, signal_transduction, tsonc
THBS2	0.66	thrombospondin 2	Cell Communication, ECM-receptor interaction, Focal adhesion, TGF-beta signaling pathway, angiogenesis, immunology
PEG10	0.66	paternally expressed 10	
POPDC3	0.66	popeye domain containing 3	
BHLHE41	0.67	basic helix-loop-helix family, member e41	Circadian rhythm

According to the upregulated gene list in Table 4.2, 26 genes seem to be upregulated under JMJD5 overexpression, not meaning that all of them are JMJD5 targets. The diversity of biological roles played by these genes makes a logical guess about function of JMJD5 even more difficult. However, most of the overexpressed genes are related with immunology and cytokines, implying a possible involvement of JMJD5 in immune regulatory processes through expression of cytokines. Angiogenesis and cell cycle were the second most common biological roles of the upregulated genes. Some of the genes were also associated with retinol metabolism.

On the other hand, as shown in Table 4.3, 37 genes were detected to be downregulated in EGEM-w4. Most of these genes were associated with lipid, sugar metabolism and biosynthesis of several organic molecules. Many of the genes were also related to immunology, again pointing to the possible immune function of JMJD5. A few members related to phospholipase C and calcium signaling pathways were also observed.

Table 4.3: 37 genes at least 1.5 fold downregulated with significance level of 0.05 in EGEM-w4 clone compared to EGEM-e1 clone

(Fold change is the ratio of the expression level in EGEM-e1 to that in EGEM-w4. Four microarray probesets that did not match with a known gene were not shown.)

Gene	Fold	Name	Defined Genelist
DIS3L2	1,51	DIS3 mitotic control homolog (S. cerevisiae)-like 2	
BCHE	1,51	butyrylcholinesterase	immunology, pharmacology
C7orf58	1,51	chromosome 7 open reading frame 58	
MYO5B	1,52	myosin VB	
LIMCH1	1,52	LIM and calponin homology domains 1	
ABHD5	1,52	abhydrolase domain containing 5	
TBC1D2	1,53	TBC1 domain family, member 2	
PPM1E	1,54	protein phosphatase, Mg2+/Mn2+ dependent, 1E	
UPK1B	1,54	uroplakin 1B	immunology
KLHL5	1,54	kelch-like 5 (Drosophila)	
GAS6	1,56	growth arrest-specific 6	immunology
CDH4	1,57	cadherin 4, type 1, R-cadherin (retinal)	Cell adhesion molecules (CAMs), cell_signaling, metastasis
CDH4	1,57	cadherin 4, type 1, R-cadherin (retinal)	Cell adhesion molecules (CAMs), cell_signaling, metastasis
C7orf58	1,58	chromosome 7 open reading frame 58	
ITM2A	1,58	integral membrane protein 2A	
SFRP1	1,6	secreted frizzled-related protein 1	Wnt signaling pathway, development
UACA	1,61	uveal autoantigen with coiled-coil domains and ankyrin repeats	
PLCE1	1,62	phospholipase C, epsilon 1	Phospholipase C-epsilon pathway, Calcium signaling pathway, Inositol phosphate metabolism, Phosphatidylinositol signaling system

TMEM45A	1,62	transmembrane protein 45A	
EPS8L2	1,63	EPS8-like 2	
FANCA	1,63	Fanconi anemia, complementation group A	BRCA1-dependent Ub-ligase activity, Role of BRCA1, BRCA2 and ATR in Cancer Susceptibility, DNA_damage, immunology
TMEM27	1,65	transmembrane protein 27	
FA2H	1,7	fatty acid 2-hydroxylase	
CCL2	1,71	chemokine (C-C motif) ligand 2	Low-density lipoprotein (LDL) pathway during atherogenesis, Msp/Ron Receptor Signaling Pathway, Pertussis toxin-insensitive CCR5 Signaling in Macrophage, Cytokine-cytokine receptor interaction
DPYSL3	1,75	dihydropyrimidinase-like 3	
ST6GALNAC5	1,75	ST6 (alpha-N-acetyl-neuraminyl-2,3-beta-galactosyl-1,3)-N-acetylgalactosaminide alpha-2,6-sialyltransferase 5	Glycan structures - biosynthesis 2, Glycosphingolipid biosynthesis - ganglioseries
ADRB2	1,82	adrenergic, beta-2-, receptor, surface	Corticosteroids and cardioprotection, Cystic fibrosis transmembrane conductance regulator (CFTR) and beta 2 adrenergic receptor (b2AR) pathway, Phospholipase C-epsilon pathway, Calcium signaling pathway, Neuroactive ligand-receptor interaction, behavior, immunology
ITM2A	1,83	integral membrane protein 2A	
PLCE1	1,85	phospholipase C, epsilon 1	Phospholipase C-epsilon pathway, Calcium signaling pathway, Inositol phosphate metabolism, Phosphatidylinositol signaling system
GREM1	1,89	gremlin 1	
GREM1	1,92	gremlin 1	
SPP1	1,95	secreted phosphoprotein 1	Regulators of Bone Mineralization, Cell Communication, ECM-receptor

			interaction, Focal adhesion, immunology
FOXF2	2,13	forkhead box F2	
NNMT	2,18	nicotinamide N-methyltransferase	Nicotinate and nicotinamide metabolism, immunology
IGFN1	2,69	immunoglobulin-like and fibronectin type III domain containing 1	
CHRDL1	2,72	chordin-like 1	
SPOCK1	4,58	sparc/osteonectin, cwcv and kazal-like domains proteoglycan (testican) 1	

4.7.2 Altered Gene Sets

Gene set enrichment analysis results are indicated in Table 4.4. Each gene set contains a certain number of cells involved in the same biological process. When the results are analyzed in detail, it is seen that highly diverse cellular pathways are upregulated in both clones. Particularly, in wild type cells, most of the enriched gene sets are related to metabolic processes and normal cellular processes, only one being directly related to cell proliferation. That was the gene set of G2-M transition of mitotic cell cycle. Interestingly, the gene set responsible for positive regulation of angiogenesis was enriched in EGEM-w4, as also observed in the case of single genes. This could be one suspected cellular process potentially regulated with the participation of JMJD5. On the other hand, in EGEM-e1 cells, several gene sets seem to be directly related to cell growth and proliferation, such as G1 phase of mitotic cell cycle, helicase activity, regulation of growth, DNA replication, etc. Accordingly, it seems that many abnormal growth pathways are active in empty cells, but the number of them is greatly reduced in JMJD5-overexpressing cells, which supports the fact that JMJD5 might have a tumor suppressor role in liver cancer. Several cell cycle-associated gene sets found to be enriched in EGEM-e1 but not in EGEM-w4 point to the potential cell cycle regulator role of JMJD5 most probably through inhibiting it.

Table 4.4: Gene set enrichment analysis of EGEM-w4 and EGEM-e1 with respect to cellular processes.

(50 gene sets are significantly enriched in EGEM-w4, and 68 gene sets are significantly enriched in EGEM-e1 with 0.01 p value.)

Gene sets enriched in EGEM-w4	**Gene sets enriched in EGEM-e1**
DOUBLE_STRANDED_RNA_BINDING	NUCLEAR_BODY
RNA_POLYMERASE_II_TRANSCRIPTION_FACTOR_ACTIVITYENHANCER_BINDING	NEGATIVE_REGULATION_OF_CELL_MIGRATION
GLUTATHIONE_TRANSFERASE_ACTIVITY	HOMEOSTASIS_OF_NUMBER_OF_CELLS
EXTRINSIC_TO_PLASMA_MEMBRANE	PML_BODY
MONOVALENT_INORGANIC_CATION_HOMEOSTASIS	RNA_HELICASE_ACTIVITY
PROTEIN_TARGETING_TO_MEMBRANE	PHOSPHOINOSITIDE_BINDING
SARCOMERE	RESPONSE_TO_ORGANIC_SUBSTANCE
AXON	B_CELL_DIFFERENTIATION
TRANSFERASE_ACTIVITY_TRANSFERRING_SULFUR_CONTAINING_GROUPS	CHROMATIN_BINDING
POSITIVE_REGULATION_OF_EPITHELIAL_CELL_PROLIFERATION	DNA_REPLICATION
RESPONSE_TO_NUTRIENT	SMALL_CONJUGATING_PROTEIN_SPECIFIC_PROTEASE_ACTIVITY
REGULATION_OF_HEART_CONTRACTION	REGULATION_OF_GTPASE_ACTIVITY
SULFOTRANSFERASE_ACTIVITY	NEGATIVE_REGULATION_OF_GROWTH
MEDIATOR_COMPLEX	TRANSCRIPTION_FACTOR_COMPLEX
AMINO_SUGAR_METABOLIC_PROCESS	RNA_DEPENDENT_ATPASE_ACTIVITY
INTRAMOLECULAR_OXIDOREDUCTASE_ACTIVITY	SEQUENCE_SPECIFIC_DNA_BINDING
PHOSPHATE_TRANSMEMBRANE_TRANSPORTER_ACTIVITY	ATP_DEPENDENT_RNA_HELICASE_ACTIVITY
INORGANIC_ANION_TRANSMEMBRANE_TRANSPORTER_ACTIVITY	MYELOID_CELL_DIFFERENTIATION
MYOFIBRIL	G1_PHASE
SH3_SH2_ADAPTOR_ACTIVITY	KINETOCHORE
SECRETIN_LIKE_RECEPTOR_ACTIVITY	MITOCHONDRIAL_OUTER_MEMBRANE
G2_M_TRANSITION_OF_MITOTIC_CELL_CYCLE	CHROMOSOMEPERICENTRIC_REGION
OVULATION_CYCLE	PROTEIN_COMPLEX_BINDING

CARBON_OXYGEN_LYASE_ACTIVITY	REGULATION_OF_RAS_GTPASE_ACTIVITY
SULFUR_METABOLIC_PROCESS	POSITIVE_REGULATION_OF_T_CELL_PROLIFERATION
PROTEIN_KINASE_INHIBITOR_ACTIVITY	RHO_GUANYL_NUCLEOTIDE_EXCHANGE_FACTOR_ACTIVITY
INTEGRIN_COMPLEX	MYELOID_LEUKOCYTE_DIFFERENTIATION
CELLULAR_MONOVALENT_INORGANIC_CATION_HOMEOSTASIS	GLYCEROPHOSPHOLIPID_METABOLIC_PROCESS
LYASE_ACTIVITY	ENDOTHELIAL_CELL_PROLIFERATION
DNA_FRAGMENTATION_DURING_APOPTOSIS	SINGLE_STRANDED_DNA_BINDING
MEMBRANE_FUSION	GLUCOSE_CATABOLIC_PROCESS
KINASE_INHIBITOR_ACTIVITY	OXIDOREDUCTASE_ACTIVITY_ACTING_ON_NADH_OR_NADPH
SPERM_MOTILITY	HEMOPOIESIS
SINGLE_STRANDED_RNA_BINDING	REGULATION_OF_ENDOTHELIAL_CELL_PROLIFERATION
POSITIVE_REGULATION_OF_ANGIOGENESIS	DNA_DIRECTED_RNA_POLYMERASEII_CORE_COMPLEX
HYDRO_LYASE_ACTIVITY	REGULATION_OF_GROWTH
CONTRACTILE_FIBER	REGULATION_OF_DNA_METABOLIC_PROCESS
PROTON_TRANSPORTING_TWO_SECTOR_ATPASE_COMPLEX	PHOSPHOLIPID_TRANSPORTER_ACTIVITY
REGULATION_OF_PH	ESTABLISHMENT_OF_ORGANELLE_LOCALIZATION
PROTEIN_SERINE_THREONINE_TYROSINE_KINASE_ACTIVITY	ATP_DEPENDENT_HELICASE_ACTIVITY
LAMELLIPODIUM	REGULATION_OF_NEUROTRANSMITTER_LEVELS
CELL_PROJECTION	CHROMOSOME_CONDENSATION
INTERCELLULAR_JUNCTION_ASSEMBLY	DEOXYRIBONUCLEASE_ACTIVITY
MICROVILLUS	NUCLEOTIDE_KINASE_ACTIVITY
DEACETYLASE_ACTIVITY	HEMOPOIETIC_OR_LYMPHOID_ORGAN_DEVELOPMENT
ANION_CATION_SYMPORTER_ACTIVITY	RESPONSE_TO_HYPOXIA

POSITIVE_REGULATION_OF_CELL_DIFFERENTIATION	MITOCHONDRIAL_MEMBRANE_ORGANIZATION_AND_BIOGENESIS
GLUCOSAMINE_METABOLIC_PROCESS	CELLULAR_PROTEIN_COMPLEX_ASSEMBLY
VACUOLAR_PART	RHO_GTPASE_ACTIVATOR_ACTIVITY
	REGULATION_OF_MEMBRANE_POTENTIAL
	STEROID_BIOSYNTHETIC_PROCESS
	ALDO_KETO_REDUCTASE_ACTIVITY
	CELL_SURFACE
	BIOGENIC_AMINE_METABOLIC_PROCESS
	OXIDOREDUCTASE_ACTIVITY_ACTING_ON_THE_CH_CH_GROUP_OF_DONORS
	HELICASE_ACTIVITY
	DNA_DEPENDENT_DNA_REPLICATION
	FATTY_ACID_METABOLIC_PROCESS
	OLIGOSACCHARYL_TRANSFERASE_COMPLEX
	BASEMENT_MEMBRANE
	RUFFLE
	REPLICATION_FORK
	G1_PHASE_OF_MITOTIC_CELL_CYCLE
	GENERAL_RNA_POLYMERASE_II_TRANSCRIPTION_FACTOR_ACTIVITY
	EXTERNAL_SIDE_OF_PLASMA_MEMBRANE
	REGULATION_OF_MYELOID_CELL_DIFFERENTIATION
	INTERLEUKIN_8_BIOSYNTHETIC_PROCESS

Gene set enrichment analysis with respect to oncogenic properties is shown in Table 4.5. Primarily enriched sets are those of p53 and β-catenin targets as expected because p53 and β-catenin are the most frequently observed mutations in hepatocellular carcinoma [5]. Interestingly, the sets enriched in EGEM-w4 and those enriched in EGEM-e1 were quite different from each other except for the sets of p53

and β-catenin. In fact, p53 and β-catenin sets were not the same at all. "BCAT.100_UP.V1_DN" and "P53_DN.V1_UP" sets were present in EGEM-w4 list, whereas "BCAT_BILD_ET_AL_DN", "BCAT_BILD_ET_AL_UP" and "P53_DN.V1_DN" were present in EGEM-e1 list. This might indicate that expression profiles of cancer-related pathways substantially altered with high levels of JMJD5, proposing a possible tumor suppression role for JMJD5.

Table 4.5: Gene set enrichment analysis of EGEM-w4 and EGEM-e1 with respect to oncogenic properties

(7 gene sets are significantly enriched in EGEM-w4 and 12 gene sets are significantly enriched in EGEM-e1 with 0.01 p value.)

Gene sets enriched in EGEM-w4	
BCAT.100_UP.V1_DN	Genes down-regulated in HEK293 cells (kidney fibroblasts) expressing constitutively active form of CTNNB1 gene
YAP1_DN	Genes down-regulated in MCF10A cells (breast cancer) over-expressing YAP1 gene
P53_DN.V1_UP	Genes up-regulated in NCI-60 panel of cell lines with mutated TP53
HINATA_NFKB_MATRIX	Matrix, adhesion or cytoskeleton genes induced by NF-kappaB in primary keratinocytes and fibroblasts
PKCA_DN.V1_DN	Genes down-regulated in small intestine in PRKCA knockout mice
ALK_DN.V1_UP	Genes up-regulated in DAOY cells (medulloblastoma) upon knockdown of ALK gene by RNAi
PRC1_BMI_UP.V1_DN	Genes down-regulated in TIG3 cells (fibroblasts) upon knockdown of BMI1 gene
Gene sets enriched in EGEM-e1	
CSR_EARLY_UP.V1_UP	Genes up-regulated in early serum response of CRL 2091 cells (foreskin fibroblasts)
BCAT_BILD_ET_AL_DN	Genes down-regulated in primary epithelial breast cancer cell culture over-expressing

	activated CTNNB1 gene
CORDENONSI_YAP_CONSERVED_SIGNATURE	YAP conserved signature
SIRNA_EIF4GI_DN	Genes down-regulated in MCF10A cells vs knockdown of EIF4G1 gene by RNAi
GLI1_UP.V1_UP	Genes up-regulated in RK3E cells (kidney epithelium) over-expressing GLI1
BCAT_BILD_ET_AL_UP	Genes up-regulated in primary epithelial breast cancer cell culture over-expressing activated CTNNB1 gene
RB_DN.V1_UP	Genes up-regulated in primary keratinocytes from RB1 skin specific knockout mice
CRX_NRL_DN.V1_DN	Genes down-regulated in retina cells from CRX and NRL double knockout mice
P53_DN.V1_DN	Genes down-regulated in NCI-60 panel of cell lines with mutated TP53
MEL18_DN.V1_UP	Genes up-regulated in DAOY cells (medulloblastoma) upon knockdown of PCGF2 gene by RNAi
CAHOY_ASTROCYTIC	Genes up-regulated in astrocytes
AKT_UP_MTOR_DN.V1_DN	Genes down-regulated by everolimus in mouse prostate tissue transgenically expressing human AKT1 gene vs untreated controls

4.8 Phenotypic Assays for Stable Clones

In order to have an insight into the function of JMJD5, any phenotypic effect of its overexpression in isogenic clones was investigated applying different methods.

4.8.1 Sulphordamine B Assay for Cell Proliferation

Figure 4.12 shows SRB results, as an indication of cell growth, for stable clones under 6-day doxycycline induction.

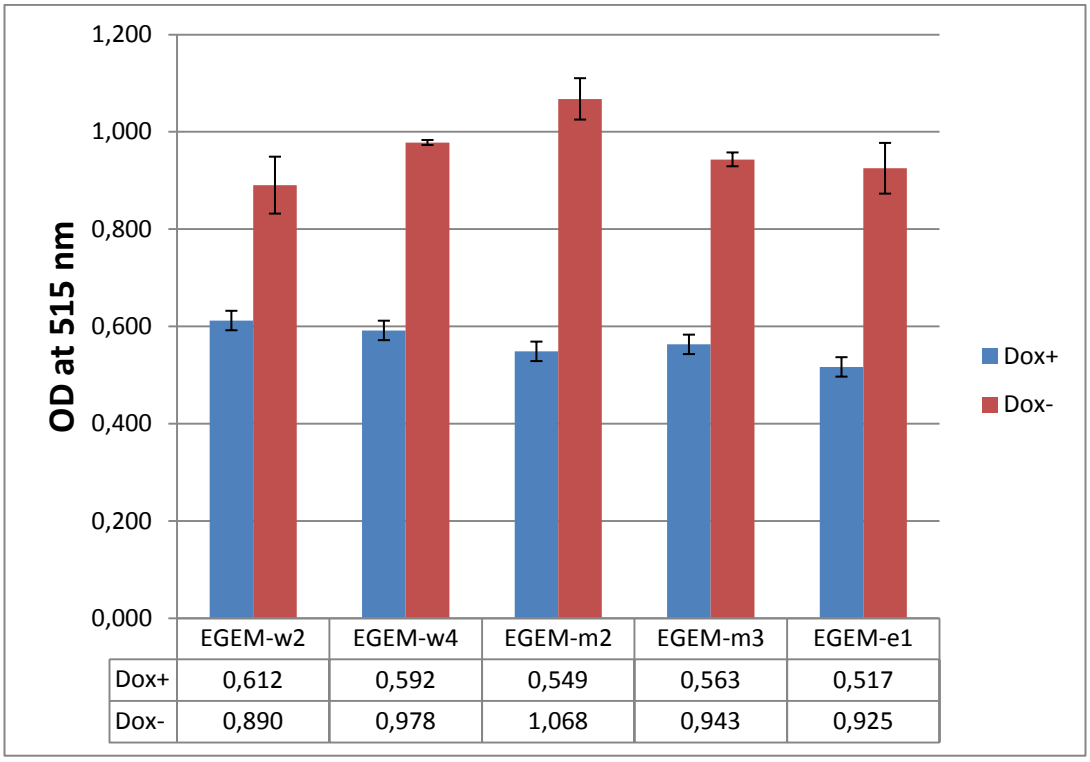

Figure 4.12: SRB readings of stable clones after 6-day doxycycline induction

(Mean OD values for triplicate samples are indicated at the bottom of the graph.)

SRB assay results indicate that doxycycline inhibits growth, decreasing OD level in all cells to almost half of Dox (-) case, due to its antibiotic activity. However, it seems that wild type clones are slightly more resistant to this drug. OD means of clones under Dox (+) conditions are also quite comparable. This result implicates that there is no drastic difference between growth rates of isogenic clones.

4.8.2 Immunofluorescence Double Staining for Bromodeoxyuridine and Flag

The reason why a substantial growth difference among the clones could not be observed quantitatively in SRB assay might be the heterogeneity of the clones for JMJD5 positivity. As observed in the previous immunoflorescence data, two type of populations, namely Flag-JMJD5(+) and Flag-JMJD5(-) are present in each clone. Even there is an effect of JMJD5 overexpression on growth, it may be tiny or unnoticeable in those mixed populations because Flag-JMJD5(-) population could compensate for that effect. In order to find out any possible effect of JMJD5 on

growth, BrdU incorporation of Flag-JMJD5(+) and Flag-JMJD5(-) cells were determined separately. In this case, instead of using Dox (-) cells or mutant cells and empty cells as negative controls, Flag-JMJD5(-) cells sitting in the same clonal culture and under same doxycycline condition with Flag-JMJD5(+) cells were used as negative controls.

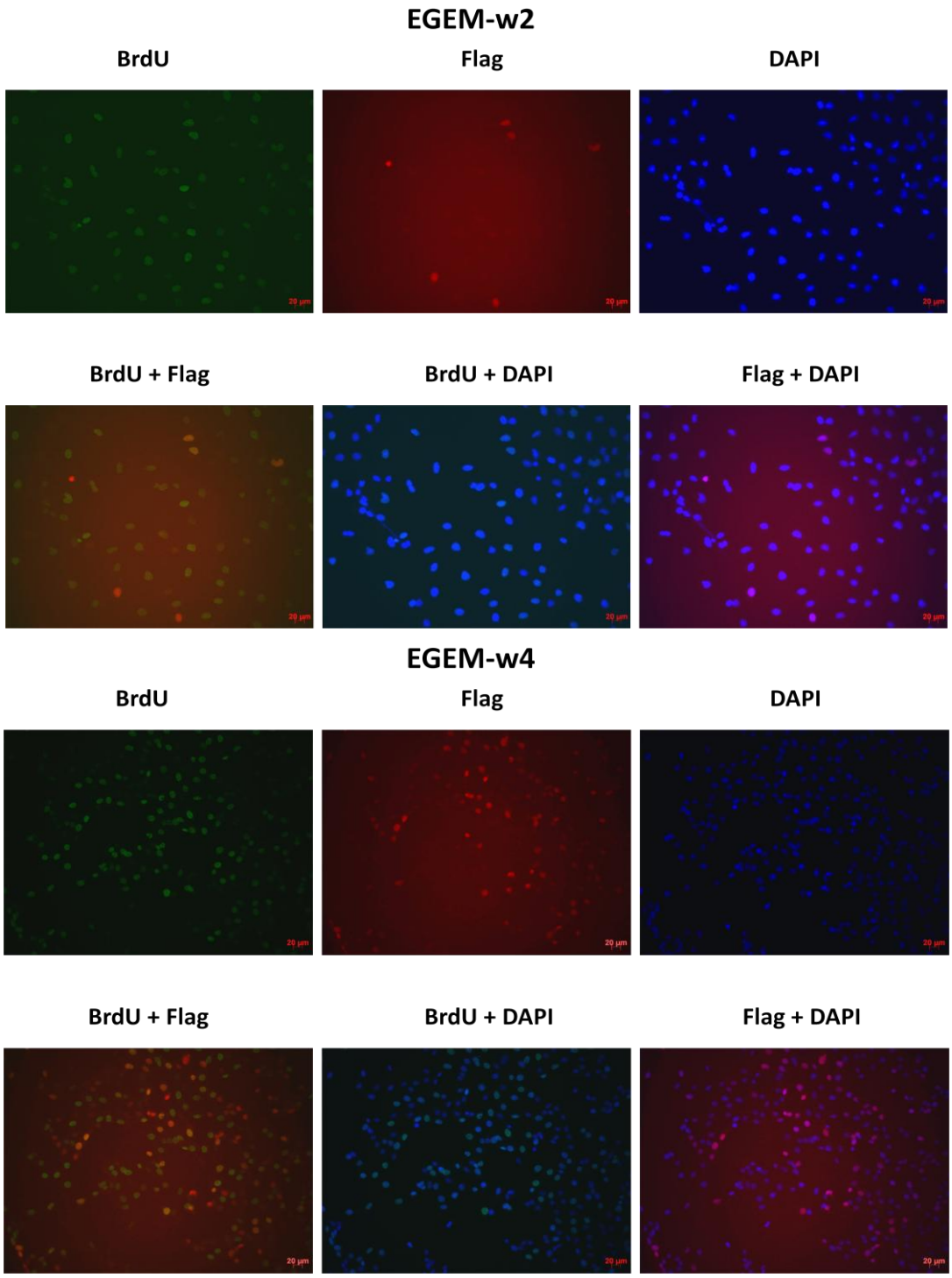

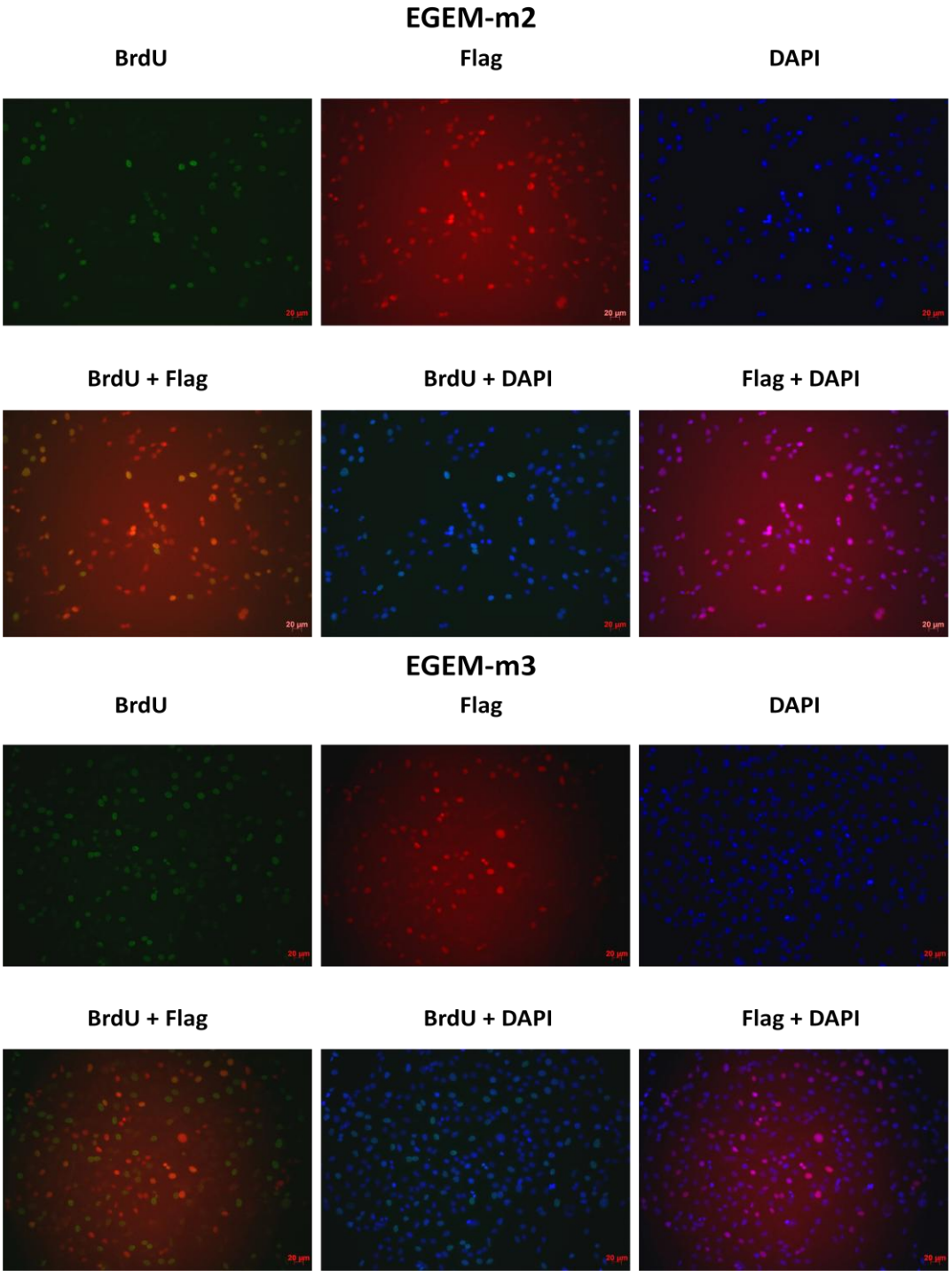
EGEM-m2
BrdU
Flag
DAPI
BrdU + Flag
BrdU + DAPI
Flag + DAPI
EGEM-m3
BrdU
Flag
DAPI
BrdU + Flag
BrdU + DAPI
Flag + DAPI

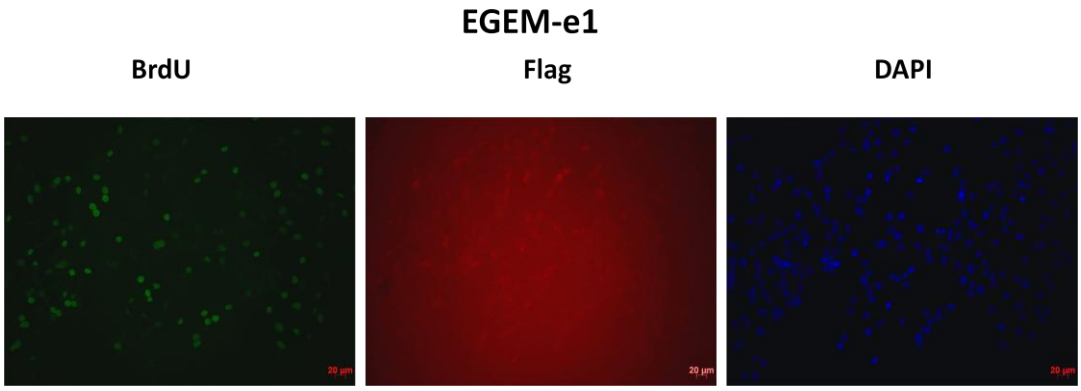

Figure 4.13: BrdU and Flag double immunoflorescence staining pictures and merged photos for each isogenic stable clone

(Images were taken at 20X.)

It can be seen from Flag + DAPI merged images that Flag and DAPI signals colocalize, suggesting that the JMJD5 localization region in the cell is nucleus. By counting the cells manually on each picture in Figure 4.13, several parameters were calculated as shown in the following bar graphs. First, BrdU and Flag positivities for each clone are depicted in Figure 4.14.

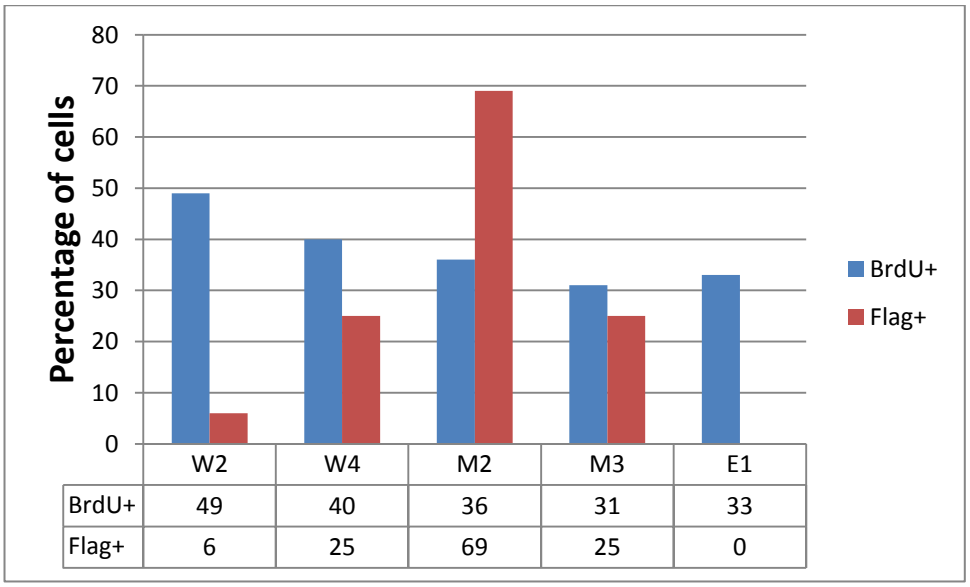

Figure 4.14: BrdU and Flag positivity percentages for each isogenic clone

(At the bottom of the graph, the percentage values are indicated.)

Accordingly, Flag positivity of the clones varies greatly, and there is a decreasing tendency in BrdU positivity from wild type to mutant and empty clones. Since the

Flag expression is variable, and the populations are not homogenous, this tendency of fall may not be dependent on type of constructs or JMJD5 levels.

On the other hand, Figure 4.15 shows the BrdU incorporation change depending on Flag expression in the same clone. According to this result, BrdU+ cell percentage in

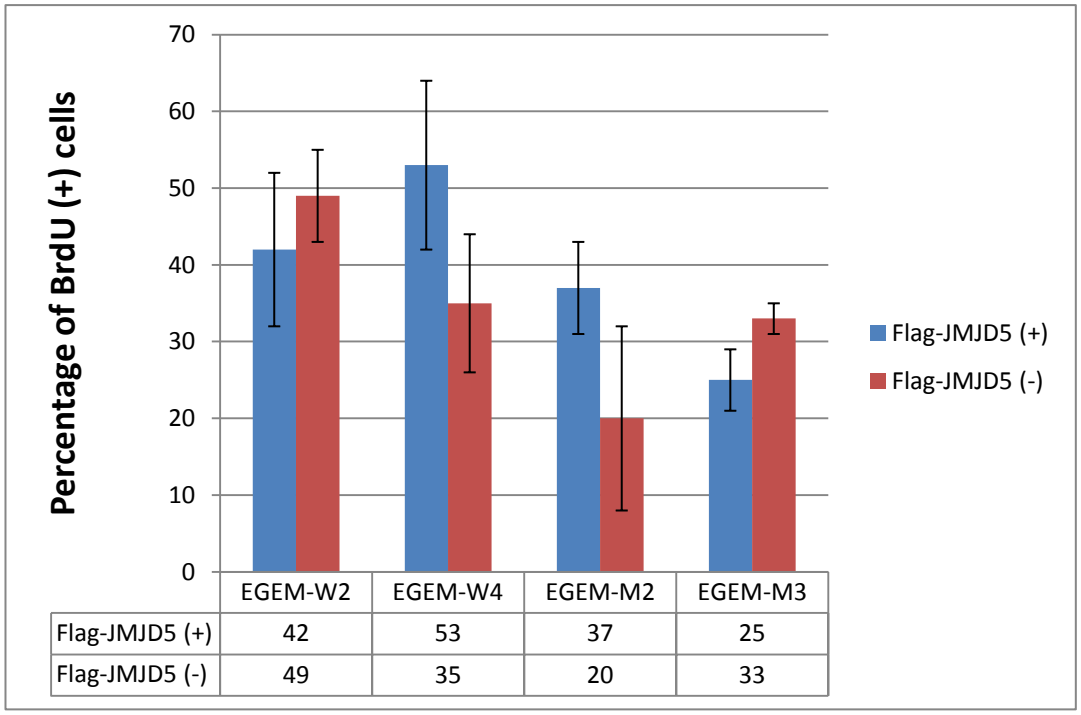

	EGEM-W2	EGEM-W4	EGEM-M2	EGEM-M3
Flag-JMJD5 (+)	42	53	37	25
Flag-JMJD5 (-)	49	35	20	33

Figure 4.15: BrdU positivity for Flag-JMJD5 (+) and Flag-JMJD5 (-) subpopulations of each clone.

(The percentages are indicated at the bottom of the graph.)

wild type clones decreases 7 % in EGEM-w2 but increases 18 % in EGEM-w4. In mutant clones, there is a 17 % increase in EGEM-m2, while there is an 8 % decrease in EGEM-m3. However, it seems that the changes in BrdU positivity between Flag-JMJD5 (+) and Flag-JMJD5 (-) populations are inconsistent and not substantially different. As a result, BrdU double staining results show the nuclear localization of JMJD5 protein; however, JMJD5 seems to be ineffective on cell growth.

4.8.3 Cell Cycle Analysis by Flow Cytometry

As our cell lines were heterogenous in terms of ectopic JMJD5 expression, we perfomed cell cycle analyses on JMJD5-positive and JMJD5-negative cells of the

same cell populations by double staining with anti-flag antibody and propidium iodide. Flow cytometry procedure with EGEM-w4, EGEM-m2 and EGEM-e1clones was applied to find out any phenotypic clue in cell cycle patterns of JMJD5-overexpressing clones. In Table 4.6, FITC signals of the clones and isotype control are shown. Isotype control has a very low FITC signal, whereas EGEM-e1 has relatively considerable background signal compared to isotype. EGEM-w4 and EGEM-m2 samples, on the other hand, have about 4-fold higher FITC signal than EGEM-e1, indicating the presence of Flag-JMJD5 expressing cells in the populations. Using the EGEM-e1 background signal as a threshold, a subpopulation of cells with higher FITC than threshold value were gated and further analyzed for DNA staining. The cell cycle patterns and average percent distributions for each cycle phase are illustrated in Figure 4.16 and Table 4.7, respectively. According to the quantitative distribution result, in both mutant and wild type clones, there are mild decreases in G1 and S phases. In contrast, G2/M phase cell fraction was raised from 16.3% in control clones to 20.4 and 19.3 % in wild-type and mutant JMJD5 clones, respectively. Thus there was 25% and 18% increase in wild-type and mutant JMJD5 clones, respectively. This slight change might be important in shedding light on the role of JMJD5 in liver cancer. Furthermore, it seems that this change is independent of H321A mutation in Jumonji C domain.

Table 4.6: Mean FITC signals for the clones and isotype control

Clone	Mean FITC signal
Isotype Control	1941.21
EGEM-e1	19277.14
EGEM-w4	79921.57
EGEM-m2	74231.30

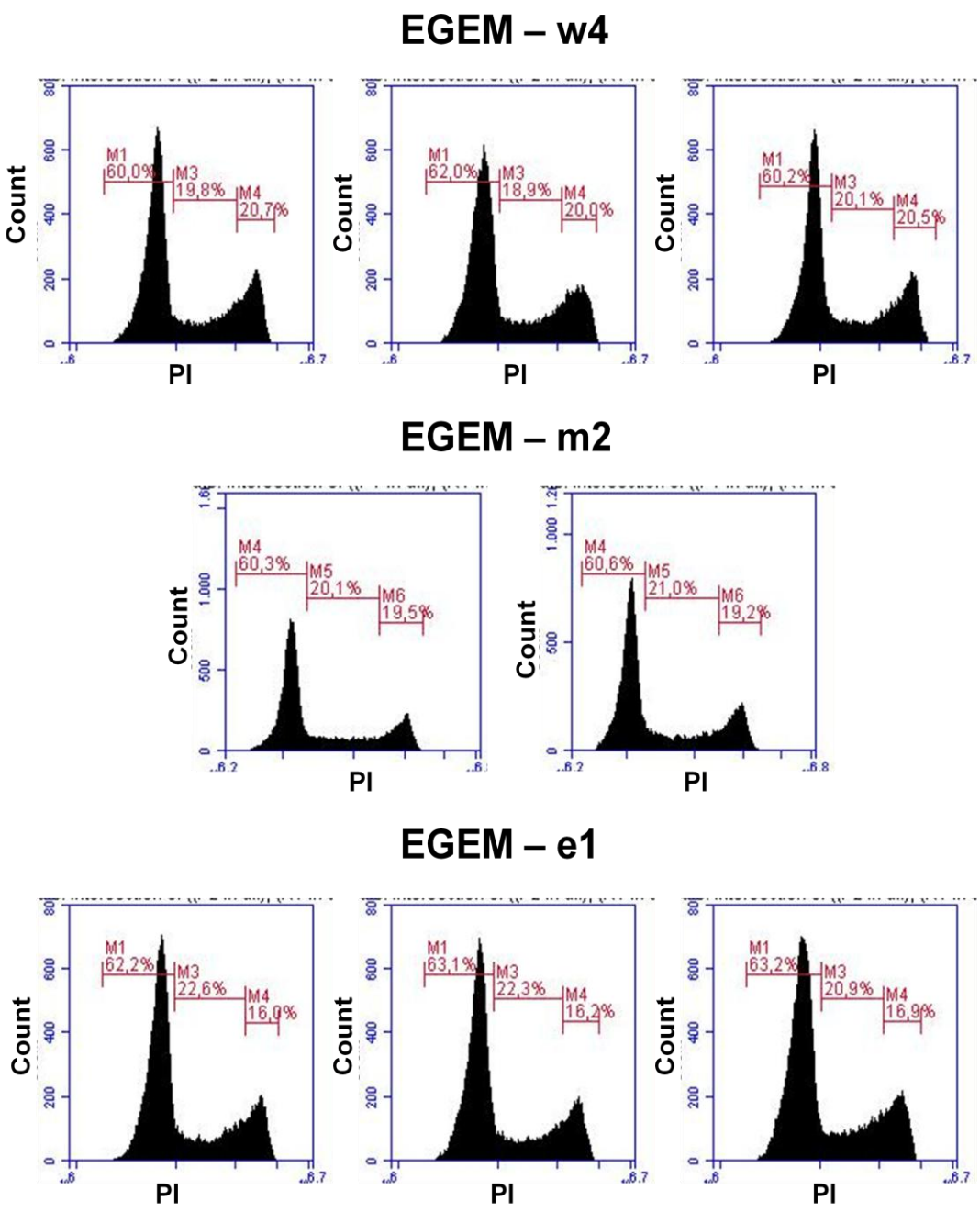

Figure 4.16: Cell cycle analysis for stable clones

(Horizontal axis indicates propidium iodide signal in logarithmic scale, while vertical axis indicates the number of cells in linear scale. The results are triplicate for EGEM-w4 and EGEM-e1 but duplicate for EGEM-m2. The percentage of cells in each cell cycle phase are indicated on the graphs.)

Table 4.7: The average percentage distribution of isogenic clones in cell cycle phases

	EGEM-w4	EGEM-m2	EGEM-e1
G1	60.74	60.47	62,85
S	19.57	20.555	21,96
G2/M	20.4	19.375	16,35

4.9 Analysis of Isogenic Sub-clones with High JMJD5 Expression

The effects of JMJD5 overexpression on phenotype, proliferation and cell cycle patterns of stable clones were either mild or unnoticeable. This could be due to a lack of effect due to JMJD5 expression or alternatively the partially positive expression of ectopic JMJD5 could hinder any potentially important effect. In order to increase the positivity of JMJD5, wild type and mutant stable clones were seeded in very low densities and allowed to form single positive colonies under optimal 9 μg/ml puromycin selective pressure. From this strategy, it was expected that single clones with 100 % JMJD5 positivity could be obtained. After a few-week selection, the emerging single cell-derived colonies were isolated, further grown in bigger plates and tested for JMJD5 positivity.

4.9.1 Immunoperoxidase Staining Analysis

In Figure 4.17, immunoperoxidase staining with Flag monoclonal antibody for some of the isolated stable clones is illustrated. All of the clones were induced with doxycycline for 48 hours.

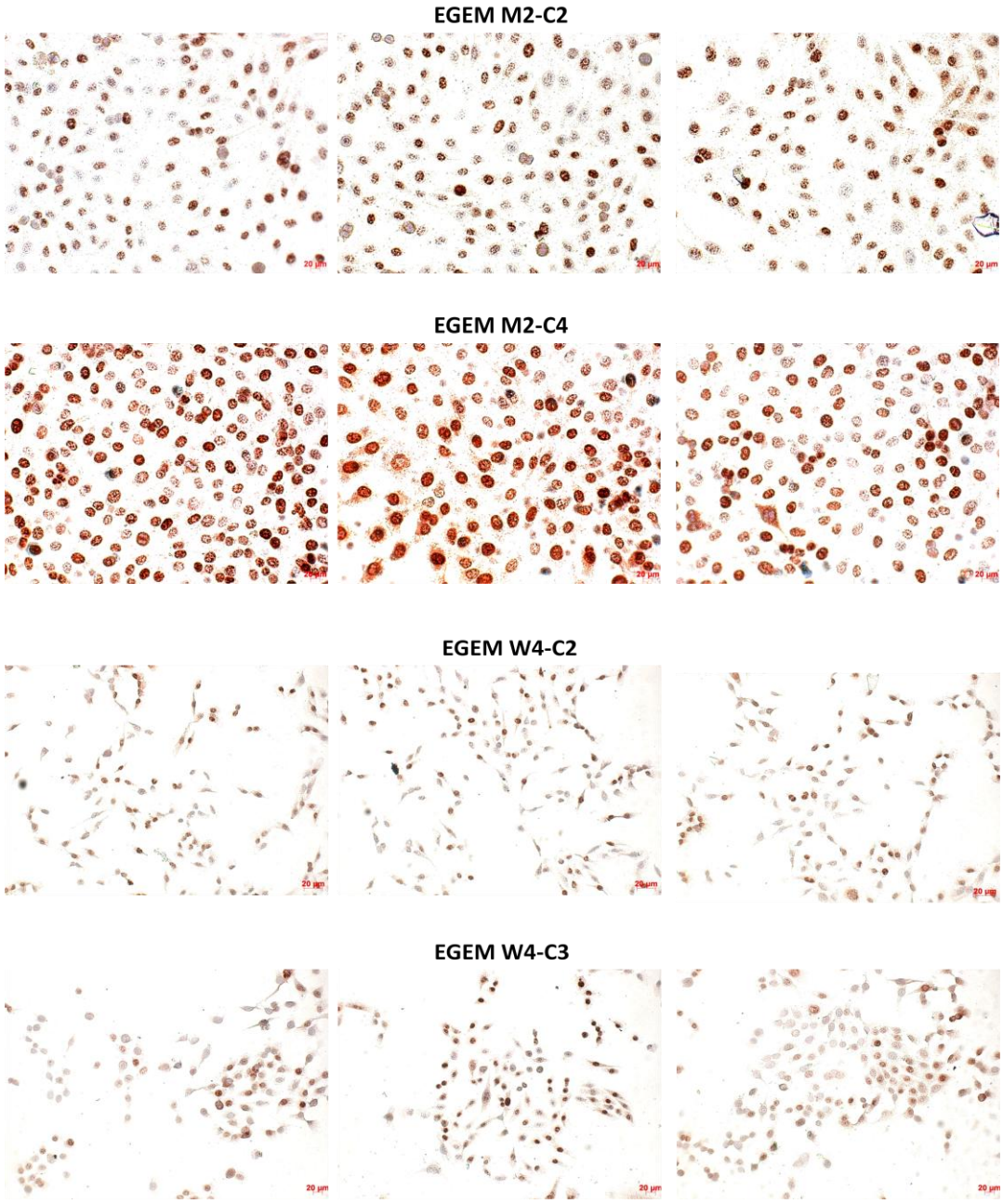

Figure 4.17: Immunoperoxidase staining for isolated sub-clones of EGEM-M2 and EGEM-W4 stable clones

(The images of EGEM-M2 sub-clones were taken at 40 X, while those of EGEM-W4 were taken at 20 X. For each sub-clone, triplicate images are shown.)

Despite the expectation of obtaining sub-clones with full JMJD5 positivity, the staining result indicates that the positivity increases greatly but not reaching to hundred percent. As shown in Figure 4.17, not only the percentage of exogenous JMJD5 expression but also the level of expression changes between clones and even

between the cells. Higher positivity and expression level are observed in EGEM M2-C4 clone compared to others. In order to quantitatively determine the JMJD5 positivity, JMJD5 (+) cells were counted and percentages were calculated as depicted in Table 4.8.

Table 4.8: Immunoperoxidase count data and the mean Flag-JMJD5 positivity of isolated stable sub-clones

Clone	Region 1	Region 2	Region 3	Average % Flag (+)
M2-C2	109/156	82/142	79/107	67
M2-C4	173/230	118/132	141/167	82
W4-C2	92/153	75/154	104/154	59
W4-C3	72/127	92/127	93/175	60

According to the counting results, percentage of Flag-JMJD5 positivity in sub-clones changes between 59 % and 82 %. It means that exogenous JMJD5 expression substantially increased from 40-50 % up to 60-80 % in these clones. Using those newly-isolated sub-clones of high positivity in later assays, the phenotypic effect of JMJD5 overexpression or mutation could be better estimated.

4.9.2 Wound Healing of Stable Sub-clones

Wound healing capacity of the cells gives an insight into their migration. As the migration ability of the cells increase, they close the wound faster. In order to investigate the contribution of JMJD5 overexpression to this property in our clones, wound healing assay was applied, and the results are shown in Figures 4.18 and 4.19.

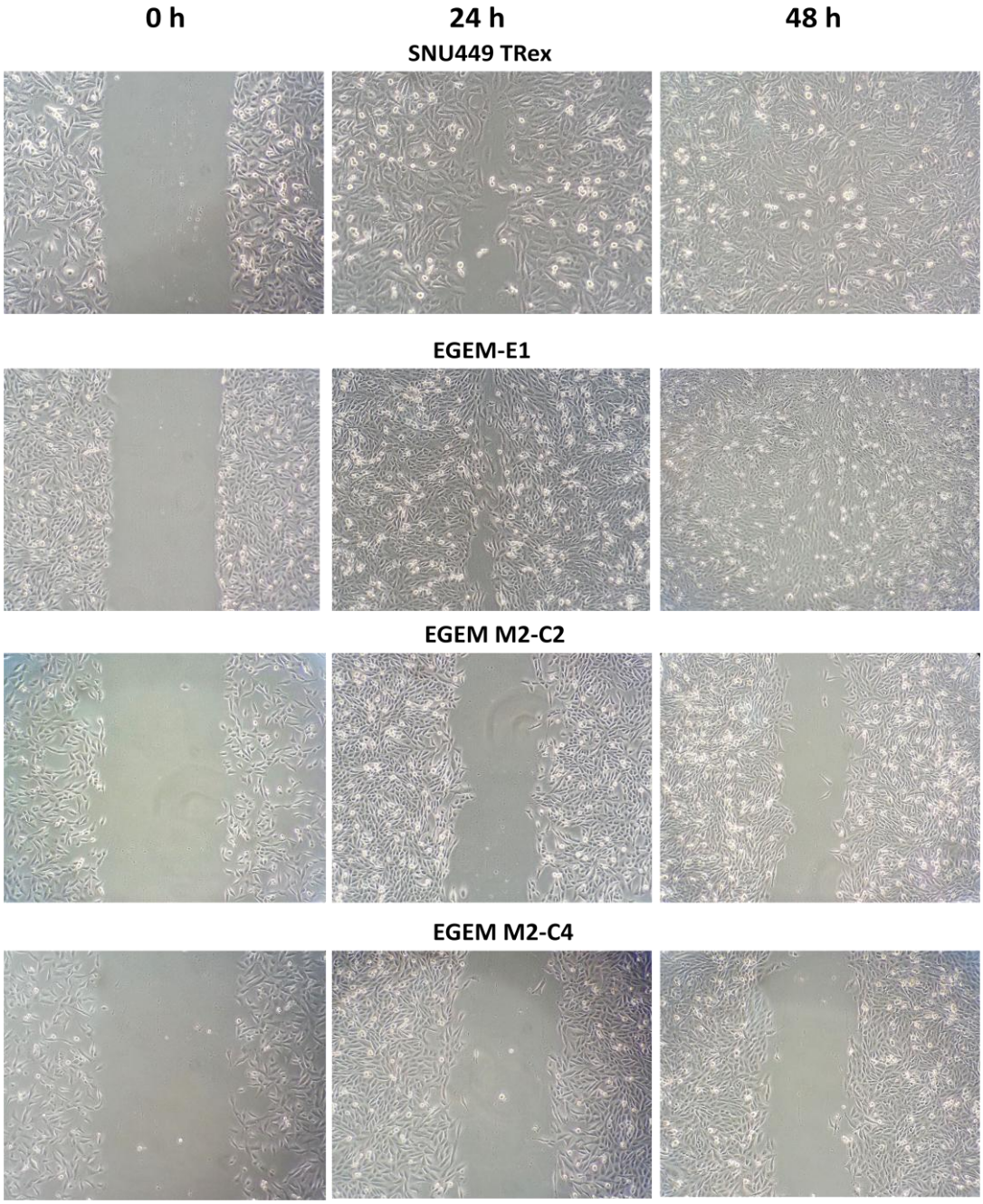
0 h
24 h
48 h
SNU449 TRex
EGEM-E1
EGEM M2-C2
EGEM M2-C4

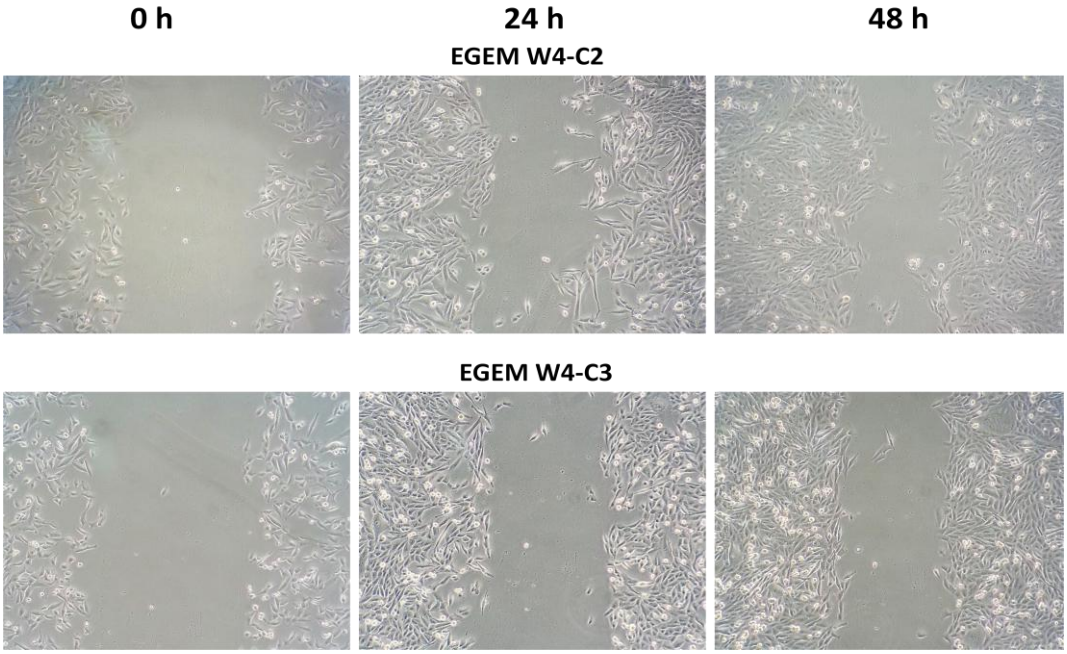

Figure 4.18: Wound healing of stable clones at 0, 24 and 48 hours

(The images were taken at 10 X.)

According to this figure, SNU449-TRex and EGEM-e1 cells close the wound quickly, with a very small gap at the end of 24 hours and a complete closure at the end of 48 hours. However, the wound healing rates in the wild type and mutant isogenic sub-clones are quite similar but much slower relative to SNU449-TRex and EGEM-e1 cells. The gaps are still quite large and clearly detectable even after 48 hours. In Figure 4.19, crystal violet staining of the cells after 48 hours is pictured. This figure better compares the scar-closing efficiency of the clones.

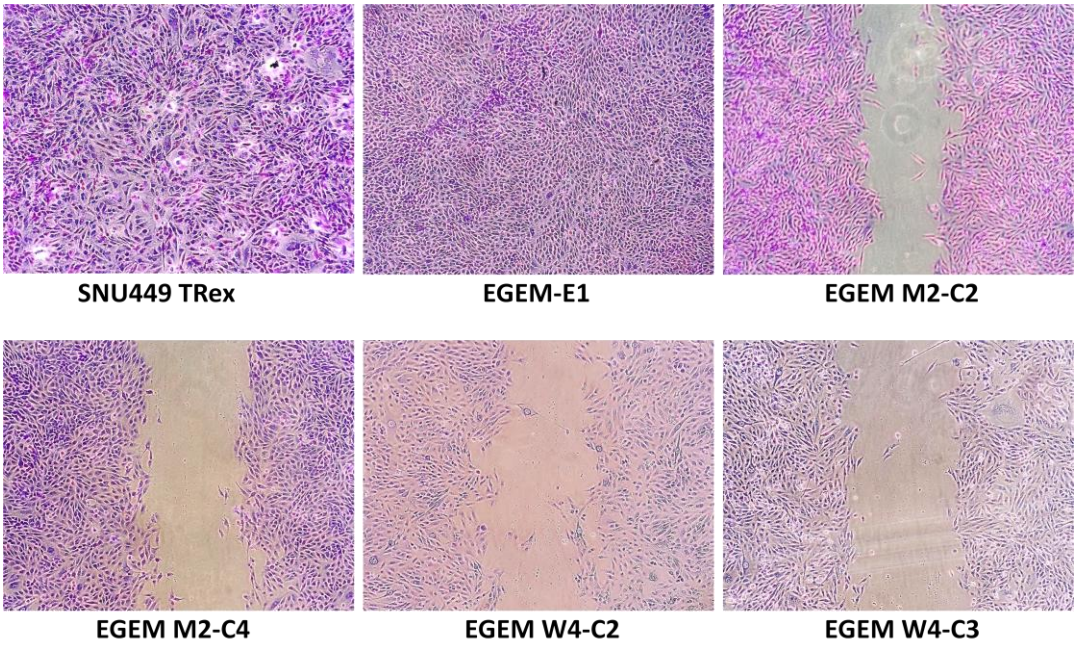

Figure 4.19: Wound healing of stable clones after 48-hour incubation

(The cells were stained with 2 % crystal violet, and images were taken at 10 X.)

The wound healing assay results indicate that the migration ability of mutant and wild type clones is much slower than empty and SNU449-TRex clones, proposing that JMJD5 protein might decelerate the motility capacity of a tumor regardless of H321A mutation.

4.9.3 Anchorage-independent Growth of Stable Sub-clones

Soft agar colony formation assay was performed to assess the effect of JMJD5 on anchorage-independent growth of stable clones. Immortal cell lines normally cannot grow in agar or agarose media because of the requirement of solid attachment to a surface. However, when these cells are exposed to activities of oncogenes or carcinogens, they are able to grow in these fluidic media without presence of attachment to a surface. This assay stringently gives clue about the transformation of the cells into malignancy, and it is also regarded to indicate the in-vivo carcinogenesis potential of cells.

Soft agar results of stable JMJD5 clones are indicated in Figure 4.20. The picture of

at 4X

EGEM-E1

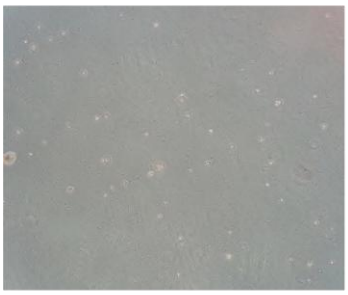

EGEM M2-C2

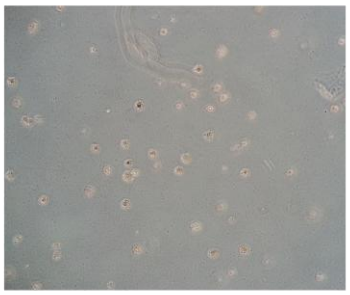

EGEM M2-C4

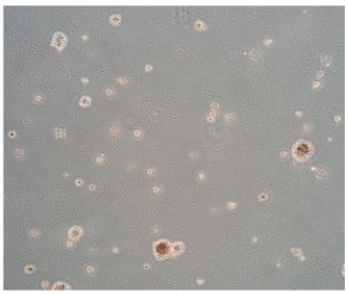

EGEM W4-C2

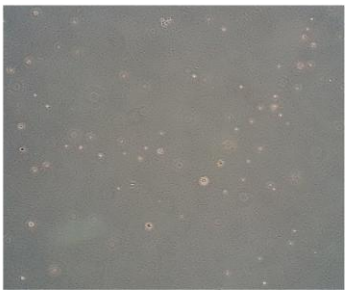

EGEM W4-C3

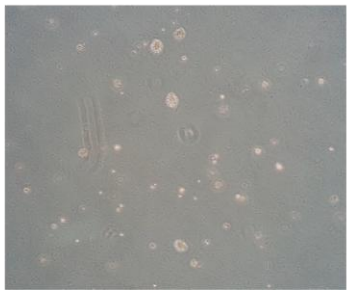

at 10X

EGEM-E1

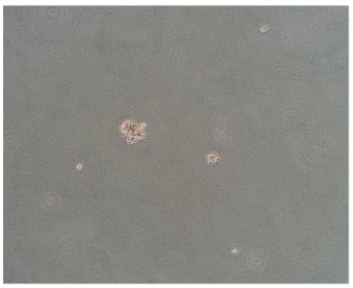

EGEM M2-C2

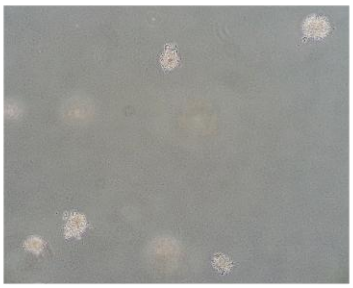

EGEM M2-C4

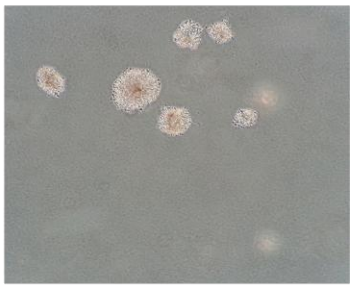

EGEM W4-C2

EGEM W4-C3

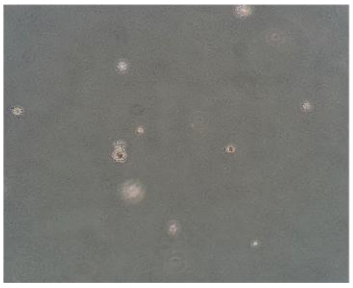

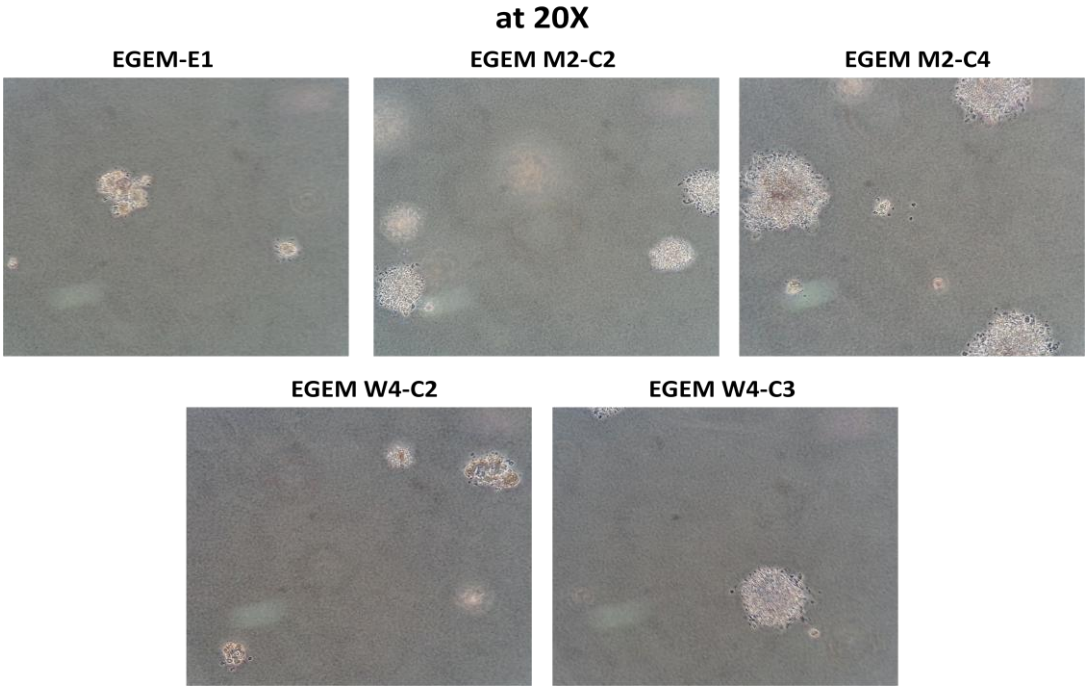

Figure 4.20: 4X, 10X and 20X pictures of formed colonies for stable clones on soft agar

plates were taken under inverted light microscope at 4X, 10X and 20X. Despite the presence of size differences among the clones, all of them were able to produce colonies in soft agar. The morphology of the colonies was similar. According to the represented images of each clone, EGEM W4-C3, EGEM M2-C2 and EGEM M2-C4 appeared to form larger and visible colonies, whereas EGEM W4-C2 and EGEM-E1 clones seemed to form smaller and hardly noticeable colonies. The colony size seemed to be increasing from empty to wild type and from wild type to mutant clones.

To obtain reproducible results, two successive experiments with two biological replicates for each clone were performed; comprising four biological replicates four each clone in total. In order to better quantify the colony formation, colony number in 11 represented regions of four replicates for each clone was counted under inverted light microscope at 4X considering the colonies in different layers, and their

mean colony number fold changes were calculated (Figure 4.21).

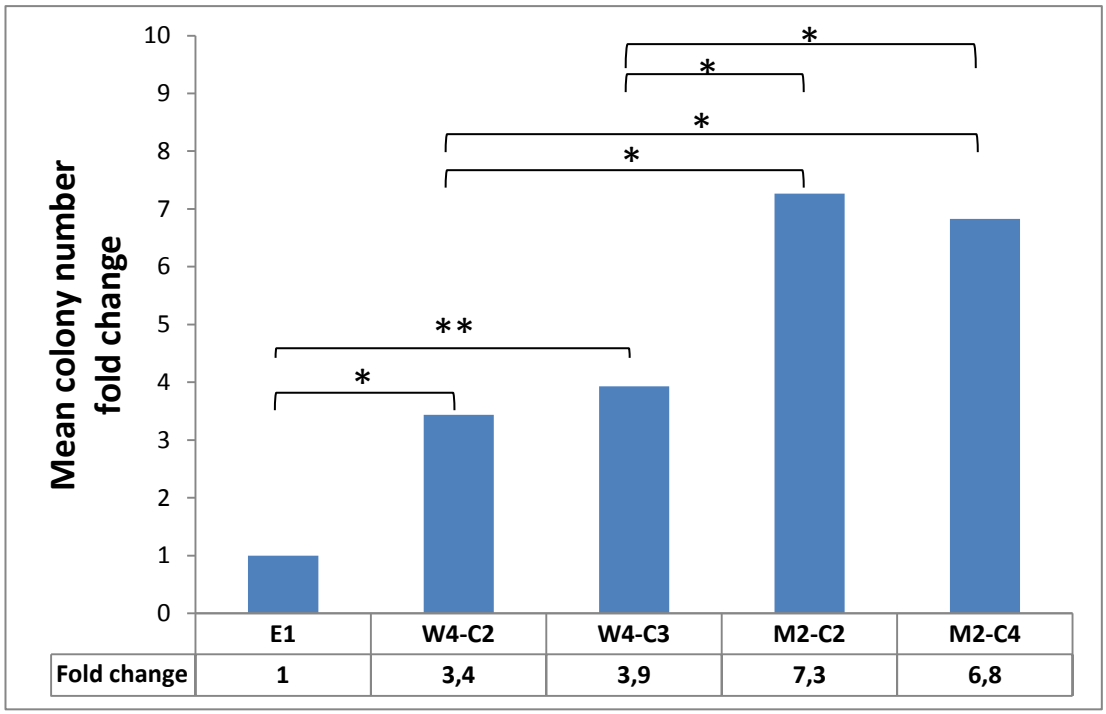

Figure 4.21: Mean colony number fold change of isogenic clones with respect to EGEM-e1 (empty) clone.

(Paired two-tailed t test with n = 11; *p < 0.05 and **p < 0.001)

As shown in Figure 4.21, EGEM-E1 had the lowest colony formation with designation of 1 fold change. EGEM M2-C2 and EGEM M2-C4 reached the highest mean colony numbers, being statistically significant compared to all wild type and empty clones. EGEM W4-C2 and EGEM W4-C3 clones formed the intermediate number of colonies, being statistically significant compared to empty clones. To sum up, soft agar assay indicated that mutant stable sub-clones had the largest size and highest number of colonies, wild type clones had the intermediate size and number of colonies, and empty clone had the lowest values for both.

4.9.4 Cell Cycle Analysis of Isogenic Sub-clones by Flow Cytometry

Cell cycle patterns of isolated sub-clones were also analyzed with FACS method to check whether the mild changes in cell cycle distribution of the cells observed in Figure 4.16 are also present in isogenic clones with higher JMJD5 levels. Table 4.9

compares mean FITC signals detected for each stable clone, sub-clone and isotype control.

Table 4.9: Mean FITC signals for the isogenic stable clones and isotype control

Clone	Mean FITC signal
Isotype Control	1941.21
EGEM-e1	19277.14
EGEM-w4	79921.57
EGEM-m2	74231.30
EGEM w4-c2	142620.50
EGEM w4-c3	149367.20
EGEM m2-c2	126274.10
EGEM m2-c4	100508.90

The increase in JMJD5 positivity observed in immunoperoxidase staining results was also confirmed with FITC signals in this table. FITC signals of the sub-clones isolated from EGEM-w4 and EGEM-m2 clones were about 1.5 – 2 times higher than the original clones. The signal from EGEM-e1 clone was considered as a background signal, and the cells having higher signals than this level were gated as JMJD5 positive cells. Then, the cell cycle distributions of these positive cells were particularly investigated, and the results are indicated in Figure 4.22.

EGEM m2 - c2

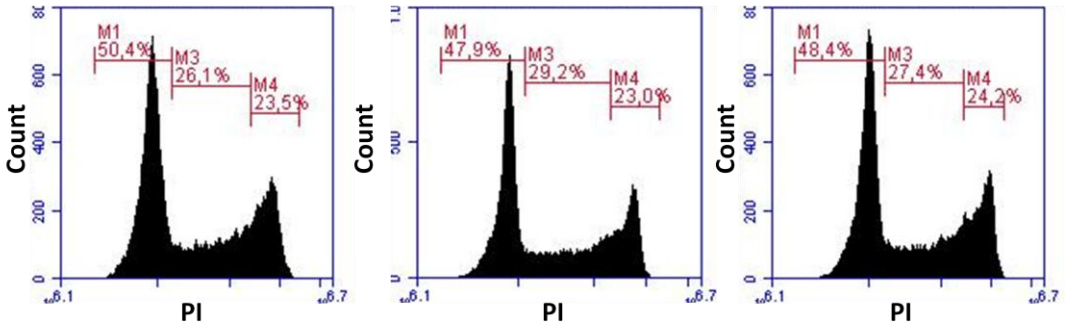

EGEM m2 – c4

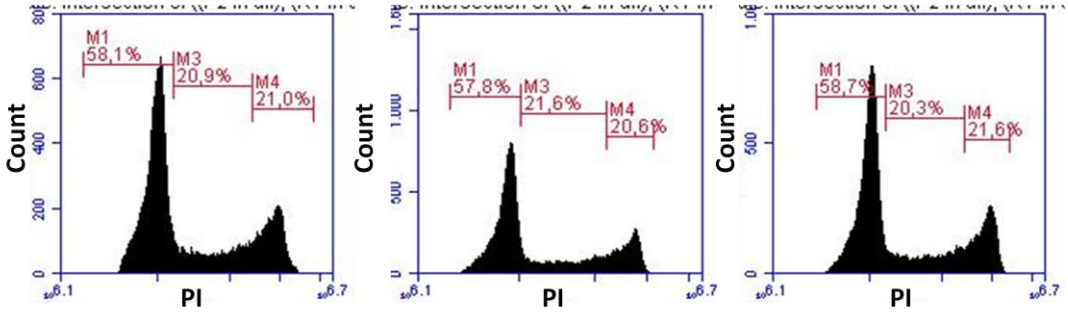

EGEM w4 – c2

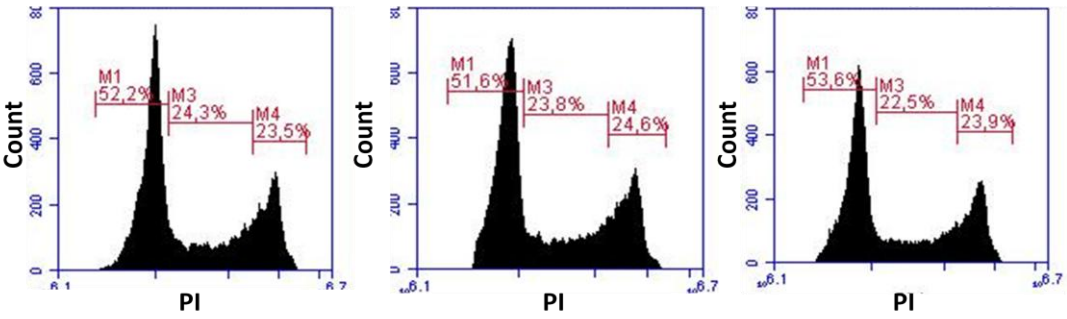

EGEM w4 – c3

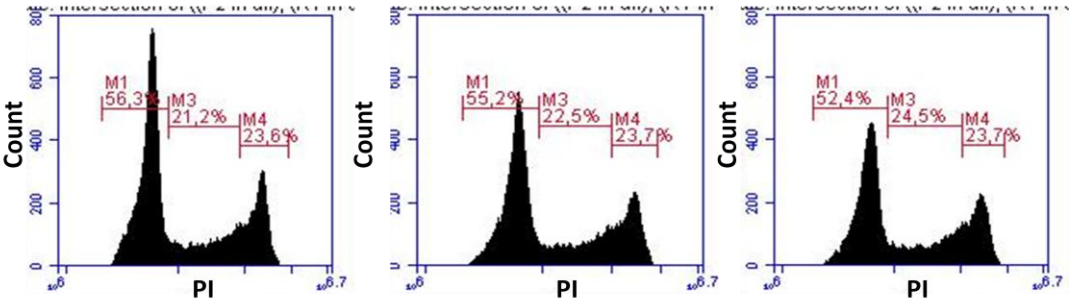

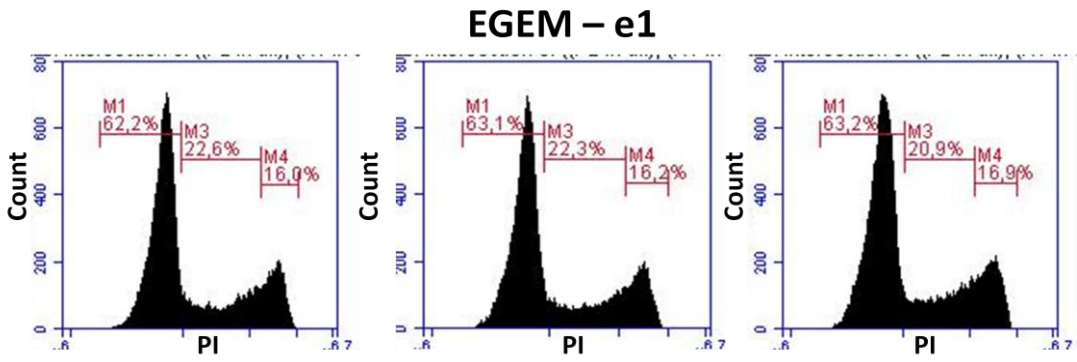

Figure 4.22: Cell cycle analysis for unsynchronous isogenic sub-clones

(Horizontal axis indicates propidium iodide signal in logarithmic scale, while vertical axis indicates the number of cells in linear scale. The results are triplicate for each clone. The percentage of cells in each cell cycle phase are indicated on the graphs.)

Using the percentages on each graph, the mean distribution percentages were calculated as shown in Table 4.10. The mild changes in G1 and G2/M distributions

Table 4.10: The mean percent distributions of stable clones in cell cycle phases

	EGEM w4-c2	EGEM w4-c3	EGEM m2-c2	EGEM m2-c4	EGEM-w4	EGEM-m2	EGEM-e1
G1	52.48	54.64	48.89	58.19	60.74	60.47	62.85
S	23.52	22.76	27.56	20.95	19.57	20.56	21.96
G2/M	23.99	23.65	23.58	21.06	20.40	19.38	16.35

of low expression clones relative to the empty clone developed remarkably in high expression clones. When compared to control clone, two wild-type JMJD5-overexpressing clones displayed consistent increase in G2/M phase cells going from 16.5 % to 23.8 % on average. This represents a 44% increase in wild-type JMJD5-overexpressing clones. There was also a consistent increase of about 35% in G2/M cells in mutant JMJD5-expressing clones. This was accompanied with a decrease in G1 phase cells.

4.9.5 Sensitivity of Stable Clones to Adriamycin

Adriamycin, also known as Doxorubicin, is a drug widely used in cancer chemotherapy. It inhibits DNA replication by intercalating double strand and stabilizing topoisomerase II complex [42, 43]. Consistent with our hypothesis, wound healing and FACS results, it can be suggested that JMJD5 could play a role in G2 arrest as a tumor suppressor. The tumor suppressor effect of JMJD5, if present, could be improved using another growth inhibitor which acts on another arrest mechanism if the interaction is synergistic. Hence, the sensitivity of the stable clones induced with doxycycline for 72 hours to various concentrations of adriamycin was investigated using SRB method. Figure 4.23 and 4.24 show the survival of clones in both qualitative and quantitative terms, respectively.

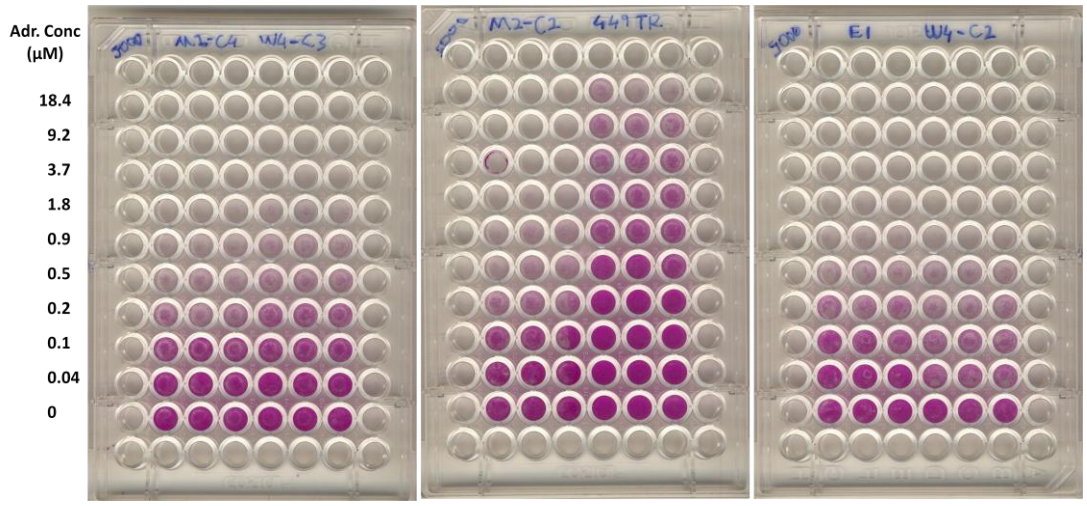

Figure 4.23: SRB staining of isogenic clones under different adriamycin concentrations on 96-well plates

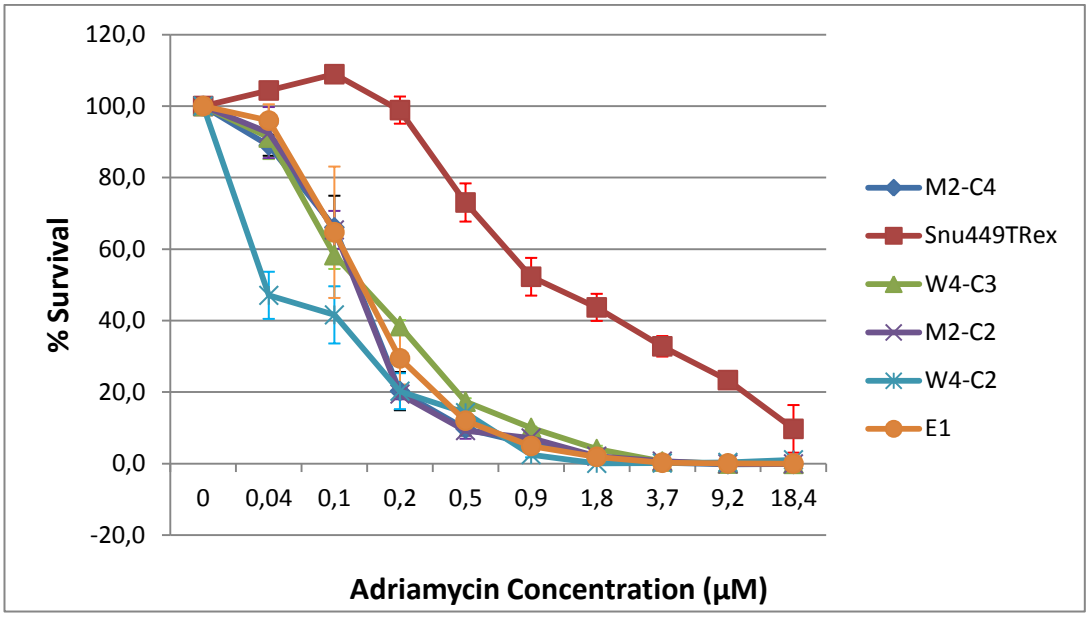

Figure 4.24: Survival curves of stable clones with respect to adriamycin concentration

According to the picture and the graphical representation, there is no considerably important difference between empty, wild type and mutant clones in terms of survival. SNU449-TRex cells, however, are more resistant to this drug than all other clones. The conclusion from this assay is that the sensitivity of isogenic clones is not affected by adriamycin treatment.

CHAPTER 5

DISCUSSION

Two preliminary studies done by our past and current group members showed JMJD5 downregulation in HCC. One of them was an in silico microarray analysis showing the smooth downregulation of JMJD5 through the increased disease stages of liver. The other study compared HCC and cirrhotic tissue sample pairs of 15 patients and revealed that JMJD5 levels reduced in HCC relative to cirrhosis in most of the patients. Two relatively recent studies on lung cancer and Blm-deficient mice also considered JMJD5 as a potential tumor suppressor gene [31, 32]. Referring to the preliminary data and literature information, in this study, it was hypothesized that JMJD5 might act as a tumor suppressor in liver, resulting in the development of cancer upon its deficiency or loss. This hypothesis was tested by applying several phenotypic, molecular biological and genetic techniques on SNU449-TRex mesenchymal-like liver cancer cell line model.

5.1 The role of JMJD5 in cell proliferation and cell cycle

Despite the several lines of evidence about tumor suppression activity of JMJD5, the counter argument is also equally supported by an important number of reports. Activating cyclin A1 expression, JMJD5 was argued to stimulate cell cycle progression of breast cancer cells [27]. In mice embryos, downregulation of p53-p21 axis was detected, suggesting an oncogenic role for JMJD5 [29, 30]. In order to find out an answer to this controversial issue, expression profiling and certain phenotypic assays showing a direct measure for cell growth were performed.

Microarray results were assessed, firstly, in this respect. Gene set enrichment analysis depending on cellular processes, shown in Table 4.4, indicated that several growth pathways are active in control cells, consistent with the nature of cancer cells.

However, the number of those active growth gene sets diminished in wild type cells. This result suggests that several growth genes and pathways might be downregulated under high levels of JMJD5, addressing JMJD5 as a potential critical regulator on several cell cycle and cell division mechanisms. The effects of JMJD5 on cell growth were further investigated using different methodologies.

SRB and BrdU incorporation assays were carried out for this purpose. In SRB experiment, the quantitative readings did not differ considerably between wild type, mutant and empty stable clones. However, one cannot claim that JMJD5 has no influence on HCC cell growth by only considering this data because of the heterogeneity of the clones for exogenous JMJD5 expression. Due to the heterogeneity, a portion of cells in the population which have strong JMJD5 levels might affect the tumor growth in some way, but this effect may not be noticed in the total population because of abundant negative cells. Those negative cells might be neutralizing the overall phenotype of the cells. Hence, BrdU and flag double staining strategy was followed to compare the BrdU incorporation rates of Flag-JMJD5 (+) and Flag-JMJD5 (-) cells in the same culture. Although there were drastic changes between the BrdU positivity of Flag (+) and Flag (-) cells within the same clone, they were not following a consistent pattern. A substantial incline in BrdU positivity occurred in a wild type or mutant clone, whereas a substantial decline occurred in the other wild type or mutant clone. That is, the results of the same type of clones were inconsistent. Because of this inconsistency, the BrdU changes could not be attributed to overexpressed JMJD5 gene. As a result, these assays were inconclusive in giving a clue on cell proliferation effect of JMJD5. To better compare the cell proliferation differences between JMJD5 wild type, mutant and empty clones; SRB assay could be repeated with high expression isogenic clones, and BrdU signal could be measured by FACS device, giving a more reliable quantitative result instead of counting with naked eye.

In the literature, several studies have reported JMJD5 as a cell cycle regulator in a H3K36me2 demethylase dependent manner. In breast cancer, induction of cyclin A1 expression by JMJD5 was shown [27]. In mouse embryos, JMJD5 was found to

have essential developmental functions through inhibition of p53-dependent cell cycle arrests and downregulation of p21 cyclin-dependent kinase inhibitor [29, 30].

In microarray data, Wnt signaling pathway components were found to be altered in a way that increases Wnt signaling under JMJD5 induction. Retinol metabolism components were also significantly upregulated under high levels of JMJD5. These pathways have been shown to be involved in developmental processes [44, 45]. Particularly Wnt, have important activatory roles in cell-cell communication, cell proliferation, differentiation and migration [45]. In addition, cellular differentiation and G2-M transition gene sets were detected to be enriched in EGEM-w4. Most interestingly, gene set enrichment analysis in empty clone gave several cell cycle progression and DNA replication-related processes, meaning they are abnormally active in liver cancer cell model. However, in wild type clone, the analysis results did not indicate most of those cell cycle-related pathways. All the literature knowledge and microarray results, collectively, point to a critical role of JMJD5 in the cell cycle and development of the organism.

Cell cycle analysis was applied to have an insight into the function of JMJD5 on the regulation of cell cycle. As a potential tumor suppressor, whether it blocks, decelerates or leads to an accumulation in any phase of the cell cycle was assessed using unsynchronized SNU449-TRex clones. Most noticeable result was that in JMJD5 stable clones cell distribution in G1 phase decreased remarkably, while that in G2/M phase increased remarkably. This change was more strongly observed as the level of JMJD5 expression increased in the sub-clones, strongly suggesting the role of JMJD5 on this phenotype. Based on this observation, it can be proposed that JMJD5 might play a cell cycle regulatory role in two ways. One way is that JMJD5 might be acting as an activator of cell cycle, facilitating the passage of G1/S and G2/M phases. Since many reports have indicated its cell cycle-activating role and requirement for developmental processes, this alternative role seems to be plausible. The other alternative way is that JMJD5 might play an inducer role in G2/M cell cycle arrest mechanisms. MCF7 breast cancer cells underwent G2/M arrest upon silencing of JMJD5, exhibiting the similar phenotype to our cells with a substantial decrease in G1 and S cell percentage but a substantial increase in G2/M cell

percentage [27]. It is also possible that JMJD5 might be acting differently depending on the context; meaning that it may be a cell cycle activator in embryos or in progenitor cells, whereas it may be a cell cycle blocker in adult cells. Additionally, it may behave as a cell cycle activator in breast cancer but as a suppressor in liver cancer. The absence of cell cycle progression-associated gene sets under JMJD5 induction also supports its suppressor effect on cell cycle of liver cancer cells. To better understand cell cycle regulation in SNU449 cells under JMJD5 overexpression, further analyses could be done by using synchronized cells.

5.2 Role of JMJD5 in cell migration and morphology

As in the case of many types of cancer, metastasis and malignant cell transformation make critical contributions to the development of liver cancer. Invasion and metastasis is one of the hallmarks of cancer [46]. Poorly differentiated HCC tumor has metastasis property [7]. Therefore, to make an inference on effect of JMJD5 on metastasis, migration of SNU449 cells under the effect of upregulated JMJD5 was investigated.

In relation to metastasis, microarray study detected an upregulation in FAP (fibroplast activation protein alpha), which is known to be upregulated in epithelial cancers and associated with epithelial-mesenchymal interactions (from NCBI-Gene); and also a downregulation in CDH4 (cadherin 4), a typical cadherin from cadherin superfamily involved in brain segmentation and neuronal outgrowth (from NCBI-Gene). Importantly, a gene set responsible for positive regulation of epithelial cell proliferation were shown to be enriched in JMJD5-overexpressing cells. NF-KB target genes involved in matrix, adhesion and cytoskeleton were also shown to be increased in wild type cells. Considering all these data, microarray results imply a potential function of JMJD5 in epithelial-mesenchymal transitions, in favour of epithelial characteristics.

Wound healing capacity is an indication for the migration of tumor cells. According to the results of the assay, the motility of the cells decreases as JMJD5 levels increase regardless of mutation in JmjC domain. This points out to the tumor suppressor role of JMJD5 as stated in the hypothesis. SNU449 cells, corresponding

to a considerably high grade of HCC tumor, have mesenchymal-like metastatic features. We would like to add here some reserves to our observations. Our observed decreased mobility in the presence of JMJD5 has not yet been confirmed by an independent laboratory (Prof. Neşe Atabey, personal communication). If our observations are confirmed, the decline observed in this property could be possibly explained by the increase in their epithelial features. The expression changes summarized above might be underlying this phenotypic alteration. As suspected molecular mediators, expression of these factors could be further investigated in protein and RNA levels upon JMJD5 overexpression. Additionally, the markers of mesenchymal to epithelial transition should also be checked. Interestingly, despite the drastic change in migratory phenotypes between the clones, no noticeable morphological difference was observed.

5.3 Role of JMJD5 in anchorage-independent colony formation

Liver injury followed by genomic instability loss is an early event in HCC development, leading to turning of normal hepatocytes into malignant phenotypes [6, 7]. Hence, to gain an insight into effect of JMJD5 on malignant transformation, anchorage-independent colony formation of SNU449 cells under the effect of upregulated JMJD5 was investigated.

Colony formation capacity of the JMJD5 stable clones was tested by soft agar assay. Intriguingly, mutant cells had the highest colony formation capacity, wild type cells had the intermediate capacity, and empty cells were the least capable clone among them. This result suggests that JMJD5 overexpression induces anchorage-independent growth and might increase tumorigenecity, mutant clone having the greatest effect. In contrast to the wound healing outcomes, soft agar assay implicates a possible oncogenic role for JMJD5. These seemingly contradictory results may be explained by the potential diversity of JMJD5 targets, as a histone demethylase in chromatin and as a protein hydroxylase in soluble nucleus [26]. Its presence in both cytoplasm and nucleus was detected in *A. thaliana*, suggesting dual functions depending on cellular location [25]. Putative interacting motifs detected on JMJD5 for nuclear receptor and methyltransferase binding also suggest participation into

complex biological networks [27]. It could briefly be stated that JMJD5 may play a tumor suppressor or tumor inducer role depending on context, location and interacting partners, affecting the overall phenotype. Assuming that JMJD5 increases epithelial characteristics, another reason could be that JMJD5-overexpressing cells tend to grow in close proximity, forming clumps due to the strong cell to cell adhesion. Hence, it should be noted that JMJD5 might seem to have induced tumor growth in soft agar assay due to increasing the expression of epithelial genes rather than carrying an oncogene property.

5.4 JMJD5 and drug sensitivity

Adriamycin, also known as doxorubicin, is a drug widely used in chemotherapy of many cancers. It acts through intercalation of DNA and stabilization of topoisomerase II complex, preventing replication of DNA and arresting the cells in S phase [42, 43].

It was estimated according to our experimental results that JMJD5 could be a potential tumor suppressor through arresting the cell cycle at G2/M phase. Since adriamycin is known to block cell cycle at S phase, JMJD5-overexpressing cells were thought to be possibly more sensitive to adriamycin treatment than empty cells. Contrary to this expectation, there was no considerable difference between the survival of mutant, wild type and empty clones. This could be due to the fact that the effect of JMJD5 upregulation on cell cycle arrest is so tiny that it is dominated by that of adriamycin. Since it is very effective on cells, even very low doses of adriamycin may be enough to arrest all the cells without any contribution of JMJD5.

5.5 The importance of H321A mutation in JmjC domain

Histidine-321 (His-321) amino acid is located in the catalytic site of JMJD5, and plays a critical role in coordination of Fe (II) with Asp-323 and His-400 [28]. It was shown that JMJD5could not carry out its demethylation activity on H3K36me2, and all the biological effects of wild type JMJD5 overexpression were reversed upon

H321A mutation, emphasizing the importance of His-321 residue in biological function of the protein [27].

Knowing the crucial role of it, the effects of H321A mutation on the phenotype and the activity of JMJD5 was also investigated in our experiments. In wound healing, flow cytometry, adriamycin sensitivity and cell proliferation assays, no phenotypic difference was detected between wild type and mutant clones of JMJD5. To be certain about unchanged phenotypes, these assays could be repeated. However, based on these observations, it can be said that H321A mutation, despite disrupting histone demethylase activity, does not influence histone demethylase-independent functions of JMJD5. Apparently, differential histone demethylase activity of wild type and mutant clone does not create any phenotypic changes detectable with these methods. The phenotypic changes observed in both wild type and mutant cells compared to empty cells are most probably caused by histone demethylase-independent functions of JMJD5. Interestingly, mutant and wild type clones significantly differed in their colony formation capacities in soft agar. Mutant clone appeared to form larger and greater number of colonies than wild type clone. This result suggests that H3K36me2 demethylase activity plays a role, to some extent, in prevention of anchorage-independent growth through yet unknown downstream interactions. Upon its loss, cells seem to gain more aggressive and tumorigenic character. Therefore, it can be said that JMJD5 has a partial tumor inhibitory role via its JmjC histone demethylase activity.

5.6 JMJD5 as a tumor suppressor in the pathogenesis of HCC

In this study, the relationship of JMJD5 with development of liver cancer was investigated applying several methods. Although JMJD5 could not be associated with a specific function in liver cancer, there is sufficiently high number of data to make an inference on the role of JMJD5 in liver tumor growth. Analysis of expression profiles showed that cell cycle-activating genes are less active, genes responsible for differentiation and genes giving rise to epithelial characteristics are upregulated in wild type cells compared to empty cells. Among our in vitro studies, two types of responses were consistently associated with JMJD5 overexpression: (1)

Increase in the fraction of G2/M phase cells; (2) increased anchorage-independent colony formation ability. We do not know how these changes will affect HCC tumor growth. The increase in G2/M phase cells could indicate increased mitotic activity which is positively correlated with tumor growth. The increase in anchorage-independent colony forming ability is used as an in vitro test for in vivo tumorigenic potential of cancer cells [47]. Thus, the overexpression of JMJD5 in HCC cells could also promote in vivo tumor growth. Primarily, these two effects would indicate a tumor promoting activity of JMJD5 expression in HCC tumors. However, this is not compatible with the decreased expression of JMJD5 in tumor cells. Microarray data itself may be misleading because it represents an increase in JMJD5 transcription, rather than an overexpression of JMJD5 protein. Our western blot experiments comparing cirrhosis and HCC provided a mixed response. Although most HCCs displayed a decreased expression, some others displayed no change or even an increased expression. This could be due to different activities of JMJD5 protein as evidenced by the fact that it may either function as a HDM or a protein hydroxylase [26]. These two independent activities may affect tumor outcome differently depending on the cellular environment. The activity of many proteins is controlled by cellular localization and protein-protein interaction which may confer differential abilities to these proteins. An excellent example for this is β-catenin.

CHAPTER 6

CONCLUSION

In this study, several consistent results were obtained from in vitro experiments as well as some inconsistent results. First, BrdU incorporation rate and S phase fraction did not change. Second, cells in G2/M are up, G1 cells are down. This can be due to accumulation of cells at G2 or M phase or a change in the progression during cell cycle: acceleration of G1 events so there is less G1 cells, or slowing down at G2 phase or partial arrest in M phase. But these changes did not affect cell proliferation rates. What it means is not known yet. Third, there was an increase in anchorage-independent colony formation. This definitely points to a promalignant change which may indicate better tumor growth in vivo. Still, this remains to be demonstrated in nude mice experiments. On the other hand, despite observing decreased cell motility, this has not been confirmed by another lab. It should be confirmed by further experiments in order to have a better comment on this data. Differences between wild-type and mutant are also not consistent, so this mutation may have no differential effect compared to wild-type JMJD5 with our tests. Somewhat in vitro data is not compatible with a tumor suppressor effect as suggested by decreased transcript expression. WB data did not show consistent decreased protein expression either, some tumors even expressing more. JMJD5 may be a tumor suppressor or promoter depending on HCC type, or cell type. Beta-catenin is a good example for this. It promotes tumor growth when accompanied by TCF factors in nucleus, but has an opposite effect as a component of E-cadherin cell-cell adhesion complex [48]. Thus, JMJD5 as an HDM or protein hydroxylase may have different effects some serving as tumor promoter, others tumor suppressor.

CHAPTER 7

FUTURE PERSPECTIVES

In vitro experiments on mesenchymal liver cancer cell line SNU449 suggested that JMJD5 might be a tumor promoter or suppressor. To provide definite conclusions for this question, two types of main experiments are missing: (1) in vitro effects of JMJD5 knock-down, (2) in vivo effects of both JMJD5 overexpression and knock-down.

Since JMJD5 seems to be downregulated from normal liver to HCC, silencing of it in the liver cells could lead to carcinogenesis. JMJD5 knock-down via siRNA or shRNAs should first be tried with cell lines which express JMJD5 in sufficiently high levels. After transiently or stably-knocked down cell lines are created, similar phenotypic assays should be performed to determine its effects on the cells.

As shown in this study, JMJD5 seems to alter migration and anchorage-independent growth of the cells, suggesting a potential link between JMJD5 and in vivo metastasis and carcinogenesis. Using these clones, xenograft liver cancer models could be created in mice, and their metastatic behavior and tumorigenic potential could be investigated under in vivo conditions. For in vivo-silencing, conditional knock-out mice for JMJD5 are required because JMJD5-deficient mice are embryonic lethal [29]. When it is knocked out, the phenotypic, morphological and biochemical changes in the liver could be traced.

In addition, cell growth assays and methodologies applied in this study, such as SRB staining and BrdU incorporation, were not very certain in determining growth promotion or inhibition of stable clones with low JMJD5 expression. These assays could be repeated with high expression clones to gain a better insight into growth phenotype of the cells. In this case, instead of counting BrdU(+) cells with naked eye, FACS technique could be used to detect the BrdU signal in quantitative terms.

Commercial kits, such as MTT and XTT cell proliferation assay kits, could also be used for more accurate results. In order to confirm that JMJD5 acts on blocking or accelerating cell cycle, flow cytometry assays can be repeated with synchronized cells. Alternatively, expression levels of proteins known to be involved in G1/S transition or G2/M arrest could be detected and compared between JMJD5-overexpressing cells and empty cells.

According to the microarray analysis results and cell migration results, it seems that JMJD5 activates certain genes responsible for epithelial characteristics and cellular differentiation, probably causing the decrease in migratory property of the cells. Whether the levels of these genes are changing in RNA and protein levels could be checked. Additionally, the change in mesenchymal to epithelial transition markers should also be investigated.

To sum up, JMJD5 could be a promising therapeutic or biomarker target in liver cancer research; hence, further studies are needed to comprehensively understand the biological role of it in HCC.

REFERENCES

[1] Farazi, P. A., & DePinho, R. A. (2006). Hepatocellular carcinoma pathogenesis: from genes to environment. *Nature Reviews Cancer*, *6*(9), 674-687.

[2] Gao, J., Xie, L., Yang, W., Zhang, W., Gao, S., Wang, J., et al. (2012). Risk factors of hepatocellular carcinoma - current status and perspectives. *Asian Pacific J Cancer Prev*, *13*, 743-752.

[3] Forner, A., Llovet, J. M., & Bruix, J. (2012). Hepatocellular carcinoma. *Lancet,379*, 1245-1255.

[4] American Cancer Society, (2010). Cancer Facts & Figures 2010. Atlanta: American Cancer Society

[5] Ozen, C., Yildiz, G., Dagcan, A. T., Cevik, D., Ors, A., Keles, U., et al. (2013). Genetics and epigenetics of liver cancer.*New Biotechnology*, *30*, 381-384.

[6] Arzumanyan, A., Reis, H. M., & Feitelson, M. A. (2013). Pathogenic mechanisms in HBV and HCV-associated hepatocellular carcinoma. *NATURE REVIEWS*, *13*, 123-135.

[7] Feo, F., Frau, M., Tomasi, M. L., Brozzetti, S., & Pascale, R. M. (2009). Genetic and epigenetic control of molecular alterations in hepatocellular carcinoma. *Experimental Biology and Medicine*, *234*(7), 726-736.

[8] Whittaker, S., Marais, R., & Zhu, A. X. (2010). The role of signaling pathways in the development and treatment of hepatocellular carcinoma. *Oncogene*, *29*(36), 4989-5005.

[9] Ozturk, M., Arslan-Ergul, A., Bagislar, S., Senturk, S., & Yuzugullu, H. (2009). Senescence and immortality in hepatocellular carcinoma. *Cancer Letters*, *286*(1), 103-113.

[10] Sharma, S., Kelly, T. K., & Jones, P. A. (2010). Epigenetics in cancer.*Carcinogenesis*, *31*(1), 27-36.

[11] Park, Y. J., Claus, R., Weichenhan, D., & Plass, C. (2011). Genome-wide epigenetic modifications in cancer. *Prog Drug Res*, *67*, 25-49.

[12] Chi, P., Allis, C. D., & Wang, G. G. (2010). Covalent histone modifications — miswritten, misinterpreted and mis-erased in human cancers. *Nature Reviews Cancer*, *10*(7), 457-469.

[13] Kanwal, R., & Gupta, S. (2012). Epigenetic modifications in cancer. *Clin Genet*, *81*, 303–311.

[14] Futscher, B. W. (2013). Epigenetic changes during cell transformation. *Adv Exp Med Biol.*, *754*, 179–194.

[15] Liu, W., Shi, Y., Peng, Y., & Fan, J. (2012). Epigenetics of hepatocellular carcinoma: a new horizon. *Chinese Medical Journal*, *125*(13), 2349-2360.

[16] You, J. S., & Jones, P. A. (2012). Cancer genetics and epigenetics: two sides of the same coin?. *Cancer Cell*, *22*, 9-20.

[17] Kooistra, S. M., & Helin, K. (2012). Molecular mechanisms and potential functions of histone demethylases.*NATURE REVIEWS*, *13*, 297-311.

[18] Hou, H., & Yu, H. (2010). Structural insights into histone lysine demethylation. *Current Opinion in Structural Biology*,*20*(6), 739-748.

[19] Cloos, P. A., Christensen, J., Agger, K., & Helin, K. (2008). Erasing the methyl mark: histone demethylases at the center of cellular differentiation and disease.*GENES & DEVELOPMENT*, *22*(9), 1115-1140.

[20] Lan, F., Nottke, A., & Shi, Y. (2008). Mechanisms involved in the regulation of histone lysine demethylases. *Current Opinion in Cell Biology*, *20*(3), 316-325.

[21] He, Y., Korboukh, I., Jin, J., & Huang, J. (2012). Targeting protein lysine methylation and demethylation in cancers. *Acta Biochim Biophys Sin*, *44*, 70-79.

[22] Kampranis, S. C., & Tsichlis, P. N. (2009). Histone demethylases and cancer. *Adv Cancer Res*, *102*, 103-169.

[23] Wagner, E. J., & Carpenter, P. B. (2012). Understanding the language of Lys36 methylation at histone H3. *NATURE REVIEWS*, *13*, 115-126.

[24] Jones, M. A., Covington, M. F., DiTacchio, L., Vollmers, C., Panda, S., & Harmer, S. L. (2010). Jumonji domain protein JMJD5 functions in both the

plant and human circadian systems. *Proceedings of the National Academy of Sciences*, *107*(50), 21623–21628.

[25] Jones, M. A., & Harmer, S. L. (2011). JMJD5 functions in concert with TOC1 in the Arabidopsis circadian system. *Plant signaling & behavior*, *6*(3), 445-448.

[26] Youn, M., Yokoyama, A., Fujiyama-Nakamura, S., Ohtake, F., Minehata, K., Yasuda, H., et al. (2012). JMJD5, a Jumonji C (JmjC) domain-containing protein, negatively regulates osteoclastogenesis by facilitating NFATc1 protein degradation. *Journal of Biological Chemistry*, *287*(16), 12994–13004.

[27] Hsia, D. A., Kung, H., Chen, H., Wright, M. E., Huerta, S. B., Izumiya, C., et al. (2010). KDM8, a H3K36me2 histone demethylase that acts in the cyclin A1 coding region to regulate cancer cell proliferation. *Proceedings of the National Academy of Sciences*, *107*(21), 9671-9676.

[28] Rizzo, P. A., Krishnan, S., & Trievel, R. C. (2012). Crystal structure and functional analysis of JMJD5 indicate an alternate specificity and function. *Mol. Cell. Biol.*, *32*(19), 4044-4052.

[29] Ishimura, A., Minehata, K., Terashima, M., Kondoh, G., Hara, T., & Suzuki, T. (2012). Jmjd5, an H3K36me2 histone demethylase, modulates embryonic cell proliferation through the regulation of Cdkn1a expression. *Development*, *139*, 749-759.

[30] Oh, S., & Janknecht, R. (2012). Histone demethylase JMJD5 is essential for embryonic development. *Biochemical and Biophysical Research Communications*, *420*, 61-65.

[31] Wang, Z., Wang, C., Huang, X., Shen, Y., Shen, J., & Ying, K. (2012). Differential proteome profiling of pleural effusions from lung cancer and benign inflammatory disease patients. *Biochimica Et Biophysica Acta*, *1824*, 692-700.

[32] Suzuki, T., Minehata, K., Akagi, K., Jenkins, N. A., & Copeland, N. G. (2006). Tumor suppressor gene identification using retroviral insertional mutagenesis in Blm-deficient mice. *The EMBO Journal*, *25*(14), 3422-3431.

[33] Fong, G., & Takeda, K. (2008). Role and regulation of prolyl hydroxylase domain proteins. *Cell Death and Differentiation*, *15*(4), 635-641.

[34] Kaelin, W. G., & Ratcliffe, P. J. (2008). Oxygen sensing by metazoans: the central role of the HIF hydroxylase pathway. *Molecular Cell*, *30*(4), 393-402.

[35] Kaelin, W. G. (2005). Proline hydroxylation and gene expression. *Annu. Rev. Biochem.*, *74*, 115–28.

[36] Webby, C. J., Schofield, C. J., Nielsen, M. L., Kessler, B., Kramer, H., Dreger, M., et al. (2009). Jmjd6 catalyses lysyl-hydroxylation of U2AF65, a protein associated with RNA splicing. *Science*, *325*(5936), 90-93.

[37] Kato, M., Araiso, Y., Noma, A., Nagao, A., Suzuki, T., Ishitani, R., et al. (2011). Crystal structure of a novel JmjC-domain-containing protein, TYW5, involved in tRNA modification. *Nucleic Acids Research*, *39*(4), 1576-1585.

[38] Wurmbach, E., Chen, Y. B., Khitrov, G., Zhang, W., Roayaie, S., et al. (2007). Genome-wide molecular profiles of HCV-induced dysplasia and hepatocellular carcinoma. *Hepatology*, *45*: 938–947

[39] de Hoon, M. J., Imoto, S., Nolan, J., Miyano, S. (2004). Open source clustering software. *Bioinformatics*, *20*: 1453–1454.

[40] Saldanha, A. J. (2004). Java Treeview–extensible visualization of microarray data. *Bioinformatics*, *20*: 3246–3248.

[41] Park, J., Hwang, Y., Chung, J., Kim, S., Lee, J., Kang, M., et al. (1995). Characterization of cell lines established from human hepatocellular carcinoma. *International Journal of Cancer*, *62*(3), 276-282.

[42] Momparber, R. L., Karon, M., Siegel, S. E., & Avila, F. (1976). Effect of adriamycin on DNA, RNA, and protein synthesis in cell-free systems and intact cells. *CANCER RESEARCH*, *36*, 2891-2895.

[43] Fornari, F., Randolph, J., Yalowich, J., Ritke, M., & Gewirtz, D. (1994). Interference by doxorubicin with DNA unwinding in MCF-7 breast tumor cells. *Mol Pharmacol*, *45*(4), 649-656.

[44] Beurskens, L. W., Tibboel, D., Lindemans, J., Duvekot, J. J., Cohen-Overbeek, T. E., Veenma, D. C., et al. (2010). Retinol status of newborn infants is associated with congenital diaphragmatic hernia.*Pediatrics*, *126*(4), 712-720.

[45] Logan, C. Y., & Nusse, R. (2004). The Wnt signaling pathway in development and disease. *Annual Review of Cell and Developmental Biology*, *20*(1), 781-810.

[46] Hanahan, D., & Weinberg, R. A. (2011). Hallmarks of cancer: the next generation.*Cell*, *144*(5), 646-674.

[47] Mori, S., Murphy, S., Gatza, M., Kim, J. W., Yao, G., Baba, T., et al. (2009). Anchorage-independent cell growth signature identifies tumors with metastatic potential. *Oncogene*, *28*(31), 2796-2805.

[48] Morin, P. (1999). Beta-catenin signaling and cancer. *Bioessays*, *21*(12), 1021-1030.